Spring 7-12-2016

The Design, Implementation, Evaluation and Results of a Race Car for the Collegiate Formula SAE Electric Competition

Quinn Jasha Bryan Sullivan
Portland State University

The Design, Implementation, Evaluation and Results of a Race Car for the Collegiate Formula SAE Electric Competition

by

Quinn Jasha Bryan Sullivan

A thesis submitted in partial fulfillment of the
requirements for the degree of

Master of Science
in
Electrical and Computer Engineering

Thesis Committee:
Robert Bass, Chair
Mark Faust
Douglas Hall

Portland State University
2016

Abstract

The Formula SAE Electric competition is a collegiate autocross event in which teams design, build, and race an open-wheeled electric race car. The main motivation is the efficiency advantage of electric motors over internal combustion motors. This thesis presents the design and evaluation of two generations of Portland State University electric race cars.

The constraints are the competition rules, finances, human resources, and time required to complete a race car in one year. The design includes the implementation of existing components: battery cells, controllers, electric motors, drivetrains, and tire data for an optimized race car. Also, several circuits were designed and built to meet the rules, including the shutdown, precharge, discharge, brake system plausibility, tractive system active light, and an electric vehicle control unit.

The car's performance was modeled with calculations and OptimumLap simulation software, then track tested for actual data. Performance data such as torque, power, and temperatures were logged, and the Formula SAE events were tested. The data were compared to the simulations and records from past competitions, and the car was 21% to 30% behind the best times.

The motor generated 410 Nm of peak torque, as expected, but the maximum power was 51 kW, 15% less than the calculated 60 kW. Compared to the best times of past competitions,

the car completed Skid-pad in 6.85 seconds (21% slower), and Acceleration in 5.65 seconds (25% slower). The first generation car was tested for range, and raced 31.4 km on a cold, wet track, so tire forces were decreased 6% to 69% from a dry track. During the 22 km Endurance test with the second generation car, there were problems with imbalanced cell voltages, limiting the test to 4.9 km. Later, there was a catastrophic drivetrain failure, and Endurance testing on a dry track was not completed.

In dynamic event simulations, a lighter, axial flux permanent magnet synchronous motor with a decreased counter EMF yielded improved times. Reconfiguring the battery pack from 200 V_{DC} 300 V_{DC} would provide 50% more peak power. Further testing is required to determine the actual average power use and making design decisions with an improved battery pack.

Dedication

To Viking Motorsports teammates and their contributions, making the electric race car possible. To Cal Watson for the opportunity and guidance in building an electric car. Special thanks to my mother for inspiring exploration and demonstrating that great opportunities are available through relentless efforts.

Acknowledgments

Gratitude is extended to Portland State University. Thank you to the thesis committee: Professors Bob Bass, Mark Faust, and Doug Hall; to the Portland State University Viking Motorsports teammates, including Michal Podhradsky, Tyler Gilbert, Nick Cho, Trevor Conant, Troy Brown, Evan Yand, Barett Strecker, Trina Wing, Nevin Scott, Keith Occena, Xander Jole, Josiah Baleilevuka, Nate Stickrod, Heber Miguel, Shastina Holmes, Justin Burris, Brantley Miller, Jarrett Lonchar, Eric Meza, Jesse Terrusa, Franklin Vang, Priyanka Chand, Bryce Rullifson, Ricky Valencia, John Talik, unofficial teammate Edith Guitron, and all of those who have helped work on the electric race car; to our industry racing advisor, Evan Waymire; to Chris Brune and Larry Rinehart of Rinehart Motion Systems for outstanding support for the RMS motor controller; to Andrew Greenberg in advising with circuit designs and interpreting FSAE rules; to all of our generous sponsors, to the donors of the crowdfunding campaign, enabling the build of the first Viking Motorsports Formula SAE Electric race car.

Contents

List of Tables

List of Figures

List of Abbreviations

- A: Amps
- AC: Alternating Current
- Ah: Amp-hour
- AIR: Accumulator Isolation Relays
- AMS: Accumulator Management System
- ARM: Advanced RISC Machine
- A_{RMS}: Amps Root Mean Square, Amps of Alternating Current
- ATF: Automatic Transmission Fluid
- AWG: American Wire Gauge
- BLDC: Brushless Direct Current
- BMS: Battery Management System
- C: Celsius
- C: Coulombs
- CAD: Computer Aided Design
- CAN: Controller Area Network
- cm: centimeter
- DC: Direct Current
- DCP: Direct Current Pulse
- EE: Electrical Engineering
- EEPROM: Electronically Erasable Programmable Read Only Memory

- EMF: Electromotive Force
- EMI: Electromagnetic Interference
- EV: Electric Vehicle
- EVCU: Electric Vehicle Control Unit
- FR-4: Flame Retardant Type 4 Woven Epoxy
- G's: gravitational force equivalent = 9.81 m/s^2
- GLVS: Grounded Low Voltage System
- hr: hour
- HT: High Torque
- HV: High Voltage
- Hz: Hertz
- HVD: High Voltage Disconnect
- IC: Integrated Circuit
- ICE: Internal Combustion Engine
- i_d: current along the direct axis
- IGBT: Insulated Gate Bipolar Transistor
- IMD: Insulation Monitoring Device
- i_q: current along the quadrature axis
- kg: kilograms
- kHz: kilohertz
- km: kilometers
- kN: kiloNewtons
- kph: kilometers per hour
- kW: kilowatts
- kWh: kilowatt hours
- LCO: lithium cobalt oxide

- LED: Light Emitting Diode
- LFP: lithium iron phosphate
- LMO: lithium manganese oxide
- LTO: lithium titanate, lithium titanium oxide
- m: meters
- ME: Mechanical Engineering
- MJ: MegaJoule
- MLEC: Master Lithium Energy Controller
- mm^2: square millimeters
- MOSFET: Metal Oxide Semiconductor Field Effect Transistor
- ms: milliseconds
- mV: millivolts
- NCA: lithium nickel cobalt aluminum oxide
- NiCd: nickel cadmium
- NiMH: nickel-metal hydride
- Nm: Newton-meters
- NMC: lithium nickel manganese cobalt oxide
- NPN: N-type P-type N-type doped layered bipolar transistor
- PCB: Printed Circuit Board
- PIR: Portland International Raceway
- PWM: Pulse-Width Modulation
- RISC: reduced instruction set computing
- RLEC: Remote Lithium Energy Controller
- RPM: Revolutions Per Minute
- RTDS: Ready-To-Drive-Sound
- SAE: Society of Automotive Engineers

- SD: Secure Digital card
- sec: seconds
- T: Tesla
- TSAL: Tractive System Active Light
- TSMP: Tractive System Measuring Points
- TSMS: Tractive System Master Switch
- VCU: Vehicle Control Unit
- Wh: Watt hours
- V_{DC}: Voltage Direct Current

1 Introduction

1.1 Motivation

In this thesis, I discuss the design, implementation, evaluation, and results of an electric race car for the collegiate Formula SAE Electric competition, including design and dynamic racing events. The main motivation is the difference of efficiencies between electric motors and internal combustion engines, as they vary greatly. Internal combustion engines are limited by the temperature differences in the Carnot cycle during gasoline combustion.

$$\eta = \frac{T_1 - T_2}{T_1} = \frac{505°K - 298°K}{505°K} = 41\% \tag{1.1}$$

The maximum efficiency, η, is based on the combustion temperature of gasoline, T_1, and the ambient temperature of the atmosphere, T_2.

This is the maximum possible efficiency for an internal combustion engine, and the actual efficiency is often much less. The electric motor datasheets state they are 74-96% efficient[1][2], possessing a much better power-to-weight ratio, and enabling the use of much lighter, smaller electric motors. This is the single greatest advantage of electric cars, and if the efficiencies of electric and combustion motors were equal, there would be no potential for improved performance with electric motors, thus, no electric race cars.

The motor efficiency gives an advantage to electric race cars, but the energy density of batteries versus gasoline is a disadvantage. Gasoline provides 12,200 Wh/kg, and the most energy-dense battery cell found was 130 Wh/kg[3], 1.1% as energy-dense as gasoline.

When possible, data-driven, quantitative design decisions are made for the design, implementation, evaluation, and analysis of the electric race car. This aids in systematically designing the race car as a package that performs well, and that can be improved upon in future iterations. In this thesis, I highlight important components, explain the design rationale, discuss the strengths and weaknesses in current designs, and develop solutions for improvements in design and dynamic performance.

1.2 Chronology

In July 2013, the Portland State University (PSU) Viking Motorsports (VMS) industry racing adviser informed the team of the results of the first US Formula SAE Electric competition, shown in Table 1.1.[4] At the time, VMS designed and built race cars with internal combustion engines, and had never worked on an electric race car. By 2011, I had converted two passenger cars to electric cars. After researching the Formula SAE rules, I was confident I could lead VMS to design and build PSU's first Formula SAE Electric race car. I took notes and reread all of the Formula SAE Electric rules, and researched the main electric car components best used for racing. This focused on lightweight, powerful components for electric cars and motorcycles, and defining the parameters of the required circuits needed. Instead of redesigning a new chassis and other components, an existing

chassis design was modified, and high quality components were reused. This eliminated the need to machine all new components, and we focused on other crucial tasks.

The VMS electric car began with two electrical engineering students and a mechanical engineering student in July 2013. In October, we registered as one of twenty teams in the second Formula SAE Electric competition in Lincoln. By the middle of the year, the project had grown to three electrical engineering students, five mechanical engineering students, and a few students from other majors. My roles included acting as the lead electrical engineer, project manager, marketer, recruiter, fundraiser, and technician in the construction of the race car.

In February, we worked to set up a simple motor test bench with the controller, motor, and a 120 V_{DC} battery pack. This allowed fine-tuning of the motor and controller parameters, provided familiarity with the controller operations and graphical user interface (GUI), and set up battery charging.

Fabrications continued from April until June, preparing the car for the competition. The PSU electric car first drove the wheels on June 19th, at the competition. The car did not pass the electrical technical inspection due to not meeting all rules, and having incomplete circuits. The amount of skilled labor required for designing and building an entire race car in a year was extremely great, and we realized the team had too few people to meet our goals of completing a high quality race car and competing in all dynamic events. The summer was spent improving the first generation car: completing circuits, track testing, fine tuning the handling, and working on a redesign to improve the car by transferring weight over the

drive wheels and reducing weight overall.

The following year, sponsorship had increased, dramatically increasing the budget, eliminating the financial constraint for design decisions. In October 2014, the team registered for the competition again. Work was done on redesigning the second generation car without sidepods, fitting all of the batteries, motor and controller in the back, eliminating significant weight. Battery containers were designed and built, but the high voltage circuitry did not get completed in time to do testing, and the car had to be withdrawn from the competition in June. The team had increased in MEs, but there were only three EEs. The time available was a great constraint, and completing the design and build of the race car was still extremely challenging. In July and August, track testing with data logging occurred.

To simplify the data, all modeling of the car is based on parameters of the second generation car. The first generation car was very similar, but 100 lbs heavier, further information in Section 3.2. The electric race car is still in progress, and registered for the 2016 Formula SAE Electric competition, but beyond the scope of this thesis.

Date	Milestone
July 1, 2013	researched Formula SAE Electric competition, results
July 2, 2013	researched motors, motor controllers, battery cells, other potential electric components
September 2013	acquired Remy motor, RMS AC controller
October 7, 2013	registered for PSU's first Formula SAE Electric competition
November 14, 2013	Oregon SAE night: raised funds needed to complete build
Feb. 26, 2014	motor and controller set up on test bench, motor rotating
March 1, 2014	fine-tuned motor, no-load bench testing completed
April 22, 2014	main chassis completed
June 10, 2014	motor, controller, shutdown components, battery boxes mounted
June 18, 2014	formula SAE Lincoln competition begins
June 19, 2014	VMS electric race car drives wheels for the first time
October 7, 2014	registered for second Formula SAE Electric competition
November 14, 2014	first track day at Portland International Raceway (PIR)
November 23, 2014	first track day at PIR in Portland rain
December 2014	redesign, started second generation car
June 2015	car not completed, withdrawn from competition
July 2015	track testing of second generation car: data gathered, mechanical failure ended testing

Table 1.1: VMS electric milestones: relevant dates from the beginning of the research in the summer of 2013 through the development, build, and testing of two generations of cars through the end of summer 2015.

Elements that are important to racing performance are the suspension and dynamics. However, these are beyond the scope of this thesis, and not included. The focus is designing the car for longitudinal forces. In Table 1.2, credit is given to those responsible for work throughout the thesis, and any time credit is not given, the work was solely accomplished by the author. The milestones give an outline for important events and a feel for the scope of the thesis from July 2013 through July 2015. Next, the relevant tasks assigned, completed, and work accomplished are credited to the appropriate students.

Tasks & Work Completed		
Subsystem	**Student**	**(year) Tasks Accomplished**
Shutdown Circuit	Quinn[5]	(2014, 2015) schematic, selected components, built circuit
Insulation Monitoring Device	Quinn	(2014, 2015) schematic, selected components, built circuit
Brake System Plausibility Device	Quinn Michal[6]	(2014) schematic, selected components (2015) redesign: schematic, selected components, built circuit
Precharge and Discharge Circuits	Quinn	(2014, 2015) schematic, simulated in MATLAB, selected components, built circuit
Reset/Latching (IMD & BMS)	Quinn Tyler[7]	(2014) schematic, selected components (2015) built circuit, redesigned schematic, replacing relays with SR latch
Tractive System Active Light	Michal	(2014) schematic, selected components, 3D printed enclosure, built circuit, (2015) redesigned circuit, built TSAL & RTDS circuits into same enclosure
Ready-To-Drive-Sound (RTDS)	Trevor[8] Michal	(2014) designed schematic, selected parts, built PCB (2015) redesigned circuit, interfaced with EVCU

Tasks & Work Completed Continued		
Subsystem	**Student**	**Tasks Accomplished (year)**
Battery Cells & Container	Quinn Xander[9]	(2014, 2015) schematic, selected components, built HV circuit connections & containers (2015) completed all welding
EVCU & BMS	Michal	(2014) schematic, selected MBED microcontroller & components, built circuit, programmed software in C, (2015) redesigned, selected GEVCU with Atmel microcontroller
Charging System	Quinn Michal	(2014) schematic, selected components, built circuit (2014, 2015) BMS functions, designed and built 2nd gen. circuit, installed on cart
Motor Controller	Quinn	(2014, 2015) schematic, selected component, wired HV, 1st gen. harness, modified GUI settings (50%)
Motor Controller	Michal	(2014, 2015) CAN bus communications, 2nd, 3rd gen. harnesses, modified GUI settings(50%)
Motor	Quinn Troy[10]	(2014) researched, calculations, and selected motor (2014) created CAD model, designed & built 1st gen. motor enclosure

Tasks & Work Completed Continued		
Subsystem	**Student**	**Tasks Accomplished (year)**
	Trevor	(2014) fabricated motor mounting, designed & built 2nd gen. motor enclosure, waterproof HV connector
Throttle (Torque Encoder)	Quinn	(2014) researched, selected 1st, 2nd, 3rd, 4th generation models, tested 1st, 2nd gen.
	Michal	(2015) tested 3rd, 4th, controller connections
Drivetrain	Quinn	(2014) simulated optimal gear reduction, selected sprockets, machined rotor shaft collar
Tires	Quinn	(2014) researched specs, selected tires
	Nick[11]	(2015) tire data, suspension, CAD models
OptimumLap Simulations	Michal	(2015) imported tracks, set up car profiles, entered torque curves, created user manual
	Quinn	(2015) modified and added car profiles, entered torque curves, compared to actual data, made conclusions
	Troy	(2013) initial setup and simulations

Table 1.2: For each subsystem, the student researched the rules, defined relevant parameters required for components, or defined the physical parameters of the circuits in terms of inputs, outputs, deliverables expected.

1.3 Formula SAE Background

SAE international is the professional association that created and continues to organize the annual racing competition. The Formula SAE competition started in late 1979 as an alternative to the existing SAE Mini Baja competition utilizing internal combustion engines. The concept behind Formula SAE is that a fictional manufacturing company has contracted a design team to develop a small Formula-style race car. The prototype race car is to be evaluated for its potential as a production item. The target marketing group for the race car is the non-professional weekend autocross racer. Each student team designs, builds and tests a prototype based on a set of rules. These rules ensure safe onsite event operations and promote clever problem solving.[12]

The first Formula SAE Electric race car competition was held in 2013 in Lincoln, Nebraska. Portland State University's race car team, Viking Motorsports (VMS), first entered the electric competition in June 2014. 2016 marks the third consecutive year that Portland State University has entered a Formula SAE Electric race car.

1.3.1 Competition Deliverables

Every year, each competition requires a Business Logic Case, Cost Report, Failure Modes Effects and Analysis Form, an Electrical Systems Form, a Design Report, and a Structural Equivalency Spreadsheet. The Business Logic Case discusses factors that require consideration for the development of a new product, including cost, identifying the market and sales volume, and profitability. The Cost Report is essentially a bill of materials. The

Failure Modes Effects and Analysis document provides a complete analysis of every possible electrical system component failure and relevant mechanical component failures that affect electrical signals, a rating of severity, likelihood of occurrence, and detectability of that failure. The Electrical Systems Form required all circuit diagrams, CAD drawings representing the car's layout and physical locations of all pertinent components. The Design Report is the overall systems engineering approach and the design of subsystems. The Structural Equivalency Spreadsheet requires CAD models of different views on the car, and shows the chassis is structurally strong enough for the competition. Also, it must be shown that the battery boxes and fasteners are able to withstand 160 kN (40 G's) of force without breaking. The documents are extensive, and demand much time to properly complete them, and there is a ten point penalty per day for missing a document deadline.

1.3.2 Technical Inspections

At each competition, the car is subject to electrical technical inspection, mechanical technical inspection, and driver safety tests. Electric race cars are much quieter than combustion race cars, therefore, a "ready-to-drive sound" and a "tractive system active light" are required. There is also a "rain test" where the low voltage and high voltage systems are turned on and the vehicle is sprayed with water for two minutes. The car passes the test if the insulation monitoring device (IMD) does not fault.[13]

Formula SAE is autocross style racing featuring several static and dynamic events. The static events are: Cost & Manufacturing, Presentation, and Design, shown in Table

1.3. The dynamic events are held on large, paved areas marked off with cones, and both combustion and electric cars compete in the same events. The dynamic events are: Skid-pad, Acceleration, Autocross, and Endurance, shown in Table 1.3. The objective in each event is to achieve the fastest time possible, and the cars are ranked according to times. Points are awarded to teams according to their position in the rankings.[13]

Event	**Max. Score**
Static Events	**325**
Cost & Manufacturing	100
Presentation	75
Design	150
Dynamic Events	**675**
Acceleration	75
Skid-pad	50
Autocross	150
Efficiency	100
Endurance	300
Total	**1000**

Table 1.3: Scoring for different static and dynamic Formula SAE events, a maximum of 1000 total points.

1.3.3 Skid-pad Event

The objective of the Skid-pad Event is to measure the car's cornering ability on a flat surface while making a constant-radius turn. The event is a figure eight course around two circles 15.25 meters in diameter, shown in Figure 1.1. The driver enters the course, maneuvers around the right circle twice, the left circle twice, then exits the course. The Skid-pad Event demonstrates the performance in angular acceleration, and the event score is 5% of the total competition score[13].

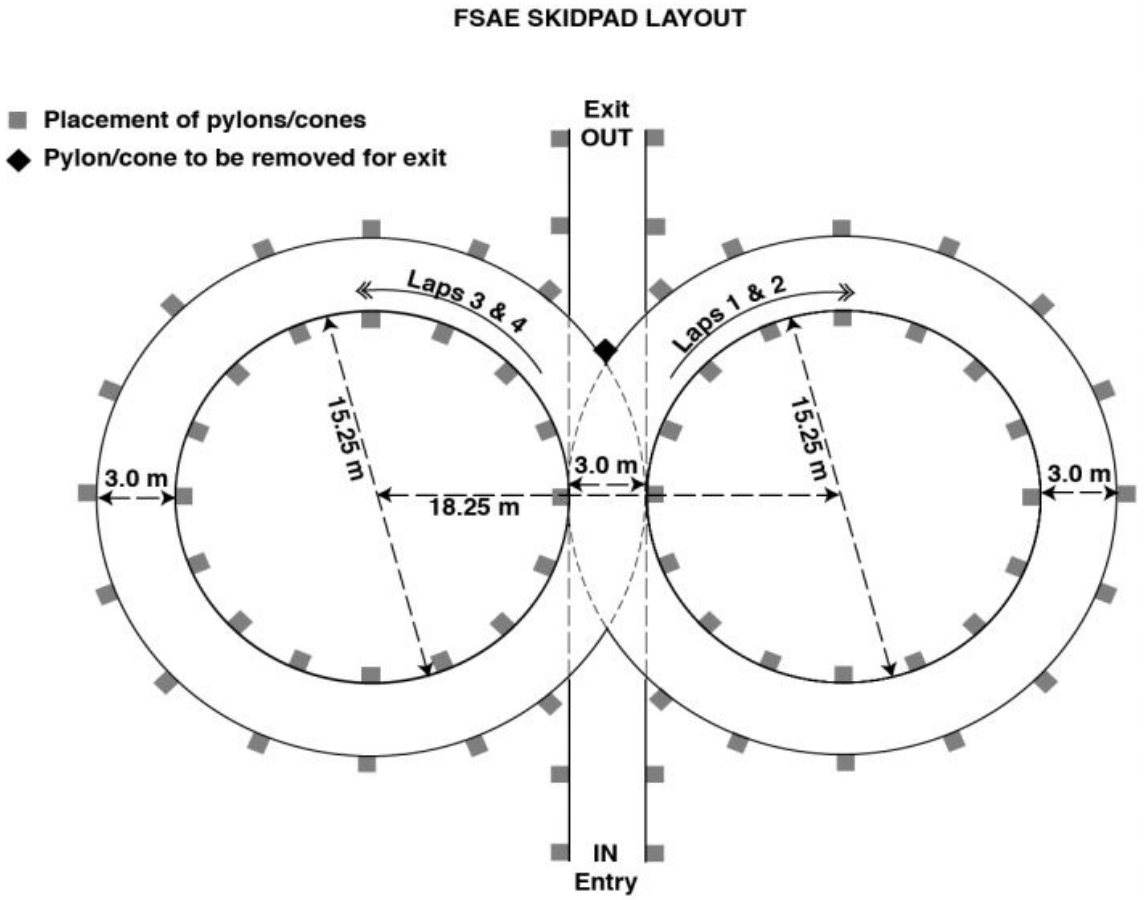

Figure 1.1: Skid-pad Course (meters).[13]

1.3.4 Acceleration Event

The Acceleration Event evaluates the car's acceleration in a straight line on flat pavement. The score is based on the time from start to finish in a seventy-five meter straight line, Figure 1.2. Then, each team's times are compared, ranked, and scored accordingly. The Acceleration Event demonstrates longitudinal acceleration, and is 7.5% of the total competition score.[13]

1.3.5 Autocross Event

The objective of the Autocross Event is to evaluate the car's maneuverability and handling qualities on a tight course without the hindrance of competing cars. The course includes straight parts, constant turns, hairpin turns, and slaloms, intended to demonstrate a combination of braking, longitudinal and lateral acceleration (Figure 1.2). The Autocross Event is 15% of the total competition score. The average speed is 40 to 48 kph, and the length is approximately 800 m.[13]

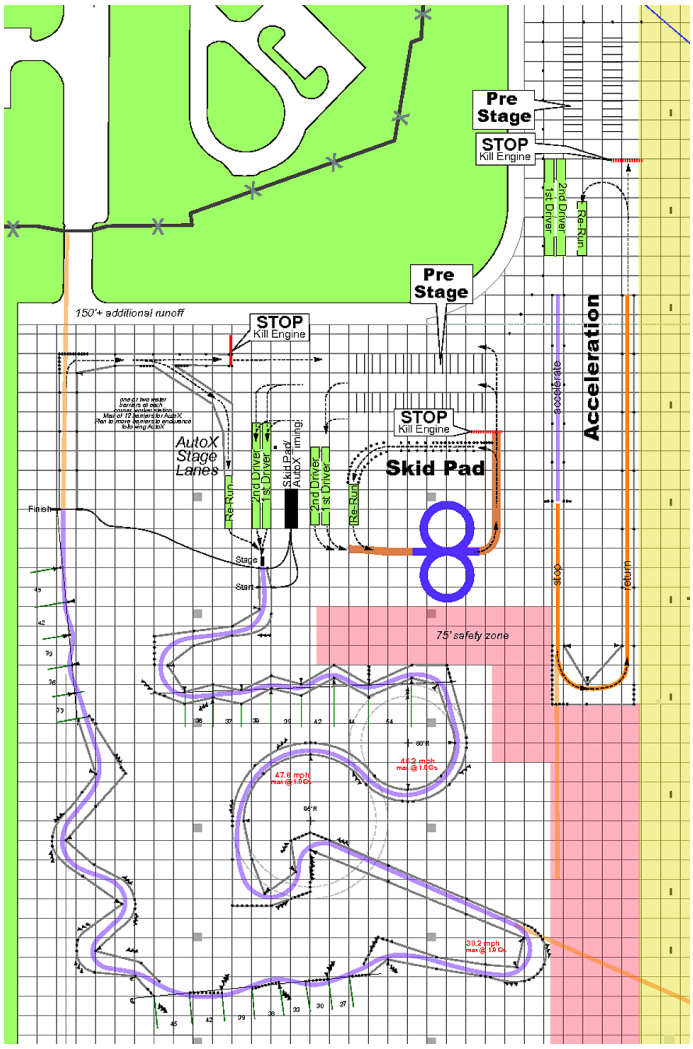

Figure 1.2: 2015 Formula SAE Lincoln Autocross, Skid-pad, and Acceleration course map, in meters.[14]

1.3.6 Endurance & Efficiency Event

The Endurance and Efficiency Event awards two separate scores from a single heat, and the objective is to evaluate the overall performance of the car and to test the car's durability and reliability over a 22 km course.[13] The car's efficiency is measured in conjunction with the Endurance Event. The objective of the Efficiency Event is to complete the event while

using the least possible amount of energy. The Efficiency score is 10% and the Endurance score is 30% of the total competition score, which will be calculated from the same heat. No recharging is allowed during an Endurance heat. Course speeds can be estimated by the following standard course specifications. The average speed should be 48 kph (29.8 mph) to 57 kph (35.4 mph) with top speeds of approximately 105 kph (65.2 mph). For electric cars that use regenerative braking, any braking energy that is recovered will be deducted from the amount of energy used after applying a factor of 90%, an estimate of round trip efficiency. The scoring rewards cars that use the least energy and incorporate regenerative braking. Shown in Figure 1.3, the Endurance and Efficiency Event demonstrates the car's durability and reliability with a more technical combination of braking, longitudinal and lateral acceleration, and efficiency.[13]

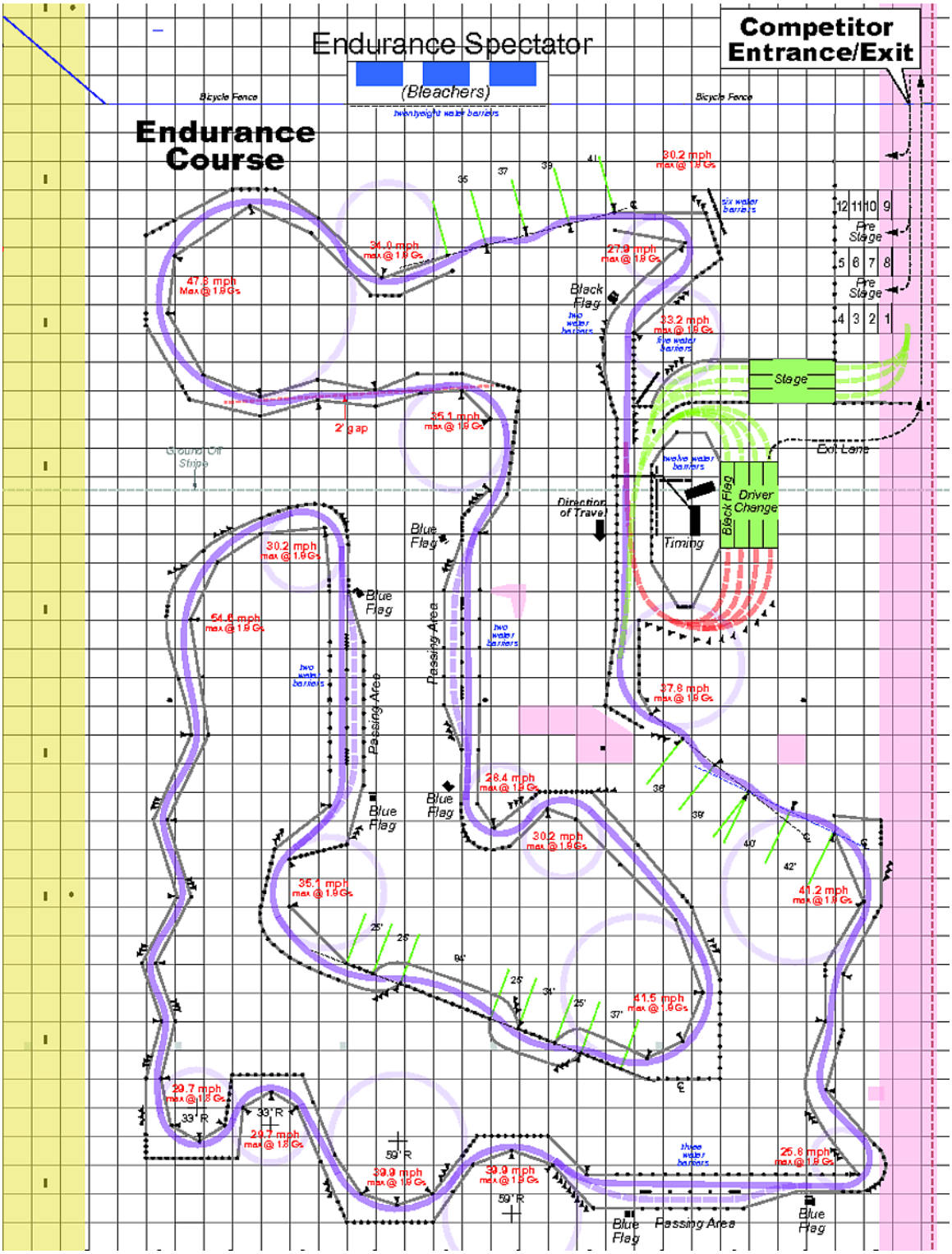

Figure 1.3: 2015 Formula SAE Lincoln Endurance Course map (meters).[14]

The Autocross and Endurance courses vary each year, and there are infinitely many options for routes with turns of varying radii and straight stretches of different lengths. The rules specify the dimensions and state that there are straights, constant turns, hairpin turns, slaloms, and miscellaneous turns. The maximum straight line distances are 77 meters in Endurance and 60 meters in Autocross.[13] Every event is conducted with only one race car on the track at a time, with the exception of Endurance, where there are multiple cars and passing lanes available. The average speed is approximately 48 to 57 kph and the maximum speed is approximately 105 kph.[13] This is relatively low for racing, and there are no obstacles, thus, much less potential for injury and damage to race cars.

2 Design Methodology

2.1 Overview

There were several design constraints, including Formula SAE rules, the VMS budget and human resources, the competition deadline in June, and the physical limitations of different components. In considering constraints on subsystem design, a procedure was developed and followed. First, we read the rules and created an outline of the allowed conditions. Second, research was conducted on commercially available solutions. Many components are off-the-shelf parts. For the circuits, there was not usually an off-the-shelf solution, and we had to design and build it. If a solution were available, the time and cost of the component would be considered and compared to a potential version we would build ourselves. If the component could affect the performance in a dynamic event, OptimumLap[15] software modeling was used to simulate changes. Third, we developed a plan for who would design, build, and test the component. This methodology considers all of the constraints, and systematically develops a solution by going through the process for all of the physical constraints of the modern components considered in design, such as motors, controllers, batteries, electronics and tires.

2.1.1 Formula SAE Constraints

The Formula SAE Electric competition provides rules that require additional safety features and constrain designs. For instance, in the American Formula SAE Electric competition, the maximum voltage is 300 V_{DC}. In 2014, the maximum power was 85 kW, and from 2015 to the present, it is 80 kW. The rules required at least ten different safety circuits, including redundant throttle and brake circuits, a flashing light to indicate active high voltage, and a high impedance measuring device between the high voltage and grounded low voltage systems. The circuits were not commercially available, and needed to be designed and built by the team, demanding a large portion of the team's time. For efficiency, time was allocated to the demands of the rules, limiting time spent on other aspects of design that were not essential to completing the car.

2.1.2 Financial Constraints

The Cost and Manufacturing Event emphasizes building the fastest car possible for the least cost. Further, the cost report lists every item on the car, and how much it would cost to build the race car. The 2014 cost report listed the car at $27,043. In comparison, the 2013 VMS combustion car cost was $12,058, 45% of the cost of the electric car. The cost report states what it would cost to create the car from scratch, not the team's actual cost. VMS decreases these costs by reusing parts from previous years, obtaining donated or discounted parts, materials and services, and machining and building components. The costs for necessary mechanical items such as the brake system, frame & body, instruments

& wiring, fit & finish, steering system, suspension & shocks, wheels & tires, and drivetrain (gear reduction, differential, half shafts) did not vary much for different designs. These components were either not changed at all or only slightly modified from the combustion designs. There are 95 different components on the car, and 40 of the components cost less than $10. To expand on the "Electric Motor & Drivetrain" subsystem in Figure 2.1, the most expensive components were constrained by cost, such as the motor ($3809), motor controller ($5203), and battery modules ($5840), totaling $14,852 of the entire budget. During the circuit design, the philosophy was to build simple, reliable, automotive-grade circuits that are robust enough to withstand heavy vibrations, accelerations, and EMI without failing and providing high quality electrical signals. The circuits designed cost less than $1500, far less than the motor, motor controller, and batteries, and these were not constrained by the budget. The design of the car also includes the cost of all materials and manufacturing processes.

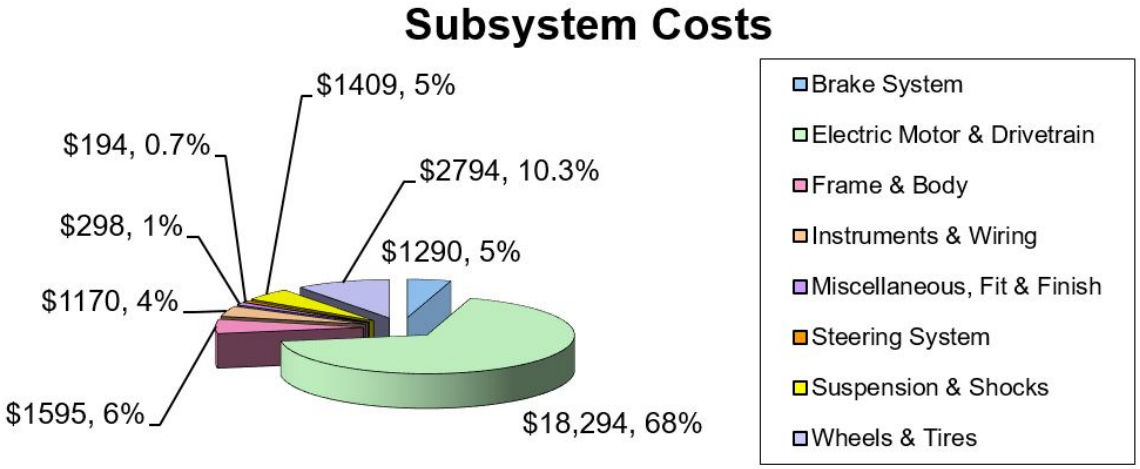

Figure 2.1: Subsystem Costs: subsystems such as brakes, frame and body, steering, suspension, wheels were not significantly changed from the combustion designs. The emphasis was the electric motor, controller, battery cells, and circuits.[5]

2.1.3 OptimumLap Model

OptimumLap[15] is software from OptimumG that allows for modeling a variety of different race car parameters for the various Formula SAE dynamic events. Shown in Figure 2.2, the team uses OptimumLap to compare the performance of different motors with varying torque and power curves, differing tire radii and frictional forces, vehicle weights, and gear ratios. The simulation data is obtained very quickly compared to the alternative of hand calculations and building an entire car. There are infinite combinations of different motors, batteries, and weights of the vehicle, and it would be impossible to create a different vehicle to track test every variable. Also, it would be challenging to hand calculate the lap time performance of the vehicle for the Autocross and Endurance Events.

The limitations of the software are that it does not allow input settings for different center of gravity heights and does not account for regenerative braking energy collected. The limitations do not discredit the value of the simulations, the parameters are simply not included and adjustable. This is compensated by adjusting for the normal force on the track, and this is verified by the tire coefficient setting in the "Driveline Model" tab that calculates the proper simulated normal force. Regenerative braking energy can be estimated and hand calculated from total energy use. When simulating in OptimumLap, the component simulated was varied, and all other parameters were kept constant, providing quick results for improving designs with quantitative data.

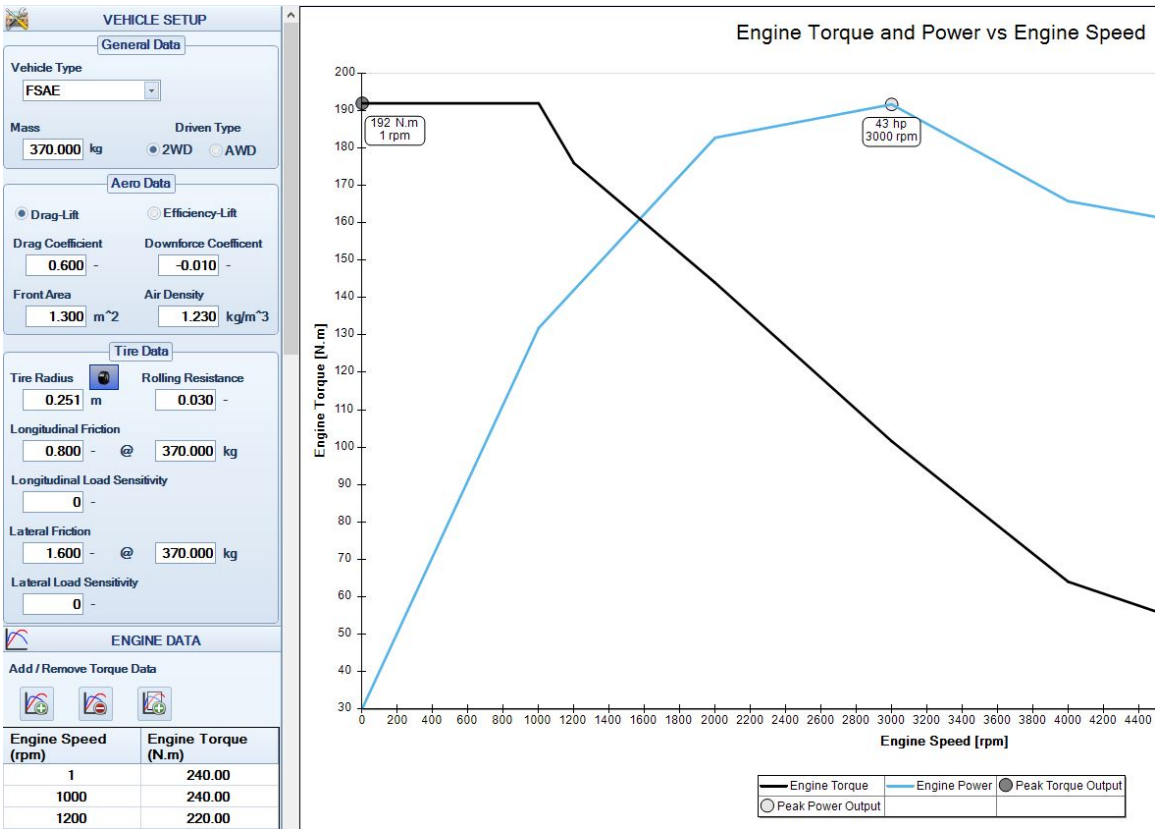

Figure 2.2: OptimumLap software allows multiple variables to be modified and tested on a particular motor. The data entered on the left column includes the total mass, the motor's torque and power curves, tire parameters, maximum RPM, power factor, gear reduction, and drivetrain efficiency.[15]

Once the car's data was entered, a simulation of vehicle mass versus lap time was conducted for a Formula SAE Autocross course (Figure 2.3).

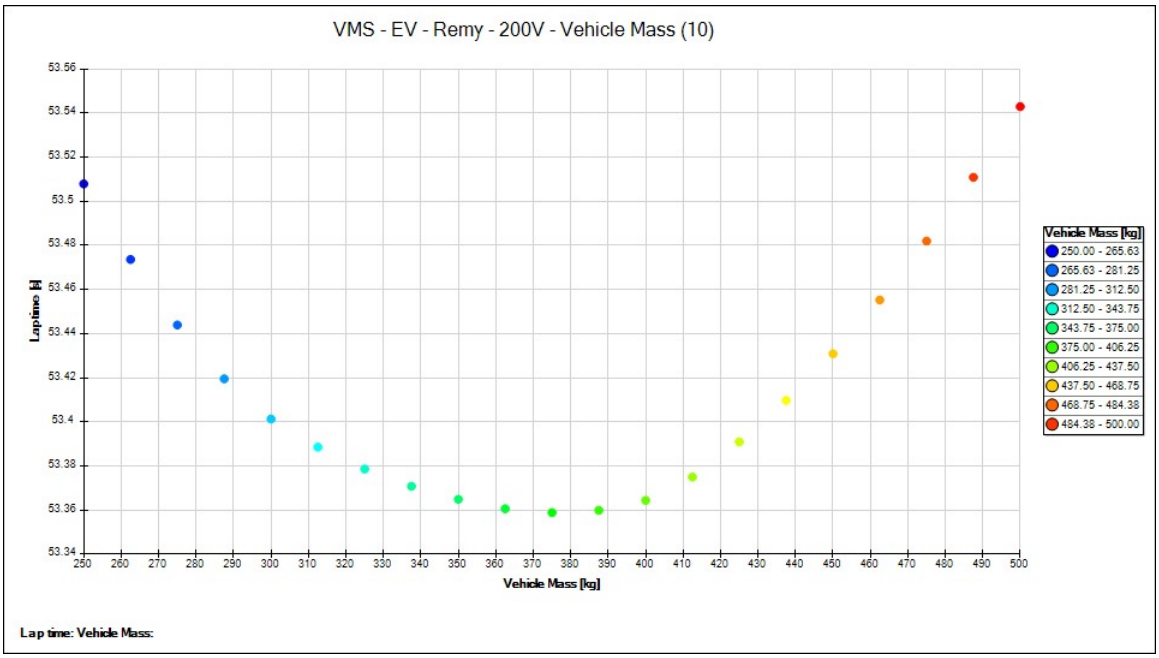

Figure 2.3: OptimumLap simulation of the mass versus lap time. The car would decrease lap time until 375 kg, then times increase as less force would be applied to the tires, decreasing acceleration.

Knowing that the car's performance improves with decreasing weight is useful for design, because weight becomes an important factor in the selection of every component. The curve is parabolic, so the lap times improve as the weight gets closer to 375 kg. For car masses less than 375 kg, the performance diminishes and lap times increase.

The overall goal was to implement new electric race car parts and not to redesign existing optimized parts. The race car frame was fabricated from a modified computer-aided design (CAD) model of a combustion car, and the car used many of the same parts. The car's mass determines the forces that can be applied to the tires, how the car performs in longitudinal and lateral accelerations, cornering and braking. Since there was not yet a car to weigh, the mass was estimated in Table 2.1 by taking the weight of the existing internal combustion engine (ICE) car, subtracting the weight of the Honda motor, and adding the weight of the

electric motor, controller, batteries, and boxes.

Parameter	change (kg)	total (kg)
2013 ICE car	0	227
remove ICE	-68	159
add motor	+52	211
batteries	+91	302
driver	+91	393
controller	+7.5	400.5
chassis weight	+7.5	408
Total		408

Table 2.1: the major mass factors in the estimated differences between the original ICE and much heavier EV version of the VMS race cars. The volume of batteries needed in an EV required a larger chassis, adding more steel members, increasing the chassis weight.

2.2 Drivetrain

The objective of the drivetrain is to apply maximum force to the tires without slipping, and reach the maximum desired speed on straightaways. The drivetrain adjusts the motor RPM speed range to the desired track RPM range, transfers the motor forces to the wheels, and consists of all mechanical components from the motor's rotor shaft to the tires. The drivetrain design is crucial to the car's performance from rest to maximum speed. In this section, I discuss the design of the drivetrain with mechanical components and efficiency calculations.

Just after the car launches from rest, a weight load transfers backwards over the rear tires, increasing the normal force on the drive wheels. This is the maximum force that can be applied to the tires. The motor's torque provides the maximum force from launch. The motor force value is usually different from the maximum tire frictional force, and the two

forces are matched with a gear reduction. The car must also accelerate to the maximum speed of 105 kph as fast as possible.

Figure 2.4: rear of car, view of drivetrain components, including chain drive, rear sprocket used in gear reduction, differential, half shafts.[16]

A smaller sprocket is fastened to the rotor of the electric motor, using a chain to drive a larger sprocket fastened to the Torsen limited-slip differential as shown in Figure 2.4. The gear reduction scales the torque and power to the desired values for frictional force and top speed using light weight aluminum sprockets and a motorcycle chain. Decreasing the

diameter of the smaller front sprocket results in significantly greater losses. This is due to greater articulation angles the chain links must move through. The work done is the product of the force (chain tension) and the distance (articulation angle). Smaller sprockets mean the chain tension must be greater and possess a greater articulation angle. Therefore, the losses are greater and the gear reduction is much less efficient.[4][17] Thus, the minimum usable front sprocket has 14 teeth.

The rear sprocket size is constrained by the maximum desired speed of 105 kph, the angle of the halfshafts, and sprocket clearance from the chassis. A greater gear reduction decreases the maximum top speed, and defines the minimum rear sprocket size (shown in Table 2.2). The halfshaft manufacturer specified the maximum angle allowed as 14° from parallel. As shown in Figure 2.4, the clearance of the sprocket from the rear bulkhead is as close as possible, and limits using a larger rear sprocket, increasing gear reduction. Therefore, the maximum rear sprocket has 44 teeth, giving a gear reduction of 3.143/1.

Since the race car is rear wheel drive, both of the wheels are connected to half shafts embedded in the limited slip differential. This allows each wheel to be driven independently, depending on the angle of the direction of travel. Either wheel can rotate faster than the other through a turn, which is ideal to deliver the maximum dynamic loads to each wheel.

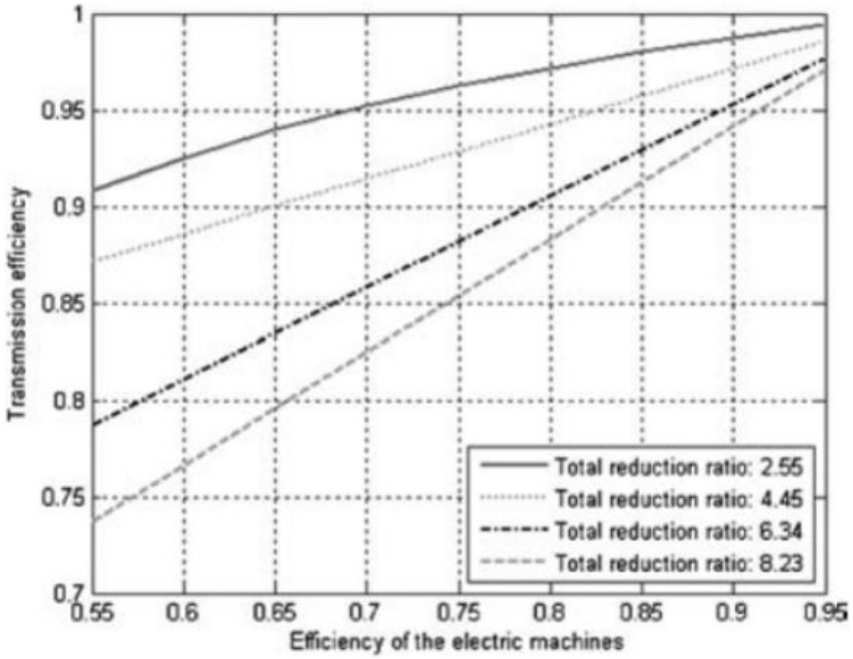

Figure 2.5: Transmission efficiency versus motor performance, efficiency decreases as gear reduction increases, a design trade-off between performance and efficiency. The 3.143/1 gear ratio VMS used is constant, and would lie between the top two lines. The motor efficiency varies from 74% to 94%. Thus, the total transmission efficiency varies from approximately 95% to 99%.[18]

The total mechanical efficiency from the rotor to the wheels is calculated from the product of all mechanical losses of each component in the drivetrain. The efficiency of a small drive sprocket, chain, and a larger driven sprocket is estimated at 96 to 99% for speeds less than 121 kph.[19] The efficiency validates the transmission efficiency findings in Figure 2.5. The estimated maximum speed is 105 kph, so this efficiency figure applies for all dynamic events. The worst case efficiency is assumed because it is easier to decrease power delivered in the controller settings than to add more power when designs are finalized. The differential manufacturer does not provide an efficiency value, but a typical passenger car differential is 97% efficient and the drive axle (halfshaft) is 98% efficient.[20] A differing

opinion is that differentials do not lose efficiency in longitudinal acceleration, only lateral acceleration.[16] Both halfshafts are 13°, creating additional losses of approximately 2.6% per halfshaft.

$$\eta = (chain)(differential)(halfshafts)(1 - 0.026)^2 \times 100\% \tag{2.1}$$

$$\eta = (0.96)(0.97)(0.98)(0.974)^2 \times 100\% = 86.6\% \tag{2.2}$$

From the motor to the wheels, the maximum force from the motor is:

$$f_{wheels} = 400(Nm)(0.866) = 346(Nm) \tag{2.3}$$

The Remy motor counter EMF equation indicates that under load, the maximum RPM is:

$$current(A) = I = \frac{200V_{DC} - \epsilon}{R(\Omega)} \tag{2.4}$$

$$\epsilon = \frac{80V_{DC}}{1kRPM} \tag{2.5}$$

$$RPM_{max} = \frac{200V_{DC}}{80V_{DC}} = 2,500RPM \tag{2.6}$$

The drivetrain was designed for the worst efficiency, but the maximum efficiency needs to be calculated with a dynamic load transfer.[5]

$$\eta_{max} = (chain)(differential)(halfshafts) \times 100\% \tag{2.7}$$

$$\eta_{max} = (0.99)(1.0)(0.98) = 97.0\% \tag{2.8}$$

$$f_{wheels} = 410(Nm)(0.970) = 398(Nm) \tag{2.9}$$

When the car is static, the amount of mass on the rear wheels is a product of the total mass and the front to rear weight bias. The load transfer equation in Figure 2.6 is used to determine the dynamic load over the rear wheels.

$$Weight_{total} = Weight_{rear} + \Delta(W) = W_T\left[\frac{l_F}{L} + \frac{acc_x}{acc_g}\frac{h_{cg}}{L}\right] \tag{2.10}$$

$$= 408\left[\frac{1.01m}{1.68m} + \frac{6.15\frac{m}{s^2}}{9.81\frac{m}{s^2}}\frac{0.33m}{1.68m}\right] = 296kg \tag{2.11}$$

The variable acc_x is the maximum longitudinal acceleration in OptimumLap simulations.

$$f_{friction} = \mu N = (0.8)(W_T)(g) = (0.8)(296kg)\left(9.81\frac{m}{s^2}\right) = 2323N \tag{2.12}$$

The value 2323 N is the maximum possible force that can be applied to cold tires.

$$Torque_{maxtires} = (f_{friction})(radius_{wheel}) = (2323N)(0.2507m) = 630Nm \tag{2.13}$$

$$Torque_{maxmotor} = \frac{Torque_{maxout}}{(\eta)(gearred.)} = \frac{(630)}{(.866)(3.143)} = 232Nm \tag{2.14}$$

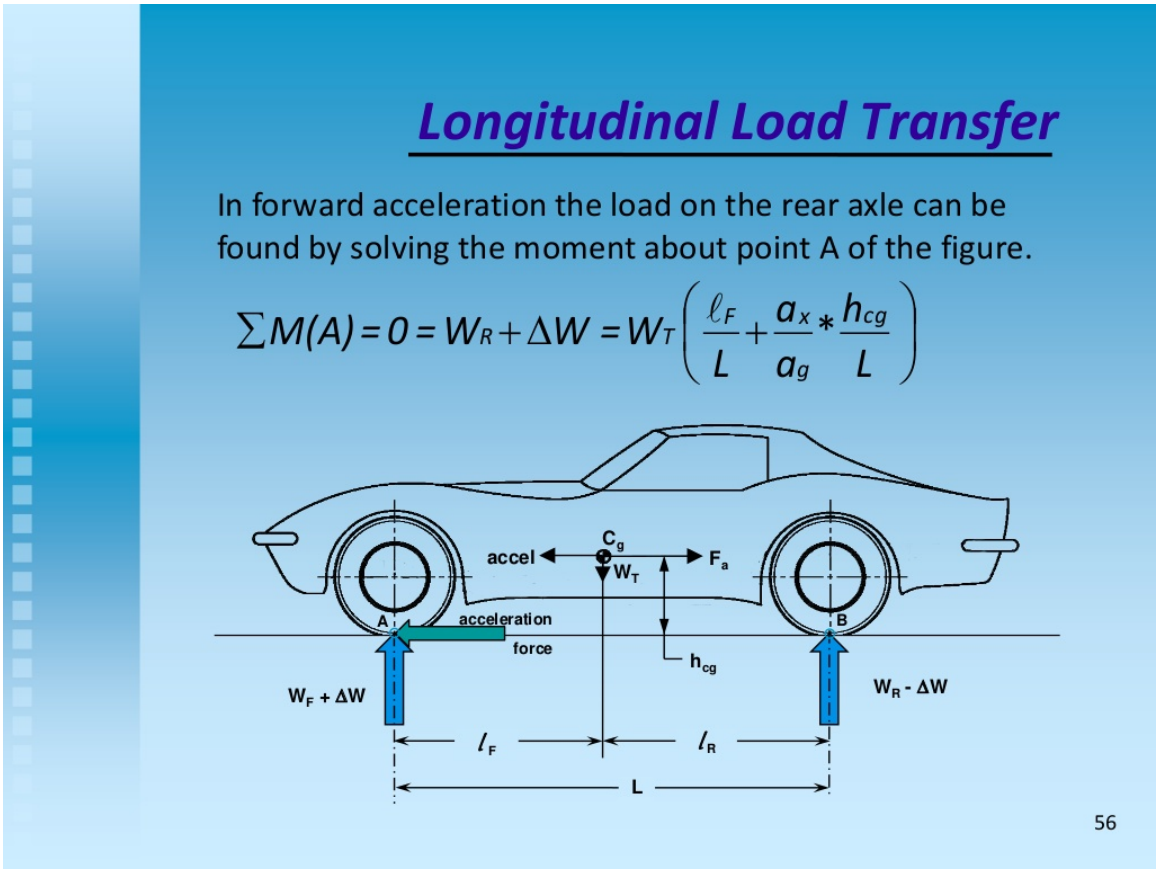

Figure 2.6: the variables used in calculating the dynamic load transfer on the rear axle during forward longitudinal acceleration.[21] This determines the maximum normal force over the drive wheels.

An OptimumLap simulation was made for the Acceleration Event, varying the gear reduction for performance using a Remy motor. Shown in Table 2.2, setting a maximum 3500 RPM at a 3.143/1 gear reduction and a 2.214/1 gear reduction, the Acceleration times were 5.39 and 5.36, respectively. OptimumLap does not have settings for electric motors and the counter EMF. A simulation was done that incorporated the counter EMF findings of a 2,500 RPM maximum motor speed, decreasing the top speed to 75.1 kph.

$$2500\frac{(rev.)}{(min)}\frac{1}{3.143(gear)}\frac{(60min)}{(1hr)}\frac{(2)(\pi)(0.2507m)}{(1rev.)}\frac{(1km)}{(1000m)} = 75.1\frac{km}{hr}(kph) \quad (2.15)$$

Max RPM	Gear Ratio	Time (sec)	Reasoning
3500	3.143/1	5.39	before RPM limitation
3500	2.286/1	5.36	improved gears for max RPM
2500	3.143/1	5.47	includes counter EMF, current gear used
2500	2.214/1	5.35	includes counter EMF, decreased gearing

Table 2.2: OptimumLap parameters modified in Acceleration to incorporate counter EMF settings to obtain ideal track time.

A 31 tooth rear sprocket with a 2.214/1 gear ratio completed Acceleration in 5.35 seconds, and the 44 tooth, 3.143/1 gear ratio completed it in 5.47 seconds. The 2.214/1 gear reduction was 2.24% faster, and had a top speed of 80.2 kph versus the 73.1 kph for the 3.143/1 gear reduction. This data was known, but the sprocket set that VMS had was the 3.143/1 gear reduction. Therefore, unless all the other tasks were completed before the 2014 competition, the 3.143/1 gear set would be used for the 2014 car and the performance would be sacrificed by 2.24% in Acceleration. The motor's rotor was machined for the smaller sprocket, and changing that sprocket could take much more time than replacing the larger sprocket. The larger 44 tooth sprocket was custom machined and had a custom bolt pattern. VMS did not have a teammate with experience to machine a new one, as machining sprocket teeth is fairly complicated. Also, there was no documentation on where it was machined or by whom, and the project would be time-intensive. The work load for designing, machining, building and testing everything on the car was too great to optimize just one sprocket. A different larger sprocket did not get machined and we used the 3.143/1 gear set. The gear ratio had been calculated and could be improved by 2.24%, but it would need to be done in the future.[5]

The VMS combustion engine has a transmission with six gears, adding weight, more

mechanical parts, and complexities of the driver shifting gears. Electric motors have a high torque from rest, allowing use of a single gear reduction to eliminate multiple gears, saving weight and time required for shifting. During testing, if the tires slip, the motor controller's maximum torque setting would be decreased until slip is eliminated, achieving maximum performance. If there is excessive slip, the gear reduction is too great, and a lesser gear reduction is necessary for better performance. In this case, the advantage of a lesser gear reduction is a greater top speed, greater acceleration near the top speed, and better times in Acceleration. The design for the drivetrain incorporated the maximum static force at rest, the motor's top speed, and the maximum drivetrain losses, resulting in 173 Nm of torque at each wheel.[5]

2.3 Tires

The force applied to the tires is proportional to the force available from the motor after a gear reduction and mechanical losses. If there is significantly more force delivered to the tires than the greatest normal force, the motor is oversized and adds excess weight, decreasing performance. If the tires do not get close to the ideal operating temperature (93°C), they never apply their maximum amount of force to the track surface. Thus, the tires would be oversized and add unnecessary weight. Selecting an appropriate tire changes track performance, and the appropriate tire varies with competition events.

Seven different Formula SAE tires were available and compared in Table 2.3: four for 10 inch diameter wheels and three for 13 inch wheels. The ten inch wheels have

Tire Size (in)	**18x6**	**18x7.5**	**19.5x6.5**	**19.5x7.5**	**20.5x6**	**20.5x7**	**20.5x7.5**
Wheel Size (in)	10	10	10	10	13	13	13
Outer Diameter (in)	18.1	18.3	19.4	19.5	21.0	21.0	20.6
Tread Width (in)	6.2	7.5	6.5	7.5	6.0	7.0	8.0
Weight (lbs)	9	10	10	11	11	11	12
Cost (US$)	170	187	168	183	216	216	231

Table 2.3: all of the tires considered are Hoosiers made from the R25B rubber compound. The tires for ten inch wheels cannot be used because the smaller rotors do not provide enough braking force. The other tires will meet the forces expected from the motor, and are compared for qualitative differences.

approximately 40% smaller brake rotor area, and it was determined that a race car heavier than 180 kg would have too much mass for the smaller brake rotors.[4] This would result in poor braking performance, would not lock the brakes to pass the brake test at the Formula SAE competition, and the car would not be safe to drive. A greater outer diameter helps with accelerating to the maximum speed, also favoring the 20.5 inch tires.

The maximum amount of force applied to Formula SAE tires increases greatly with tire temperature. The cold tires at ambient temperature possess a coefficient of friction of μ = 0.6 to 0.8.[22] Hot tires at 93°C increase to μ = 1.5.[23] This is a simplification, as the tire forces are non-linear with changes in vertical forces, and the μ value decreases with an increasing normal load. Therefore, a wider tire (greater tread width) can accept more increase in normal force before reaching the limiting condition that occurs when the entire tread width is in contact with the pavement. This favored the wider seven inch and eight inch tires. Wider tires perform better only if the peak operating temperature is reached during the event.[4] This temperature is only reached during the Endurance and Efficiency

Event (400 points), and all of the other dynamic events (275 points) must be completed with cold tires. During Endurance it takes several minutes to reach the peak tire temperature. Lincoln has had hot weather above 32°C, favoring wider tires that can heat up more quickly, gaining more traction. The six inch and seven inch tires are $15 less per tire, decreasing the overall cost. All three of the 20.5 inch tires would work well and have advantages in different scenarios. The remaining variable for the final three tires considered was tire width; OptimumLap does not have a setting for tire widths and was not used. It was best to compromise between a wide tire and a narrow tire and use seven inch wide wheels and Hoosier 20.5x7" tires.

2.4 Motors

For Formula SAE autocross racing, a motor with a high torque output and a high power-to-weight ratio is desirable. High torque allows a race car to accelerate and decelerate quickly. This is particularly important for the longitudinal acceleration of Acceleration, Autocross, and Endurance and Efficiency events. All of the motors our team analyzed have high torque of at least 100 Nm, with maximum torque at zero revolutions per minute.[24][25][26] New motors are created every year by manufacturers with improved efficiencies, torque densities, and less weight. Hence, in 2014 and 2015, motor research was conducted to assess new or alternative motors and compare potential options to the current selection with calculations and simulations. If a potential motor performs significantly better in simulations and has greater overall design benefits, a new motor would be selected.

2.4.1 2014 Motor Models

Several constraints helped narrow down my search for a motor. The Formula SAE rules allow a maximum voltage of 300 V_{DC}, and a maximum power of 80 kW.[13] In general, no component should exceed the electrical limits provided on the data sheet, but the rules allow for exceeding the motor's maximum current and temperature ratings.[13] This does not appear to be an advantage, as the motor torque and power outputs are limited by the internal magnetic field, and increasing current beyond the datasheet specifications does not result in more torque or power. There are copper losses in the stator windings of AC motors and armature of DC motors, and the losses increase with temperature. For a temperature increase from 20°C to 140°C, the resistivity of the copper windings would increase from 1.59×10^{-8} to 2.32×10^{-8} Ωm, an increase of 46%.

$$R = \frac{(\rho)(l(m))}{A(m^2)} \tag{2.16}$$

ρ= resistivity (Ωm), *l*= total length of the conductor (m), *A* = cross-sectional area of the conductor (m^2).

Further temperature increase could create an overtemperature fault, damage the winding insulation, motor terminal insulation, conductors, or components connected to the high voltage cables in the motor controller. Due to the risks of motor and related component damage, we did not attempt to exceed the motor current ratings.

Some electric cars have multiple motors, a performance advantage from driving all four wheels. However, for simplicity, minimizing weight, and financial constraints, a single motor and a differential were chosen for delivering power to the rear wheels for the electric

race car. This constrained the maximum motor load to the finite frictional force on the rear tires from the mass of the car, solved in Equation 2.12. Once that was calculated, I researched different types of motors, including series DC motors and permanent magnet synchronous motors (PMSMs).

Different motor technologies are compared because their topologies, construction, and power generation vary greatly. The prospective motor's characteristics included: weight, torque and power curves, and efficiency. These were entered into OptimumLap and simulated for the Formula SAE events for lap times. Table 2.4 summarizes the characteristics of the two motors considered for the 2014 car.[5]

Motor make	**Remy**	**Netgain**
Motor model	HVH250-115S	TransWarp 7
Motor type	PMSM	Series DC
Number Poles (N-S)	10	2
Weight (kg)	52	50
Rotating Mass (kgm^2)	0.069	unknown
Cooling medium	oil	air
Max efficiency (%)	94	91
0 RPM efficiency(%)	74	unknown
Max bus voltage (V_{DC})	700	144
Max current	300 (A_{RMS})	340 (DC)
time at max current (sec)	30	unknown
Peak speed (RPM)	10500	3600
Peak torque (Nm)	400	100
Peak power (kW)	80	21
Continuous speed (RPM)	1800	unknown
Continuous torque (Nm)	270	unknown
Continuous power (kW)	60	unknown
Torque-to-weight ratio Nm/kg	7.7	2.0
Cost (US $)	3,800	2,260
Skid-pad time (s)	5.84	6.82
Accel. time (s)	6.28	8.57

Table 2.4: 2014 Potential motor comparison, the ideal motor has high power and torque, low weight. Many motors were researched, but most were not good candidates due to being very heavy or having too little power. All data is from datasheets except the last three lines. The peak power is limited by the 200 V_{DC} value of the battery pack and the controller to 60 kW, any value above that is not usable. The torque-to-weight ratio is a factor used to quickly compare the torque densities of the motors.[5]

2.4.2 Series DC Motors

Because of their simple controls and low cost, DC motors have been utilized in electric racing since at least 2000 in the White Zombie electric drag race vehicle.[27] However, DC motors are not as efficient as other types, and there are motors with greater torque and power densities. DC motors have brushes, which wear down over time and need to be replaced, increasing maintenance. When the brushes wear, they emit a carbon dust that could ignite

under high temperatures.

Regenerative braking is not available in DC motors, which is a drawback because it can increase the range of passenger EVs by about 10 to 15%[28], possibly more in racing. Regenerative braking also increases the efficiency score at the Formula SAE competition.[13] It is possible that the increased range from regenerative braking would allow for scaling down the battery pack 15% or more and decrease weight, creating faster lap times.

The Netgain TransWarp 7 series DC motor was researched and its characteristics were compared and simulated against other performance electric motors. The motor costs $2,260, $1,540 less than the Remy motor, weighs 50 kg, 2 kg lighter than the Remy, but had less torque and power. Low torque can be compensated with a greater gear reduction if the peak RPM is high, but the motor peaked at 3600 RPM, limiting the performance at either 0 RPM or top speed. The motor had slower times in Skid-pad by 16.8% and Acceleration by 36%, and is 58 cm in length, too large for the chassis without completely redesigning the chassis and suspension arms. Also, the motor does not have any sensors to monitor the rotor position, which is vital to get feedback and monitor variables such as torque and speed. It is possible to add external sensors for measuring the RPM, current, and voltage, but these added complications that would require much more time. Due to the low torque, low RPM range, and significant weight resulting in decreased performance, I did not select the Netgain TransWarp 7 series DC motor for the 2014 car.

2.4.3 Permanent Magnet Synchronous Motors

Permanent magnet synchronous motors (PMSMs) are the most common motors implemented in production electric vehicles. In this section, I discuss the differences in the rotor, the role of the magnets, and the characteristics of the Remy HVH250-115S motor.

There are two types of AC PMSMs: surface-mount permanent magnet motors and internal permanent magnet motors. Surface-mount motors are less expensive to manufacture because they use adhesive to mount the magnets in place instead of embedding the magnets within the rotor, shown in Figure 2.12. A drawback is surface-mount motors are not as mechanically robust, especially at greater motor speeds. Interior permanent magnet motors are more complicated to manufacture, making them more expensive. The motors have magnetic saliency, meaning the inductance varies at the motor terminal depending on the rotor position due to the magnets in the rotor.[29]

Cogging torque is the interaction of the magnetic poles to the teeth (steel structure) of the laminations.[30] At low speeds just above rest, the magnetomotive force from the magnets is much greater than the reluctance force generated by stator current. As a result, some PMSMs can feel jerky, as the rotor "clicks" from pole to pole. As the inductance varies, the reluctances are unequal. The variation in inductances can generate a smooth torque output by shaping the motor currents in the controls software.[28]

The three phases, abc, are modeled in two dimensions shown in Figure 2.7 as a dq reference frame locked to the rotor because the phase labels a,b, and c are no longer the reference. Thus, it's not the significance of the phase label, just the proximity to the nearest

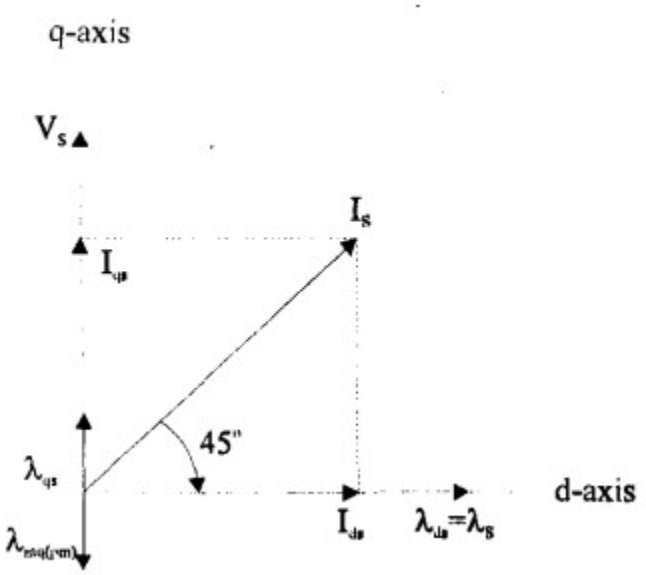

Figure 2.7: The two-dimensional dq-axes representing the q-axis, torque producing current, and d-axis, field weakening current.

phase "firing" current and the rotor position in relation to that phase. In the rotor, space occupied by a magnet is in the d-axis, the flux direction, and iron in the q-axis, which lags behind 90°.[28] To simplify, the i_q current produces torque, and i_d current produces field weakening.[31]

Field weakening allows the rotor to rotate faster than base speed, producing the rated power by lowering the field flux, alleviating some counter EMF. Once the counter EMF is decreased, a greater current flows to increase the speed range of the motor. The d-axis and q-axis have a large difference in inductance[28], allowing internal PMSM to exploit field weakening settings. Field weakening creates a potential advantage for PMSMs to have a greater top speed and power at high RPMs.

The PMSM rotor varies from other motors. Rare earth magnets increase the flux density in the air gap, increasing the motor power density and torque-to-inertia ratio. If the

motor's rotor exceeds the temperature limit, the magnets are at risk for demagnetization. In neodymium-iron-boron magnets, the flux density increases with temperature, and the temperature limit is high, as it varies from 100°C to 180°C. This is the magnet composition with the greatest flux density at 1.25 tesla (T), and a composition used in PMSMs[28], but none of the motor manufacturers researched disclosed their exact rotor magnet composition. In the Remy HVH250-115S motor, the magnet over-temperature rating is the same as the stator winding insulation temperature rating, 165°C.[25] Unless there is much unexpected heat, it was not anticipated there would be overheating issues in the motor. Remy Motors states permanent magnets deliver higher performance at higher cost, while induction rotors offer moderate performance at a lower price.[24]

The Remy HVH250-115S PMSM utilized a unique, proprietary rectangular "high voltage hairpin" stator winding to fit a larger conductor in the same space to generate greater torque density. As shown in Figure 2.8, the hairpins interlock and "produce a superior slot fill, up to 73% versus 40% for typical round-wire windings.[24] Therefore, the length to wrap around 180° from one turn to the next is less, and this reduces heat, increases torque 27% and power 34%, compared to similar sized PMSMs. Also, the volume was reduced 22%, and the mass reduced 13%. The rotor has interior-buried permanent magnets, which is a more robust mechanical design that is less likely to suffer from magnets chipping.

Figure 2.8: Remy HVH250 cutaway, internal permanent magnet rotor and stator with rectangular windings for increased torque density.[32]

The Remy PMSM was researched and its characteristics such as mass, cost, and simulated track times were compared to other performance electric motors. The motor costs $3800, $1,540 more than the Netgain motor, and is 2 kg heavier at 52 kg, but has four times as much torque, more than any motor researched. The motor had the fastest simulated time in Skid-pad and the Acceleration event. An internal resolver is built into the motor for measuring the rotor position and temperature of the stator windings, which is ideal to obtain feedback and monitor variables such as torque and speed. Due to the high torque, track simulation performance, and internal sensors, I selected the Remy HVH250-115S PMSM for the 2014 car.

$$Torque = T_e = \frac{3P}{2}[\lambda_f i_q + (L_d - L_q) i_d i_q] \tag{2.17}$$

From Equation 2.17, the number of pole pairs is P, λ_f is the flux linkage, L_d and L_q

are the inductances when modeling phases a, b, and c into the two-dimensional dq plane. Within the brackets, the first part is the product for torque generated by the magnets, and the second part is the reluctance torque generated by the stator current.

$$P = 10, \lambda_f = 7.1mWb, T_e = 410Nm, i_q = 425A_{RMS}, i_d = 0 - 425A_{RMS} \tag{2.18}$$

At peak torque, all of the variables are known except L_d, L_q, and i_d. Remy does not provide the values for L_d and L_q, but the maximum values are fixed, and i_q is the field weakening current, an adjustable parameter set from 0 to 425 A_{RMS} in the controller's software.

The torque and power parameters of the Remy motor are limited by the voltage and current. The voltage used was 200 V_{DC}, and the maximum current of the Remy is 300 A_{DC} (425 A_{RMS}). Therefore, the maximum torque is the same value regardless of voltage, but the torque "breaks" at a lesser RPM due to the counter EMF shown in Figure 2.9. In Figure 2.10, the maximum power scales linearly with the maximum voltage, and the maximum power at 200 V_{DC} is 50% less than the voltage at 300 V_{DC}. In Figure 2.11, it shows from launch to peak torque the motor is 74% efficient. But, as the RPMs increase, the efficiency increases to a maximum of 94% at 2000 RPM, which was greater than the other motor researched.

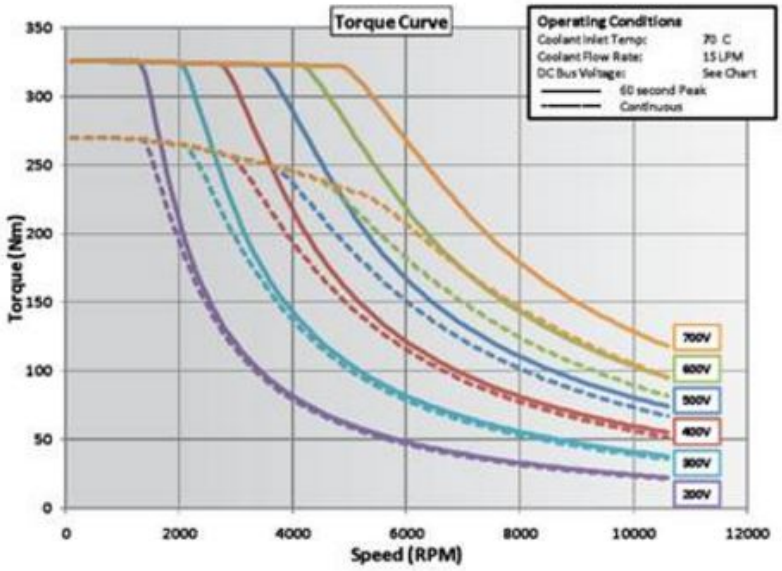

Figure 2.9: Remy PMSM Torque Curve, maximum torque is possible to 5000 RPM at 700 V_{DC}(orange), rules allow for 300 V_{DC}(aquamarine), we used 200 V_{DC}(purple), and torque "breaks" at 1400 RPM, using much less of the possible torque area, decreasing acceleration and limiting the motor's performance.[24]

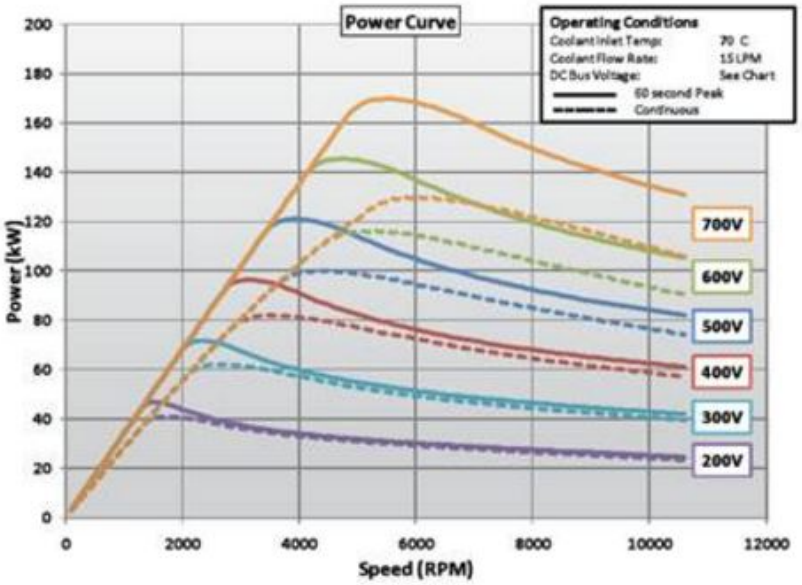

Figure 2.10: Remy PMSM Power Curve, maximum power possible is 170 kW at 5500 RPM and 700 V_{DC}(orange). Rules allow for 300 V_{DC}(aquamarine), peaking at 70 kW and 2200 RPM. 200 V_{DC}(purple) was used, and torque "breaks" at 1400 RPM, using much less of the possible power area, decreasing acceleration and limiting the motor's performance.[24]

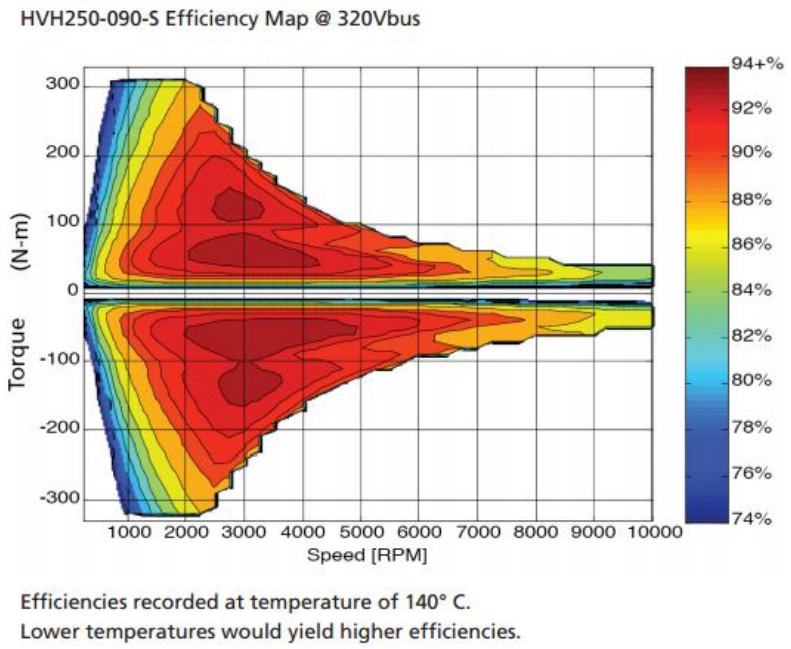

Figure 2.11: Remy HVH250 motor efficiency, the speed range is 0 to 2500 RPM, resulting in efficiencies ranging from 74% to 94%. Notice the footnote that this is recorded at 140°C, and is improved at lower temperatures, the efficiency in the race car could be greater.[25]

2.4.4 2015 Motor Models

For the 2015 competition, new motors were considered for improved performance in all of the Formula SAE dynamic events. The current motor (Remy HVH250 PMSM) performed adequately, but is heavy in comparison to other motors (Table 2.5). Thus, alternative motors were discovered and simulated in OptimumLap for potential use in the race car.

The main characteristics considered for the 2015 motor include the torque, power, maximum RPM, motor weight, torque density, efficiency, and cooling. Other considerations include the counter EMF waveform, cogging, torque ripple, and field weakening. I considered several motors, weighing the advantages and disadvantages of each type. A motor was

selected with the best combination of characteristics, and simulated track performance.[5]

For the 2015 electric race car, three new models of motors and the Remy motor used in 2014 were considered. The Remy, Emrax, and Parker data were taken from datasheets[1][2][33] and key specifications are summarized in Table 2.5. The GM induction motor did not have an accessible datasheet, only a document with a couple of specifications.[34] Since a GM eAssist induction motor was available, it was bench tested at Rinehart Motion Systems and results entered. In this section, I compare the characteristics of the four different motors.

Motor make	Remy	GM	Emrax	Parker
Motor model	HVH250-115S	eAssist	228	GVM210-050J
Motor type	PMSM	Induction	PMSM	PMSM
Number Poles (N-S)	10	8	10	12
Weight (kg)	52	15	12.3	25
Rotating Mass (kgm^2)	0.069	unknown	0.0421	0.00824
Cooling medium	Dexron VI oil	water	water	water
Max efficiency (%)	94	75	96	unknown
0 RPM efficiency(%)	74	unknown	86	unknown
Max bus voltage (V_{DC})	700	115	450	350
Max current (A_{RMS})	300	306	340	234
Time for max current (sec)	30	30	120	unknown
Peak speed (RPM)	10500	4000	6500	8000
Peak torque (Nm)	400	70	240	79
Peak power (kW)	80	25	100	58
Continuous speed (RPM)	1800	unknown	5000	6166
Continuous torque (Nm)	270	unknown	38	125
Continuous power (kW)	60	15	42	32
Torque-to-weight (Nm/kg)	7.7	4.7	19.5	3.16
Cost (US$)	3,800	*480	3,200	6,270
Skid-pad time (s)	5.84	9.02	5.93	6.75
Accel. time (s)	6.28	11.44	6.27	8.14

Table 2.5: 2015 comparison of different motor characteristics, the Remy was used in the car in 2014. All data is from datasheets except the last three lines. The peak power is limited by the 200 V_{DC} value of the battery pack and the controller to 60 kW, any value above that is not usable. Overall, the motors were much lighter but still powerful, DC motors were eliminated from consideration and replaced with PMSMs. All of the motors have feedback sensors for temperature, rotor position and speed.
*The GM eAssist motor is not available for purchase from GM, it is only available in GM production cars from 2007-2014.
**The Remy is able to use oil cooling, but we did not use oil or any cooling.

2.4.5 Induction Motors

Induction motors have advantages and disadvantages in their physical characteristics and total costs. As shown in Figure 2.12, the rotor component of the motor does not use rare-earth magnets, but more abundant elements such as aluminum. Tesla Motors is the only automotive manufacturer known to use induction motors, and implements a proprietary

induction motor with a copper rotor with approximately half the electrical and thermal resistivity of aluminum.[35] As the motor's speed increases, the friction, windage, and stray losses increase. However, at greater speeds, the motor's core losses decrease, making the rotational losses constant.[36] Both induction and permanent magnet synchronous motors (PMSM) have stator copper losses and core losses, but only induction motors have rotor copper losses. Induction motors cost less and have less cogging torque because there are not permanent magnets in the rotor.[28]

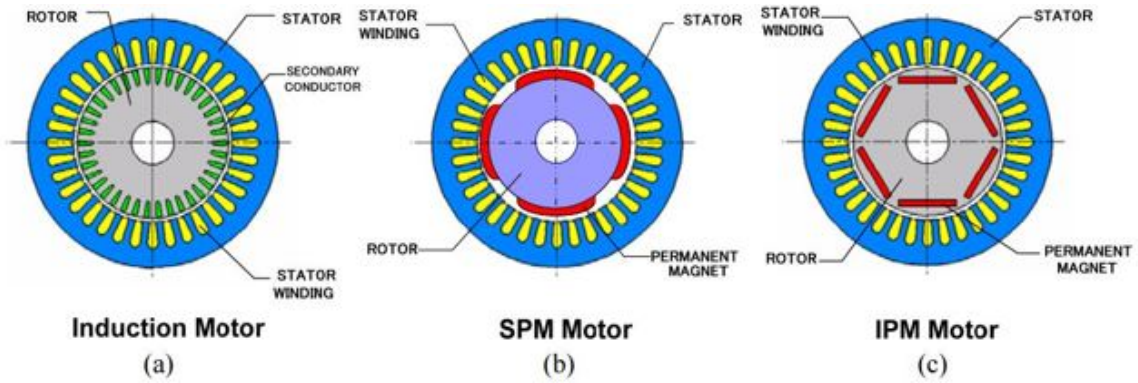

Figure 2.12: cross-sectional views of AC motors, including induction, surface-mounted permanent magnet, and interior-buried permanent magnet. Note the stator windings are similar, the differences are in the rotors.[29]

Figure 2.13: GM eAssist induction motor cutaway of motor housing showing stator windings and rotor cage with aluminum bars, which varies from the smooth exterior of the Remy PMSM.[37]

2.4.6 GM eAssist Induction Motor

A GM induction motor was researched and its torque, power, speed range, cost, and efficiency were compared to other performance electric motors. The skin effect results in AC conductors, and as frequency increases the current concentrates near the outer surface of the conductor.[36] At electrical frequencies, especially those greater than 300 Hz, there are additional losses from the skin effect.[38] The maximum RPM of the motor is 4000 RPM and solved for the electrical frequency in Hertz (Hz), f_e:

$$f_e = \frac{(n_{sync})(P)}{120} = \frac{(4000RPM)(8)}{120} = 267Hz \tag{2.19}$$

n_{sync}=maximum speed (RPM), P=number of pole pairs.

At the maximum speed, the motor speed is 60% greater than the Remy motor, and is within 11% of 300 Hz. The motor likely starts to experience additional losses from the skin effect.

The eAssist motor was discontinued and not commercially available for purchase new. The motor can only be found in 2007-2014 GM hybrid vehicles, or possibly from second-hand sellers. Because these motors can only be obtained as used models, it is not a fair comparison to directly match their cost against that of new motors. Also, the motor would probably not have a warranty or customer support for this application that GM did not authorize. The motors have been purchased from $105 to $480, which is 85% to 92% less than all three of the other motors. As shown in Figure 2.13, the motor is the second lightest at 15 kg, but it produces significantly less torque and power, resulting in an 82% slower time than the best in Acceleration and 54% slower time in Skid-pad. Due to the simulated track performance and motor characteristics, I decided not to select the GM eAssist induction motor for the 2015 car.

2.4.7 Parker GVM210-050J PMSM

The Parker GVM210-050J PMSM motor was researched, and its torque, power, speed range, cost, and efficiency were compared to other performance electric motors. The motor costs significantly more than the others at $6,270, $2,470 more than the second most expensive motor. This motor is the second heaviest, 25 kg, which is 12.7 kg heavier than the lightest

motor. The Parker motor had a relatively low torque at 79 Nm, but could develop 58 kW of power, close to the maximum 60 kW of the motor controller. In the OptimumLap simulations, the motor was 15.6% slower than the Skid-pad leader, Remy, and 30% slower than the leading Emrax in the Acceleration event. Due to the high cost and simulated track performance, I did not select the Parker GVM210-050J PMSM for the 2015 car.

2.4.8 Remy HVH250-115S

The Remy PMSM was compared to three different motors for use in the 2015 car. This is the same motor used in 2014, and there are advantages to using a motor the team is familiar with: it saves time in designs, we do not have to change motor data on all of the documents, it is track proven and predictable. The cost is $3800, $2470 less than the Parker motor, but $3,380 more than the GM motor and $600 more than the Emrax motor. This motor is the heaviest at 52 kg, but has at least 160 Nm more torque than the other motors researched. The motor had the fastest simulated time in Skid-pad and was .01 seconds (0.04%) slower in the Acceleration event. The motor has a resolver for measuring the rotor position and temperature of the stator windings, which is ideal to obtain feedback and monitor variables such as torque and speed. Due to all of these characteristics, the Remy was our second choice behind the Emrax. There was not enough time to make such a major design change, so we used the Remy HVH250-115S PMSM for the 2015 car.

2.4.9 Emrax 228

The Enstroj Emrax 228 motor was researched and its characteristics were compared to other performance electric motors. The Emrax was the first axial flux motor researched, the previous motors were radial flux motors. As shown in Figure 2.14, the axial flux motor has magnetic flux lines parallel to the rotor and shaft, radial flux lines are perpendicular to the rotor and shaft.[39]

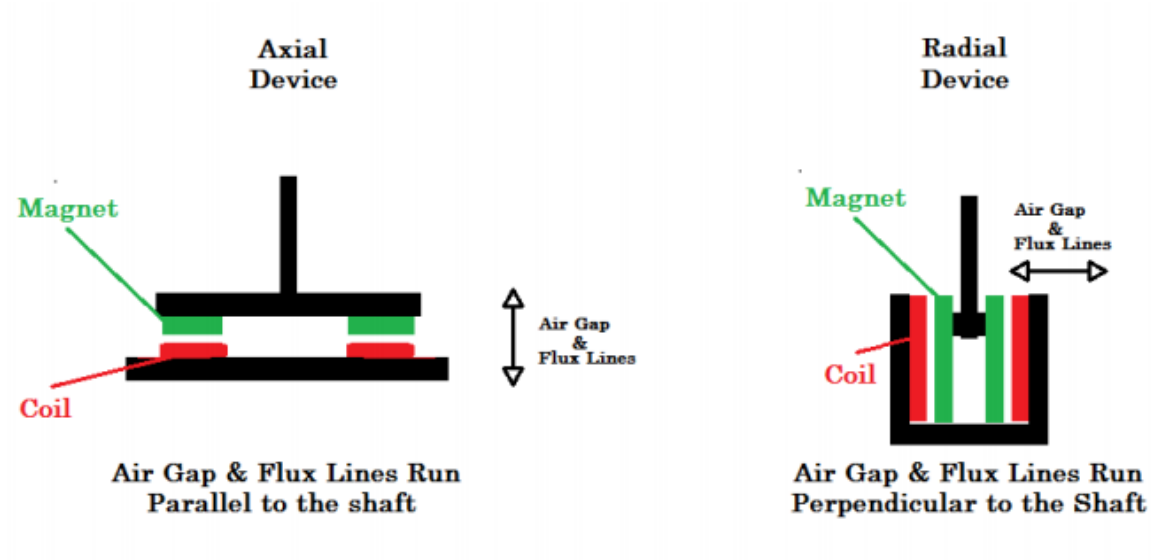

Figure 2.14: Axial flux versus radial flux. Under conditions with a high number of poles and width to diameter ratio, axial flux has a greater power density than radial flux motors.[39]

The axial flux motor topology has electromagnetic advantages over radial flux motors. Axial flux eliminated torque cogging, as the rotor spins smoothly at low speeds just above 0 RPM, and a traditional radial flux motor jolts from pole to pole. When the number of poles is ten or more, and the width to pole ratio is <0.3, this motor topology can provide both a greater torque and greater torque density than radial flux permanent magnet motors.[40] The

Emrax motor width to pole ratio is solved in Equation 2.20[2]:

$$\frac{width(mm)}{diameter(mm)} = \frac{86(mm)}{228(mm)} = 0.377 \tag{2.20}$$

This suggests the torque would be 140 Nm. The Emrax motor achieves 240 Nm, exceeding those findings. The torque density is 19.5 Nm/kg, compared to the 7.9 Nm/kg of the Remy. The Remy requires a thick metal outer casing on the outer diameter to provide a rigid housing for the motor, and the Emrax rotor rotates about the outside of the motor. Therefore, the Emrax motor requires only a thin scatter shield of metal on the outer diameter, saving significant weight. These factors all favor the axial flux Emrax motor over the radial flux Remy motor.

The motor costs $3,070 less than the Parker and $600 less than the Remy, but $2,720 more than the GM motor. This motor is an axial flux PMSM, and is 86% efficient from 0 RPM, 12% more efficient than the other motors. The efficiency is up to 96% between 1500 and 3500 RPM. The Emrax motor is the lightest and creates 240 Nm of torque, second to only the Remy, but one-fourth of the weight. In the OptimumLap simulations the motor was 1.5% slower than the Skid-pad time leader, Remy, and the fastest in the Acceleration event by 0.16%, ahead of the Remy. Due to the affordable cost, extremely light weight, and high performance in the track simulations, the Emrax 228 radial flux PMSM would have been the ideal selection for the 2015 car. However, this motor was not used due to time constraints, and the Remy motor was used.

2.5 Motor Controllers

Motor controllers are paired with every motor to accept inputs such as the analog throttle signal, fault signals, and drive electrical power to the motor by controlling a sinusoidal or pulse width modulated high powered signal. The automotive application is challenging for controller electronics because there is a large variation of work load, temperature changes, and acceleration in multiple directions. Therefore, the controller needs to be reliable, robust in challenging conditions, and powerful. Ideally, the controller is versatile for various motors such as induction and PMSMs, maximizes the power output of the motor, and is lightweight. In this section, I discuss the characteristics of various power devices, and the motor controller selected.

2.5.1 Power Transistors

Each of the various power devices used in motor controllers has specific characteristics.[28] The power devices are vital to the performance of an electric race car, and if one fails the competition is likely over for that car. The desired power device does not require a high frequency, as a low switching frequency below 20 kHz is enough for the greatest motor speed. The power device has a short duty cycle as there are multiple devices switching on and off and the maximum power time period is less than 7 seconds. The device must have a high voltage of 150 to 300 V_{DC}, and a high current up to 300 A_{DC}. This narrowed the selection to insulated gate bipolar transistors (IGBTs) and metal oxide semiconductor field effect transistors (MOSFETs).

2.5.2 IGBTs versus MOSFETS

In the late 1990's, the inexpensive, original Curtis DC motor controller models utilized MOSFETs to drive 500 A_{DC} peak to the motor, but limit the nominal voltage to 144 V_{DC}.[41] Newer generations of MOSFETs are proven, capable devices for breakdown voltages below 250 V_{DC}. MOSFETs prevent thermal runaway, as they have a positive temperature coefficient. The steady state losses are less, and there is a body-drain diode for free-wheeling currents. IGBTs have a negative temperature coefficient, and if pushed to the temperature limitations, could create a thermal runaway. There is some debate between IGBTs and MOSFETs for the breakdown voltage range 250 to 1000 V_{DC}.[42] At this time, IGBTs tend to provide better performance for voltages greater than 250 V_{DC} with short duty cycles. MOSFETs are more efficient in minimizing conduction and switching losses at frequencies greater than 50 kHz, but the losses are much closer at frequencies below 50 kHz, the range for this application. The newer, higher-end controller models use IGBTs to reach the 80 kW max limitation[13], and are water-cooled to prevent thermal runaway. Motor controllers with IGBTs are preferred.

2.5.3 RMS PM100DX AC Motor Controller

AC controllers require advanced feedback control and setup, but deliver a much greater power-to-weight ratio and performance. The DC current is inverted to a sinusoidal waveform. Flux weakening enables a constant power mode by applying a stator flux in opposition to the rotor magnet flux, allowing for smooth torque output.[28] In the case of a short-circuit

fault, it is more likely that the motor power will simply fail to generate power, and not be a "runaway". The Rinehart Motion Systems PM100DX provides 100 kW peak power and is water-cooled by a patented heat exchange system (shown in Figure 2.15), regulating the IGBT temperatures.

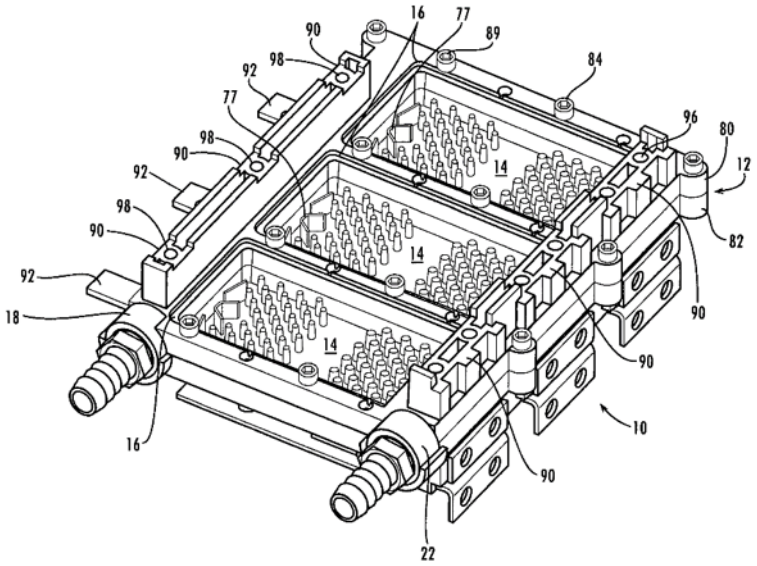

Figure 2.15: The RMS heat exchanger is a proprietary component with protrusions to maximize cooling.[31]

The controller is rated at 100 kW peak at 400 V_{DC}, continuous 200 V_{DC}, the power output is much less[31]:

$$P_{mech} = \frac{V_{DC}}{\sqrt{2}}\sqrt{3}A_{RMS}PF\eta_{motor}(kW) \tag{2.21}$$

$$P_{mech} = (141.4)(\sqrt{3})(340)(0.8)(0.90) = 60kW \tag{2.22}$$

The controller can be used on either PMSMs or induction AC motors. The controller uses IGBTs, and the switching frequency is twelve kHz, much quicker than the maximum

RPM of the motors. The controller is 97% efficient, and 3% of all energy on the input is consumed as heat.[31] The value is not used in motor efficiency calculations, but is useful for modeling the battery pack for an accurate amount of energy for 22 km of racing. The RMS controller provides customizable variables on a graphical user interface (GUI), allowing us to quickly improve the performance by changing the variables in the controller software. A sample of the GUI is shown in Figure 2.16.

EEPROM List

Symbol	ADDRESS	VALUE
Ia_Offset_EEPROM	0x0126	2048
Ib_Offset_EEPROM	0x0127	2048
Ic_Offset_EEPROM	0x0128	2048
DC_Volt_Limit_EEPROM_(V)_x_10	0x0104	2900
DC_Volt_Hyst_EEPROM_(V)_x_10	0x0105	300
DC_UnderVolt_Thresh_EEPROM_(V)_x_10	0x0117	1500
Inv_OverTemp_Limit_EEPROM_(C)_x_10	0x0106	950
Mtr_OverTemp_Limit_EEPROM_(C)_x_10	0x0121	2000
Zero_Torque_Temp_EEPROM_(C)_x_10	0x015e	1400
Full_Torque_Temp_EEPROM_(C)_x_10	0x015d	1000
Accel_Pedal_Flipped_EEPROM_(0=N_1=Y)	0x0114	0
Pedal_Lo_EEPROM_(V)_x_100	0x0107	0
Accel_Min_EEPROM_(V)_x_100	0x0108	10
Coast_Lo_EEPROM_(V)_x_100	0x0109	20
Coast_Hi_EEPROM_(V)_x_100	0x010a	50
Accel_Max_EEPROM_(V)_x_100	0x010b	490
Pedal_Hi_EEPROM_(V)_x_100	0x010c	499
Motor_Torque_Limit_EEPROM_(Nm)_x_10	0x0110	600
Regen_Torque_Limit_EEPROM_(Nm)_x_10	0x0111	50
Braking_Torque_Limit_EEPROM_(Nm)_x_10	0x0112	150
Kp_Torque_EEPROM_x_10000	0x012d	100
Ki_Torque_EEPROM_x_10000	0x012e	4
Kd_Torque_EEPROM_x_100	0x012f	0

Figure 2.16: The RMS GUI allows the user to reprogram any parameter in the motor controller, quickly fine-tuning variables and maximizing performance. The parameters also allow for creating safety redundancies for protecting components and preventing exceeding limits for speed, temperature, and set limits for other faults.[31]

After bench testing the motor and before test driving the car, the torque and maximum RPM were set at a very low level to keep the driver and spectators safe. During the first track day at PIR, the car was test driven for several minutes at low torque. Once it was driven

for several minutes and inspected for mechanical quality, the torque and maximum RPM settings were increased, and it was driven faster to test the acceleration.

Parameter	Start	Final	Result
Motor Torque Limit (Nm)	160	450	increased torque, acceleration
Max Speed (RPM)	2000	4000	set max speed to 129 kph
Motor Overspeed Limit (RPM)	2500	5000	sets motor fault RPM for safety
Speed Rate Limit (RPM/sec)	1000	5100	increased motor speed quickly
IQ Limit (A_{RMS} peak)	150	425	increased torque-producing current
ID Limit (A_{RMS} peak)	120	425	increased field-weakening current
Motor Overtemp Limit (°C)	160	200	temp sensor error, overridden
Break Speed (RPM)	3000	1700	decreased per Remy datasheet
Regen Torque Limit (Nm)	30	50	increased regen braking
DC Volt Limit (V_{DC})	400	290	decreased to meet rules in regen
DC UnderVolt Limit (V_{DC})	150	120	per battery datasheet limits

Table 2.6: RMS GUI settings: modified torque and speed rates to gain performance, adjust fault parameters for safe operations of motor speeds, battery overvoltage and undervoltage.

The GUI settings were altered to improve the track times, shown in Table 2.6. The maximum speed was less than the setting, and the setting was a safety precaution as a redundancy to prevent a runaway car. The 290 V_{DC} setting is based on the rule requiring a 300V_{DC} maximum[13] during regenerative braking. The regenerative torque limit could be increased and fine-tuned, adding to the efficiency. The break speed is the speed on the datasheet when there is a "knee" in the torque curve, and the torque drops sharply from the maximum. The DC undervoltage limit prevents the battery pack from draining to a voltage less than 120 V_{DC}, possibly damaging the pack and violating the rules. The motor overtemperature setting was originally set to 160°C and was working fine, but it began to give a fault that would return after resetting it. The rotor was never getting close to the temperature limit, so it was not a concern, and it was set to 200°C, and the fault did not

return. Through these GUI settings, we were able to improve the performance of the car and set safe fault parameters.

2.6 OptimumLap Endurance Modeling

As the car's characteristics for the drivetrain, tires, and motor were defined, the car was modeled in OptimumLap for performance in several Formula SAE Endurance courses. Each Endurance course varied slightly in the average speed, percent accelerating, percent braking, and total length, shown in Table 2.7. This data was used to estimate the total energy use of the electric race car for the Endurance course.

Formula SAE Course	**Germany 2012**	**Mich. 2012**	**Lincoln 2012**	**Mich. 2014**	**Average**
Distance (m)	1424	1099	1170	1070	1206
Time per lap (s)	118.15	70.7	93.4	86.53	95.43
Total Laps	15	20	19	20	18.2
Actual Distance (km)	21.35	21.98	22.2	21.40	21.70
Total time (min)	30.4	23.6	29.3	29.7	29.0
Energy Use (kWh)	5.04	4.36	3.28	4.22	4.27
Average Speed (kph)	47.69	58.63	47.67	48.68	49.5
Acceleration %	68.45	73.9	50.95	65.44	64.75
Braking %	30.73	24.98	48.46	32.76	33.95

Table 2.7: OptimumLap Endurance modeling was conducted for various tracks to simulate the actual distance, lap times, braking, accelerating, and total energy use. The acceleration and braking percentages are close to 100%, but do not include the percentage for coasting.

During simulations, the race car's parameters remained constant, but there was some variation in the Endurance course simulations in terms of distance, energy use, average speed, percent braking, and percent accelerating. The average of the actual distances is only 1.4% less than 22 km. The energy use calculation is based on the energy to complete 22 km,

not the actual distances. Energy use varies drastically, and the Lincoln 2012 course required 54% *less* energy than the Germany 2012 course. However, the Germany 2012 course is 18% above the average energy use of 4.27 kWh. The Germany 2012 course did not produce the greatest average speed or possess the greatest acceleration percentage ratio, but the course required the most energy at 5.04 kWh, and that value will be used as an estimate for the amount of energy required for the electric race car.

Useful information can be estimated from calculations based on the data presented in the Endurance simulations. This includes time racing, continuous power, and the continuous current. The average power in kW can be calculated from the average speed in kph and the energy used in kWh.

$$time_{Endurance} = \frac{distance(km)}{speed(kph)} = \frac{22(km)}{47.7\frac{km}{hr}} = 0.461hr \tag{2.23}$$

The continuous power is the ratio of energy used to time racing:

$$kW_{continuous} = \frac{5.04(kWh)}{0.461(hr)} = 10.9kW \tag{2.24}$$

The continuous current is approximately the ratio of continuous power to the nominal voltage:

$$I_{continuous} = \frac{kW_{avg}}{V_{nom}} = \frac{10.9(kW)}{172.8(V_{DC})} = 63.1A \tag{2.25}$$

The continuous current is needed to properly size the high voltage components. The main fuse, high voltage conductor size, and related components in the high voltage path are determined by this value.

2.7 Batteries

The considerations for batteries are the cell current output, energy density, cell weight, costs of battery cells and cell monitoring, and meeting the Formula SAE Electric rules. As shown in Figure 2.17, in the last twenty-five years, battery cells for electric vehicles have evolved from lead acid to nickel cadmium, nickel metal hydride, to lithium ion. The ideal battery pack is made of reliable, powerful cells with a high energy density to complete the Endurance event and a high specific power to meet the power needed to create maximum torque. The battery cells that were best suited for use in the Formula SAE competition are mass-produced lithium ion batteries that cost less than one dollar per Watt-hour (Wh). For these reasons, the team selected lithium ion batteries for use in the VMS Formula SAE Electric car. This section discusses the battery cell selection, battery pack characteristics, cell monitoring and controls, and battery containers.

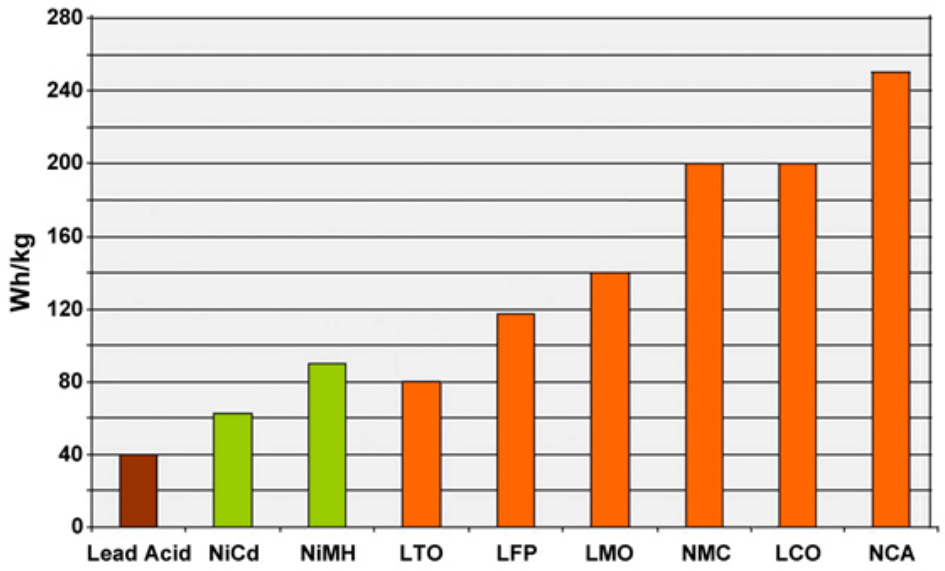

Figure 2.17: Battery specific energy levels (Wh/kg) based on the cathode chemistry, lithium cobalt oxide (LCO) and lithium nickel cobalt aluminum oxide (NCA) are promising cell candidates, but cells with those chemistries with at least 10 Ah per cell are not readily available at this time. For the cells available, lithium iron phosphate (LFP) and lithium nickel manganese cobalt oxide (NMC) cells have a better energy-to-weight-ratio over the other nickel chemistries.[43]

Research by Professor Dahn of the Waterloo Institute for Nanotechnology found that NMC and LFP chemistry cells were more resistant than other chemistries to the negative battery degradation that occurs over time with recharges.[44] Therefore, it was ideal to select either a NMC or LFP battery cell.

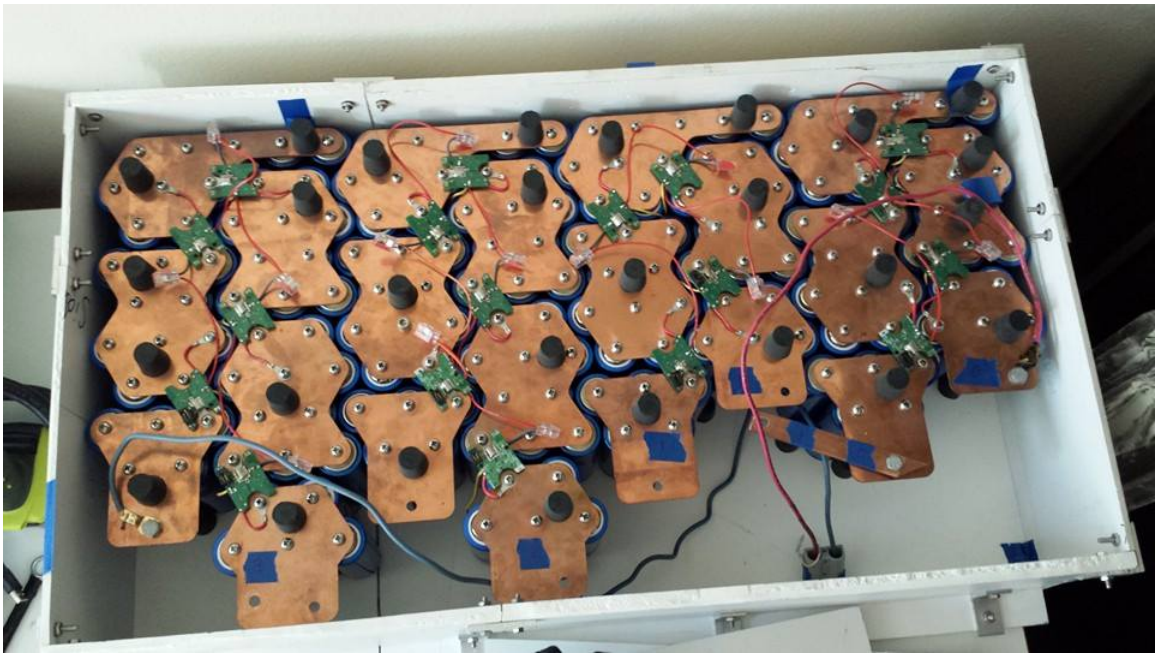

Figure 2.18: Six kWh cylindrical LFP battery pack with copper bus bars for parallel and series connections. Printed circuit boards for monitoring voltage, current, and temperature.[45]

The VMS Formula SAE Electric car's battery pack was a design that improved upon the battery pack design for my personal electric car, shown in Figure 2.18. My personal car's battery pack was built using lithium iron phosphate (LFP) cylindrical cells. Making multiple parallel connections with cylindrical style cells adds complexity and weight. There were five cells in parallel, and the cells were either bolted or welded together. The bus bar was large, and covered most of the surface on the top and bottom of all cells with conductive high voltage copper. This increased the risk of connecting the batteries to the chassis ground. The large bus bar added a few pounds of weight, which is undesirable. To immobilize the cells in all directions, the container had to clamp down on all sides. This was difficult because the battery pack requires a pcb (printed circuit board) on the top that can not have pressure on

it. Hence, I redesigned the battery pack to minimize weight, improve safety, and decrease unnecessary costs in manufacturing and materials.

2.7.1 Battery Chemistry Selection

The overall performance of the car relies on minimizing battery pack weight by designing for power and energy density. The weight of the battery pack is approximately 22% of the entire weight of the race car. At the maximum voltage, the cell must supply enough current for both peak torque and peak power to the motor.

Manufacturer	**Model**	**Wh/cell**	**Cost/cell ($)**	**Wh/kg**	**W/kg**	**$/kWh**
Enerdel	CP160-365	65.6	36	130	2028	625
Headway	38120S	32	19	97	970	594

Table 2.8: Cell Comparison for Enerdel NMC and Headway LFP, emphasis placed on energy density, favoring Enerdel cells.

Table 2.8 shows the parameters for the two final lithium ion cells. The LFP Headway cell energy density for the bare cells is 97 Wh/kg [46], and the NMC Enerdel cell energy density is 130 Wh/kg.[47] The Enerdel cost per cell is much greater at $36 versus $19, but the Enerdel cell has much more energy in the cell. The cost per kWh is $625 versus $594, 5.2% more for a cell with much better energy and power density. The densities of the two cell types differ, and the volume of the LFP battery pack would be too large for the motor bay, and require building a larger chassis, adding significant weight.[5]

2.7.2 NMC Cells for the Formula SAE Car Battery Pack

The battery cells selected are a 16 Amp-hour (Ah) NMC cell made by Enerdel. The total amount of energy in a cell is the product of the amp-hours and voltage, equal to 65.6. However, the usable energy is the area under the discharge curve in Figure 2.19. The discharge rate in C is the ratio of continuous current to the Ah rating. The continuous current was solved in Equation 2.25, and there are two cells in parallel, doubling the Ah capacity.

$$C = \frac{I_{cont}}{Ah} = \frac{63.1(A)}{(2cells)16Ah} = 1.97C \tag{2.26}$$

The cell discharge rating is approximately 2C, shown in aquamarine in Figure 2.19. The discharge curve is useful, but very vague, and there is not a formula provided to calculate the exact curve. Implementing a linear approximation from 0 Ah and 4.1 V_{DC} to 15 Ah and 2.5 V_{DC}, the usable energy is approximately 49.5 Wh per cell, 75% of the total energy.

The cells are contained in professionally manufactured modules of twenty-four cells. The modules contain aluminum heat sinks, cell tab connections, a slight compression to prevent the cells from undesirable swelling, and insulation around all sides. Within each module, there are twelve cells in series, and two in parallel. There are four modules in the battery pack, with the specifications as shown in Table 2.9.

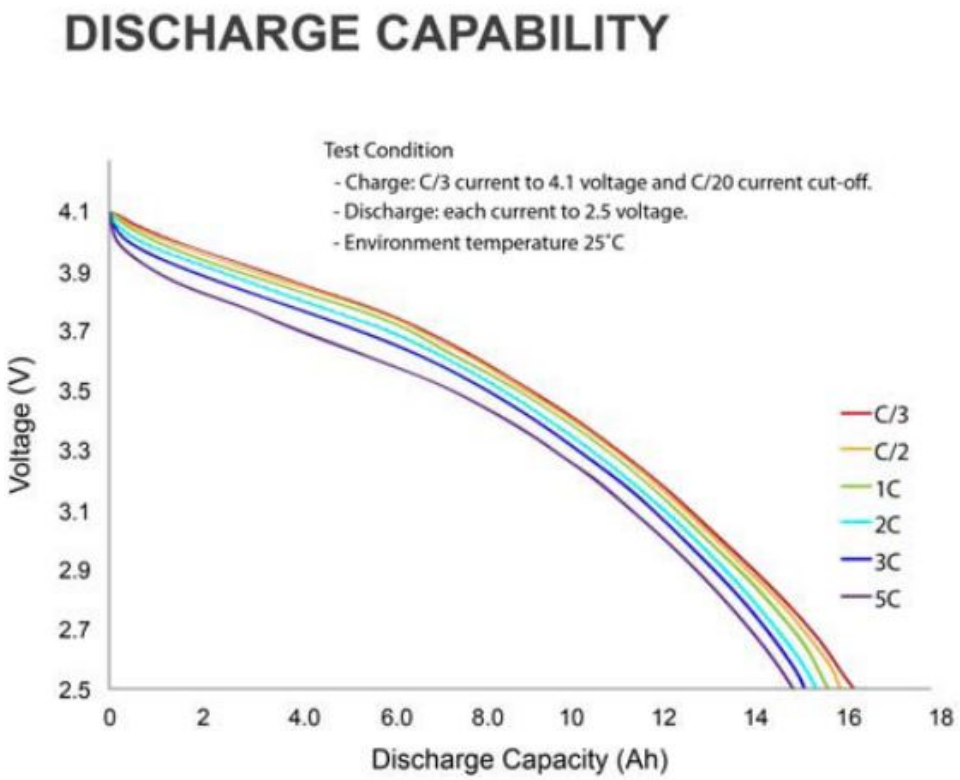

Figure 2.19: The Enerdel discharge capacity is the area under the curve for the respective C rating. This is the usable energy for each cell, and during a heavier load, the discharge capacity decreases slightly.[47]

Specification	**Value**
Maximum Voltage	196.8 V_{DC}
Nominal Voltage	172.8 V_{DC}
Minimum Voltage	120.0 V_{DC}
Battery Configuration	48 series 2 parallel
Maximum Voltage per container	98.4 V_{DC}
Battery Ah	32
Maximum Battery Current	480 A for 10 sec
Nominal Current	120 A
Maximum Charging Current	120 A
Total Cells	96
Total Capacity	6.30 kWh
Usable Capacity	4.75 kWh
Number of Cell Stacks <120 V_{DC}	2

Table 2.9: Battery Pack Specifications include maximum voltages, discharge and charge currents, energy of cells and total pack.

The maximum DC voltage from 48 cells in series is 196.8 V_{DC}. Each cell is 16 ah, and there are two in parallel. The cells will output up to 480 A_{DC} peak, or 120 A_{DC} continuously. The total capacity is 6.3 kWh, but the usable energy is 25% less, 4.75 kWh, which is the total amount of energy that can be discharged during the Endurance Event.

The usable energy of the battery pack is very close to the amount of energy required to complete Endurance at peak performance. The OptimumLap simulations found the most energy required was 5.04 kWh in Germany 2012, but the average energy use was 4.27 kWh. Three out of four modeled Endurance events require less energy than 4.75 kWh. If regenerative braking energy decreases total energy required by 15%, the Germany Endurance course requires 4.28 kWh. Track testing will be useful for including regenerative braking energy, determining actual energy use, validating the OptimumLap model, and the hand calculations.

2.7.3 Battery Monitoring & Control

Each pair of cells is connected by a flexible printed circuit board (pcb) to a RLEC (remote lithium energy controller) board that performs real-time control and monitoring of the battery modules. The RLEC sends the cell voltages, temperatures, and faults in 25 ms (milliseconds), and each board does cell balancing of 24 cells: twelve in series, two in parallel. The MLEC (master lithium energy controller) requests cell data by sending broadcast CAN messages with cell balancing commands, and then commands to individual RLECs. The RLEC boards contain a 37.5Ω balance resistor for current balancing cells.[48] The battery modules were

received with RLEC boards and software, but not MLEC master units, because there was not any available and these are not sold, requiring us to find a different master unit for the batter management system (BMS).

The lithium cells need to be monitored for over-current, under-voltage, over-voltage, over-temperature, and under-temperature faults. Lithium cells are voltage-sensitive, and just one event exceeding 4.10 V_{DC} per cell or falling below 2.50 V_{DC} could permanently damage the cell. The entire battery pack needs to be top-balanced, making sure that all of the cells were as close to each other at 4.10 V as possible. The over-temperature specification limit for discharging is 65°C, but the datasheet limits the maximum allowed temperature to 55°C.

BMS Component	**Cost** $	**Water-proof**	**Time Required**	**Conclusion**
Elithion	1,700	no	least	too expensive, not waterproof
Orion	1,225	no	least	too expensive, not waterproof
custom EVCU	500	yes	most	affordable, more appealing

Table 2.10: Variables of a battery management system, the main differences are the time for developing a custom unit, and the cost.

The decision was either to replace the RLEC boards and implement an off-the-shelf battery management system (BMS) or create a custom Electric Vehicle Control Unit (EVCU). The car requires an electronics unit that monitors and manages the battery cell voltages and faults, analog and digital inputs, outputs, and data logging. The BMS options only manage the battery cells, and are not a complete control unit. The custom EVCU option allows for hardware selection, provides the software and hardware for the BMS functions, and logs data. As shown in Table 2.10, a high quality, custom EVCU would possibly do better in the Design Event and cost $725 less, but risked not finishing the car for the June

competition. Both of the off-the-shelf units are designed for use inside passenger cars and are not waterproof. These would require additional enclosures and wiring harnesses, adding weight and expenses. The benefits of consolidating hardware and creating a custom EVCU outweighed the challenges and time constraints of hardware development and reverse-engineering the software required to communicate with the RLEC boards. We decided to create a custom EVCU, discussed in more detail in Section 2.8.1.[6]

2.7.4 Battery Container

The battery cells, high voltage fuses, insulation monitoring device (IMD), contactors, and high voltage components are contained in waterproof containers that can withstand 160 kN (40 G's) of force horizontally.[13] The Formula SAE rules allow use of either steel or aluminum to construct the containers, which can be constructed by welding or using positive locking fasteners.[13] The team made the containers using laser cut steel[5] and welded the boxes.[9] An electrical insulation material rated to UL94-V0 fire resistance was required.[13] G-10/FR-4 is an industrial laminate sheet with characteristics of high strength, great dielectric properties, chemical resistance, and a maximum continuous operating temperature of 141°C .[49] FR-4 sheet was placed on all interior container surfaces to make the containers fire resistant and to electrically insulate the battery containers.[5]

As shown in Figure 2.20, the FR-4 sheet lines all interior surfaces, and contains the contactors, IMD, HV LED indicator boards, HV fuse and cables, precharge and discharge relays, and battery modules. The HV cables enter the lower left and exit the upper right, and

Figure 2.20: Battery container from the second generation car, designed from steel to secure the battery modules and high voltage components.

head to the motor controller and energy meter. The box is made from steel, and designed to withstand 160 kN of force horizontally.[11]

2.8 Electrical Systems

The competition requires many safety circuits and systems that interact with and control the electric drive system. In this section, I discuss how components behave and interact under

different circumstances to generate faults, including the EVCU, shutdown circuit, precharge and discharge, IMD, brake system plausibility device, torque encoder, and charging system.

2.8.1 Electric Vehicle Control Unit

The EVCU acts as a BMS of all battery cells, performs data logging, and manages the processing of different dynamic inputs and outputs for the entire car. These include analog inputs such as the 12 V_{DC} sensor input, two throttle pedal signals[13], and digital inputs such as the shutdown circuit status, brake light switch status, insulation monitoring device (IMD) status, and the brake system plausibility device. In 2014, the first generation EVCU (Section 2.7.3) was made, shown in Figure 2.21 .[6] It uses a standard Linux operating system including drivers for all peripherals. Communication is executed with controller area network (CAN) serial data.

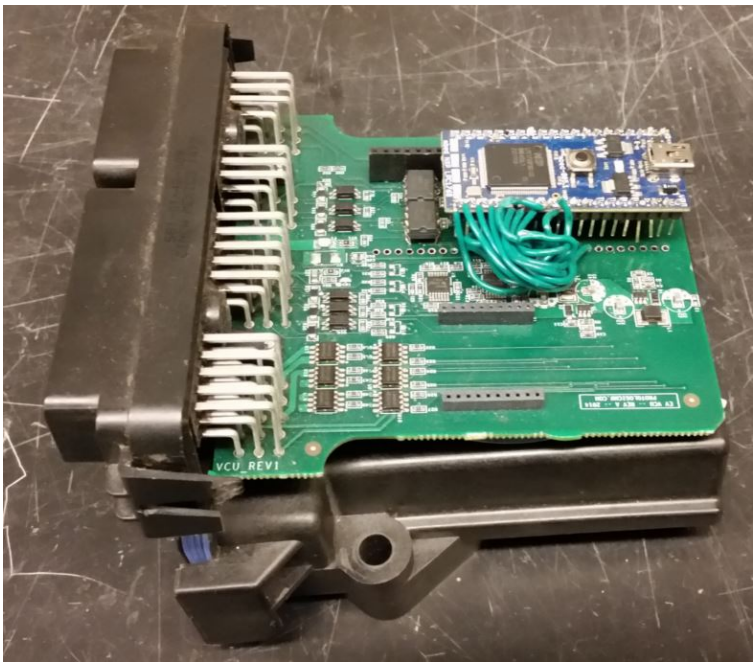

Figure 2.21: 2014 EVCU: First generation, custom board, MBED microcontroller, antenna in waterproof cinch case.

CAN is a message broadcasting system designed for automotive use that does not have a single host, varying from other communications protocols. USB and ethernet communications send large blocks of data to the entire network, but devices connected to the CAN bus "talk" with other devices directly. The purpose of this is to reduce complex, bulky wiring harnesses with versions that have two wires per device, saving on the cost of copper and reducing weight. Also, CAN has high immunity from EMI and has the ability to self-diagnose problems and repair data errors. This feature is valuable, as high frequency AC electric motors emit a large amount of electromagnetic noise. Each device on the CAN bus has a CPU, CAN controller, and transceiver to send data.[50] Each CAN message begins with a bit to synchronize the nodes, an identifier, up to 64 bits of data, a redundancy check,

an ending bit, and a bit for the time required.[51] CAN is used in the EVCU and motor controller, and is an advantage for protecting data from EMI, communicating between two devices without a host computer, and simplifying wiring.

The motor controller CAN protocol requires a "heartbeat" message sent once every 500 ms, or a fault results. The CAN controls the inverter, motor direction, and torque. Without the broadcast message, the controller assumes something is wrong, stops operations, and sends a fault message. The CAN messages give the status on modes, indicating if the transceivers are in transmit mode, receive mode, acknowledging power down, and the current state. CAN messages are key for control of the motor, adjusting parameters, diagnostics and monitoring parameters.[52]

Data from the motor controller are logged on the secure digital (SD) card in the EVCU, which allows us to monitor and analyze crucial data that displays the car's track times and performance. The data logged includes: temperatures of the motor controller gate driver board, motor, battery cells, voltages and currents of individual cells, high voltage DC, high voltage AC, the motor phase angle, frequency, power, flux, and torque. During track testing, the data was also sent to a wireless interface provided realtime data on a laptop through telemetry.

An Android tablet with internal accelerometer sensors was mounted to the car to collect data such as the acceleration in x,y, and z dimensions, and the ambient temperature. The sensors are capable of providing raw data with high precision accuracy, useful for three-dimensional device movement.[53] The acceleration and temperature data were logged on

the SD card.

The 2015 EVCU is an off-the-shelf, open-sourced product from EVTV named the "GEVCU", which was designed to accept a variety of accelerator pedals, motors, and motor controllers. It is an adaptable unit that allows versatile changes in software, and has a basic USB serial interface to fine-tune the motor controller for each application. Automotive manufacturers create electronic components that use CAN messages. The messages can be made somewhat generic with the EVCU controlling them through "CAN opener" software developed by EVTV.[50]

The GEVCU is based on an Arduino Due microcontroller with an Atmel ARM CPU. As shown in Figure 2.22, the GEVCU has four analog inputs, four digital inputs, eight digital outputs, and two independent CAN bus controllers built into the chip. The CPU does not contain CAN transceivers, so two Texas Instruments galvanically-isolated CAN transceivers were used, which prevent noise currents from entering through the chassis ground.[54]

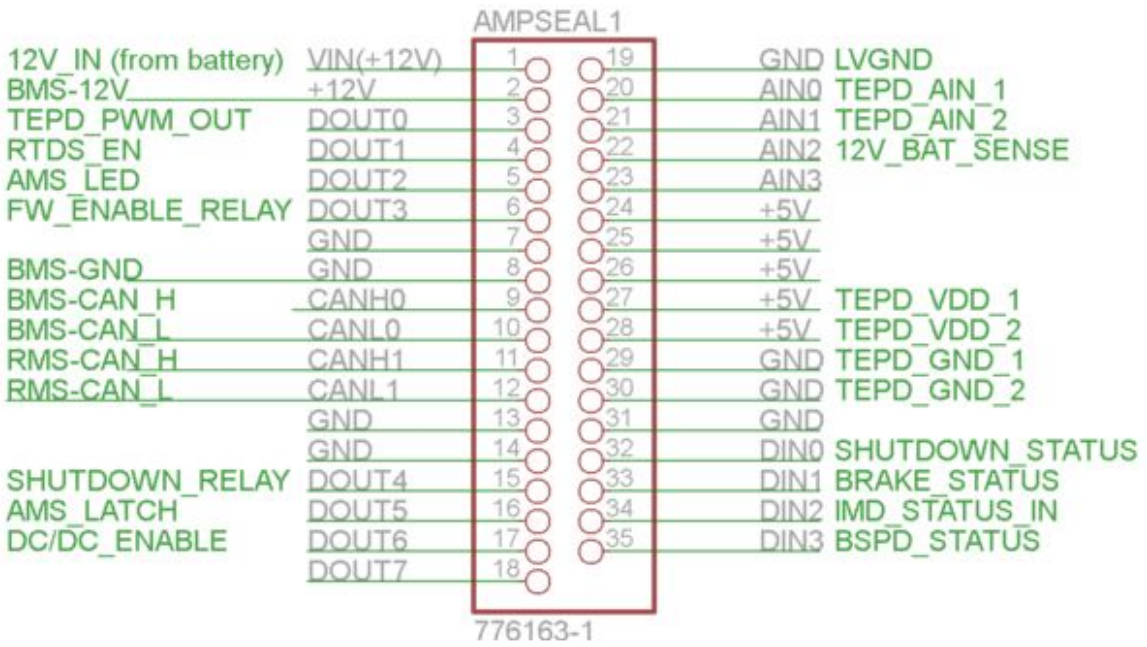

Figure 2.22: GEVCU analog and digital inputs and digital outputs include 12V, grounds, torque encoder, BMS (AMS) faults, CAN, ready-to-drive-sound, latching relays, DC/DC converter, LED status lights for the shutdown circuit, brake light, IMD, and brake system plausibility device. The pertinent data is sent to the Edison data logger and stored.[6]

The GEVCU uses a waterproof, thirty-five pin AMPSEAL connector, and manages all of the terminating resistors. The DUE CAN library allows for simple C++ commands for managing the CAN communications. Any device on the CAN bus is able to transmit and receive data. Michal Podhradsky programmed the GEVCU, as it needed the addresses defined and data from the motor controller, provided by RMS documentation.[31] Also, software was created to collect, send, and log data in the Edison board. One negative aspect of the GEVCU is that the USB port on the opposite end is not a waterproof connector, and could be problematic for the rain test. We used tape as a temporary solution, but discontinued use of the GEVCU in 2016 with a waterproof design.

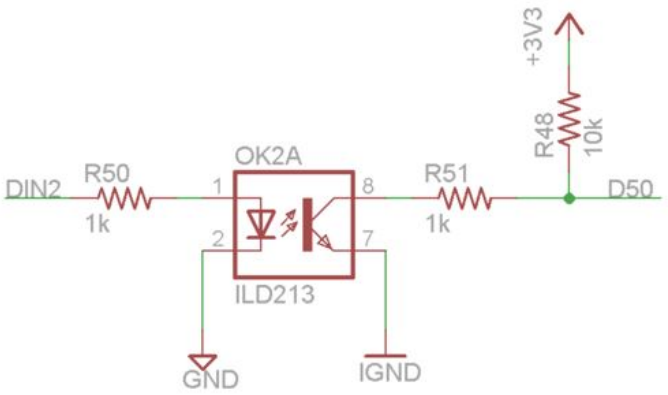

Figure 2.23: An EVCU digital input, DIN2 from the AMPSEAL connector, and D50 goes directly to the Arduino chip. The EVCU has pull-up resistors, normally high, that invert the logic. If there is an input voltage, the EVCU reads logic low.[6]

The digital outputs are connections from the EVCU to peripherals, including the torque encoder PWM signal, ready-to-drive sound, LED indicators, and relay drivers. As shown in Figure 2.24, DOUT0 and DOUT1 are from the AMPSEAL wiring harness, D4 and D5 are outputs from the Arduino chip. When the logic is high, it connects the input to the low voltage ground, and conducts. When logic is low, the input is floating and does not conduct.[6] The digital outputs are vital to enabling the high voltage to low voltage (DC/DC) converter, enabling relays for various states of operations for the car, and driving important LEDs to inform the human driver of conditions.

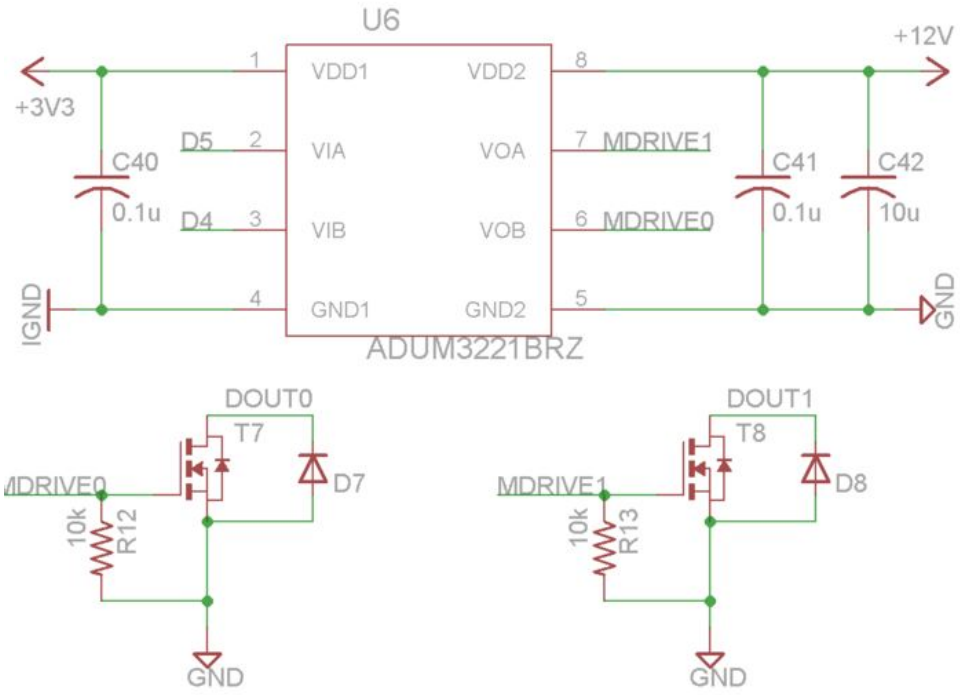

Figure 2.24: EVCU digital outputs, the torque encoder PWM and ready-to-drive enable signals .[6]

The analog inputs are used for some of the peripheral signals that feed into the EVCU, including the torque encoder signals and the 12 V_{DC} battery sensing input. The inputs on the electric car such as the torque encoder and brake signals from the human driver are relatively slow at approximately 150 ms maximum, so the signals were sent through a 100 Hz resistor-capacitor (RC) filter to eliminate excessive EMI.

Since the internal Arduino analog-to-digital converter is 3.3 V_{max} and has a 12-bit resolution, we can measure voltage from 0 to 8.5 V_{DC}, and the resolution is 8 mV. For sensing 12 V_{DC}, we need to add another voltage divider at the input. The analog input circuit is vital to the torque encoder input signal that determines the motor output, and sensing the voltage of the low voltage (12 V_{DC}) system, shown in Figure 2.25.

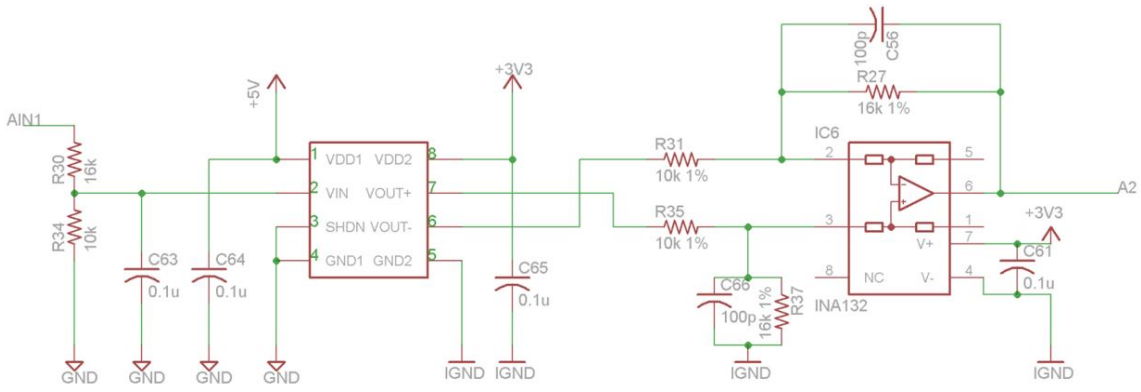

Figure 2.25: EVCU analog input example from the GEVCU connector, A2 is an analog input fed directly to the Arduino chip.[6]

2.8.2 Shutdown Circuit

The shutdown circuit contains the safety components in the electric race car that interrupt the continuity of the circuit, resulting in a fault and opening the contactors. Shown in Figure 2.26, the IMD, BMS, high voltage disconnect, and interlocks are inside the battery boxes. One shutdown button is on the dashboard, the inertia switch is under the dashboard, the brake over travel switch and BSPD are at the pedals. Both master switches are located on the right side of the motor bay, and a shutdown button is located on both the left and right sides of the motor bay. Figure 2.27 provides a high level circuit diagram from Formula SAE with all of the shutdown components connected in series, and Figure 2.28 shows the custom application the team created for the shutdown circuit.

During a fault in the shutdown circuit, both the positive and negative poles of the battery high voltage are opened, eliminating the high voltage system from conducting. The high voltage connectors have safety interlocks that open the shutdown circuit when the high

voltage connectors are removed from the battery boxes, eliminating contact with the high voltage system.

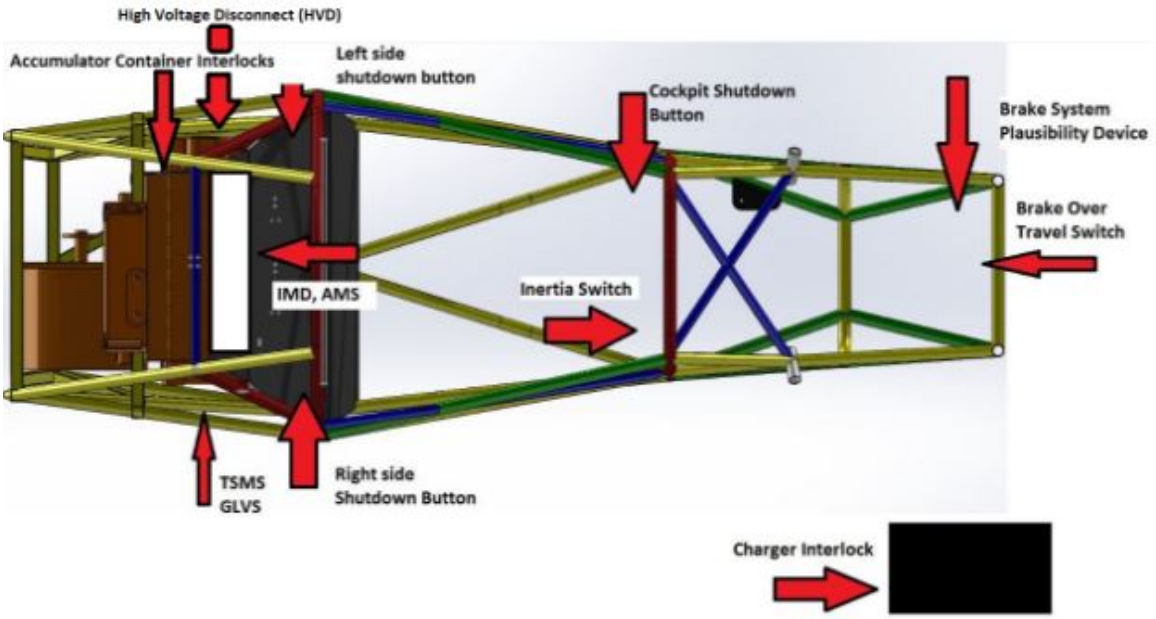

Figure 2.26: A top view from a CAD model indicates where each of the circuits is located in the race car.[11][5]

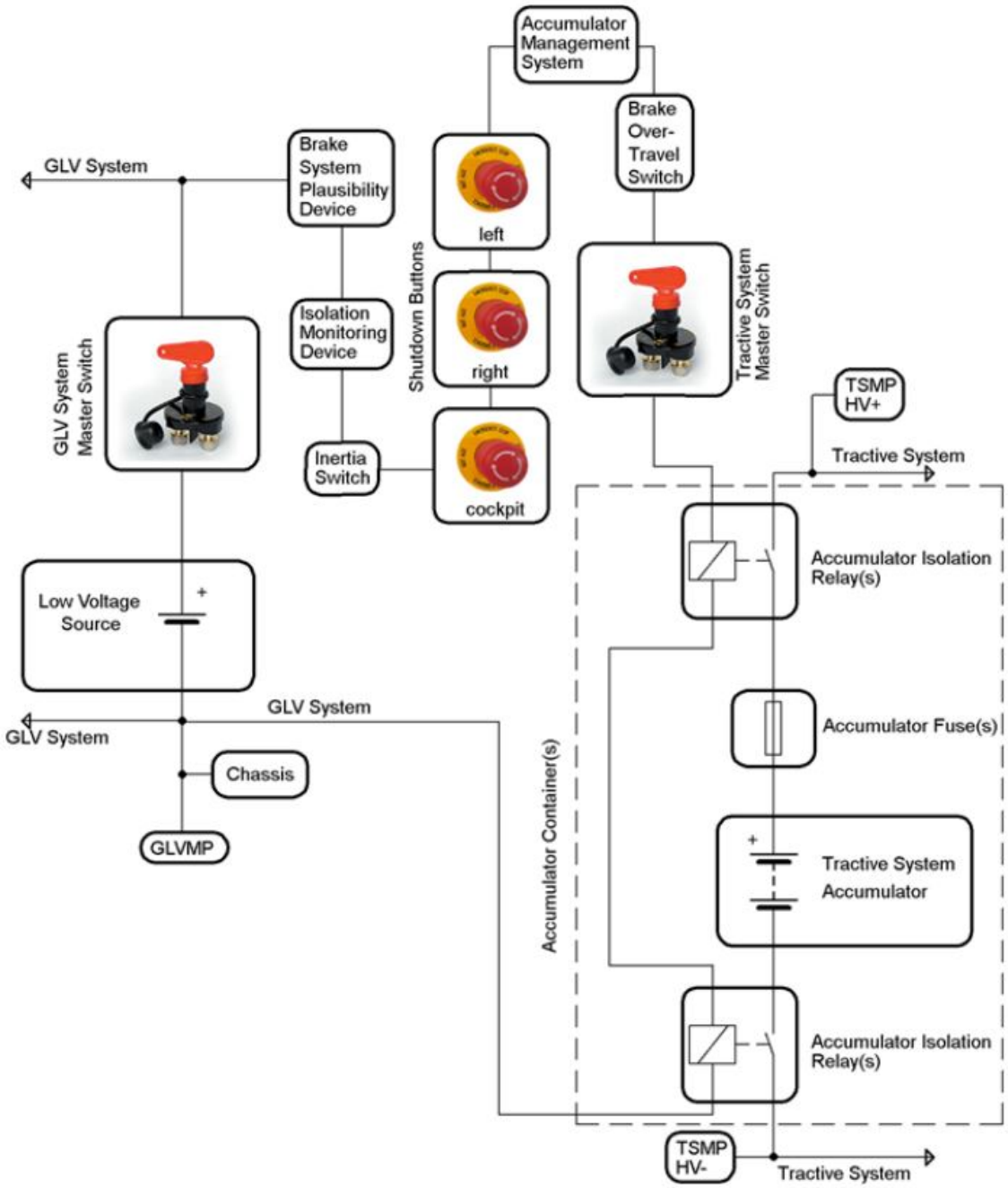

Figure 2.27: Formula SAE Safety Shutdown Circuit

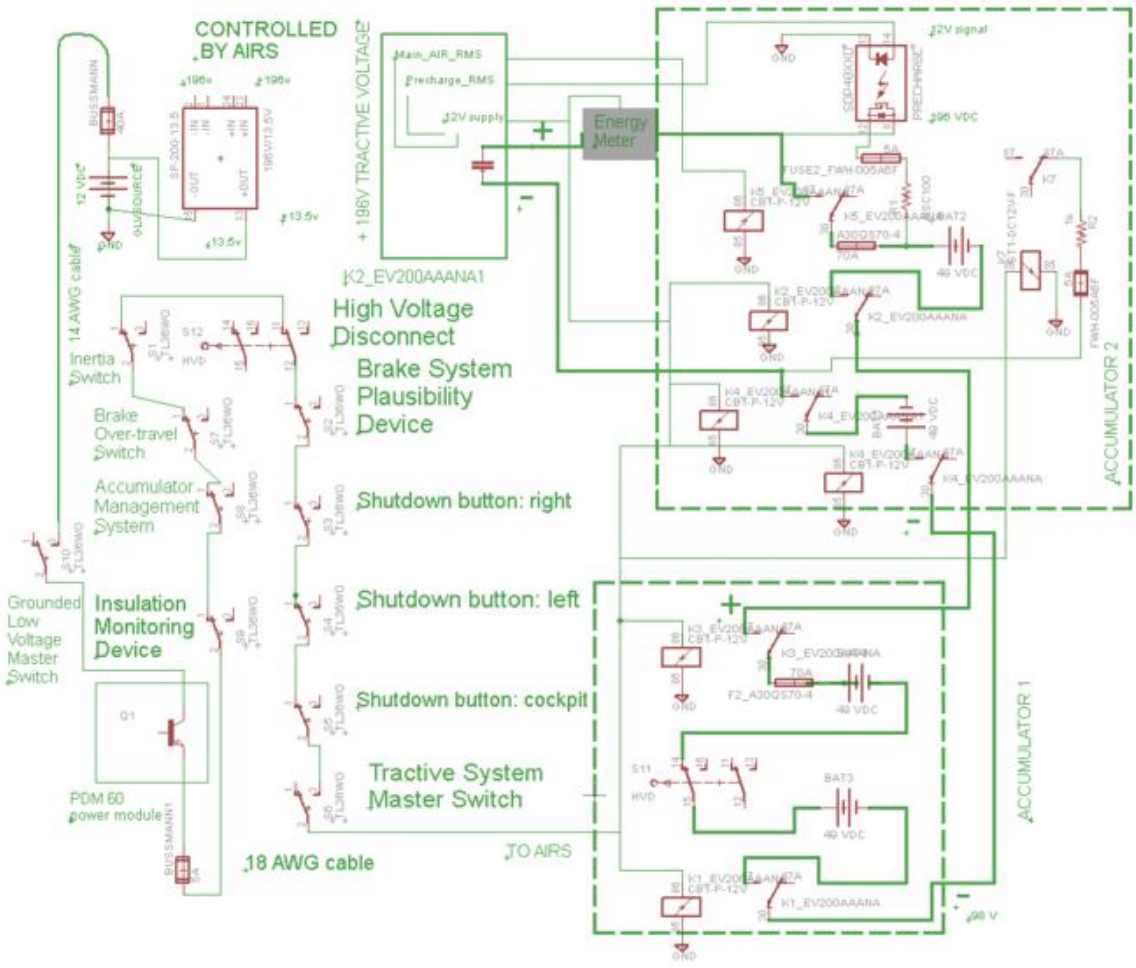

Figure 2.28: VMS Safety Shutdown Circuit, a detailed version integrating circuit connections specific to our electrical systems.

If the circuit is opened by the BMS or IMD, the circuits latch and the tractive system is disabled until manually reset by another person (not the driver). By design, the driver cannot reactivate the tractive system with cockpit controls, and can't physically reach the reset buttons in the rear of the car, or use remote reset.[13] The two master switches will remove the 12 V_{DC} supply, and open the accumulator isolation relays (AIRs) when switched off.

2.8.3 Precharge and Discharge

The motor controller has 280 μF of capacitors on the DC input. To avoid damage or early component failure from repeated inrush currents over time, precharging the capacitors to 90% of the maximum voltage is required. The battery current can be a maximum of 250 A_{DC}. However, utilizing a parallel circuit with a power resistor (shown on the output HV in Figure 2.28) the precharge circuit was designed to deliver a small maximum current of 200 mA_{DC}.[5]

The motor controller has an internal high-impedance, low-power EMI filter across the DC terminals that dissipates a small amount energy. However, the energy needs to be dissipated and the capacitor voltage must be below 60 V_{DC} in five seconds, and the internal filter did not dissipate the energy in time. Most datasheets required a bulky heatsink, which takes up valuable space in the battery box, but this was avoided by utilizing a larger 100 W resistor at a derated 50 W power rating to avert overheating damages.[5]

2.8.4 Insulation Monitoring Device

The insulation monitoring device (IMD) is an automotive-grade circuit board manufactured by Bender that continuously monitors the electrical insulation resistance between the active HV conductors of the drive system and the chassis earth ground. The response value of the IMD is set to 500 Ω/V_{DC}, related to the maximum tractive system operation voltage. The tractive system maximum voltage is 196 V_{DC}, so the IMD is at 98 kΩ.

Once the low voltage power is switched on, the IMD performs a Speed Start measurement.

This provides the first estimated insulation resistance during a maximum time of two seconds. The Direct Current Pulse system continuously takes insulation measurements. Faults in the connecting wires or any functional faults will be recognized, and drive a relay open in the shutdown circuit.

Since the IMD provides a "LOW" signal when there is a fault, the signal is run through an inverter to provide a "HIGH" signal in the event of a fault. The signal is fed to the gate of a NPN transistor, shown in Figure 2.29. The transistor is needed to drive a larger 100 mA current through the emitter to the coil of a relay, switching open the shutdown circuit and closing a circuit with an LED fault indicator light on the driver's dash display.[5]

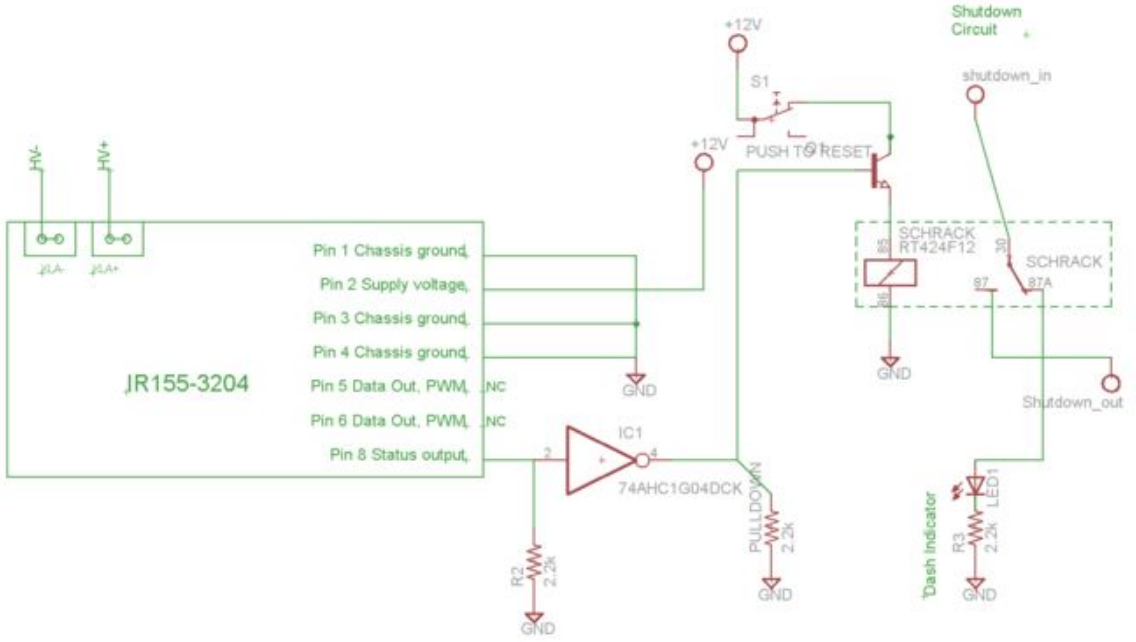

Figure 2.29: The IMD circuit closes the shutdown circuit in normal operation mode, and drives an LED in fault mode.[5]

2.8.5 Brake System Plausibility Device

The Brake System Plausibility Device (BSPD) is a non-programmable component that opens the shutdown circuit if there is simultaneous motoring power and "hard braking".[13] Further, if there is 5 kW or more of power being delivered to the motor and "braking hard" occurs without locking the wheels at the same time for more than 500 ms, the device must fault.[13] Under these conditions, the BSPD opens the shutdown circuit. “Braking hard” is a vague term in the Formula SAE rules, and challenging to quantify. I determined we would not try to interpret the rule, and simply use any amount of braking from the brake pedal signal for BSPD operation. A brake pressure sensor was tested, but it was difficult to work with and it was decided that time was best spent on other electrical tasks. A brake light switch was used in the final schematic to indicate when braking occurred, shown in Figure 2.30. Formula SAE rules state using the low voltage throttle input that commands 5 kW is not allowed. The actual high voltage current and voltage need to be measured.[13]

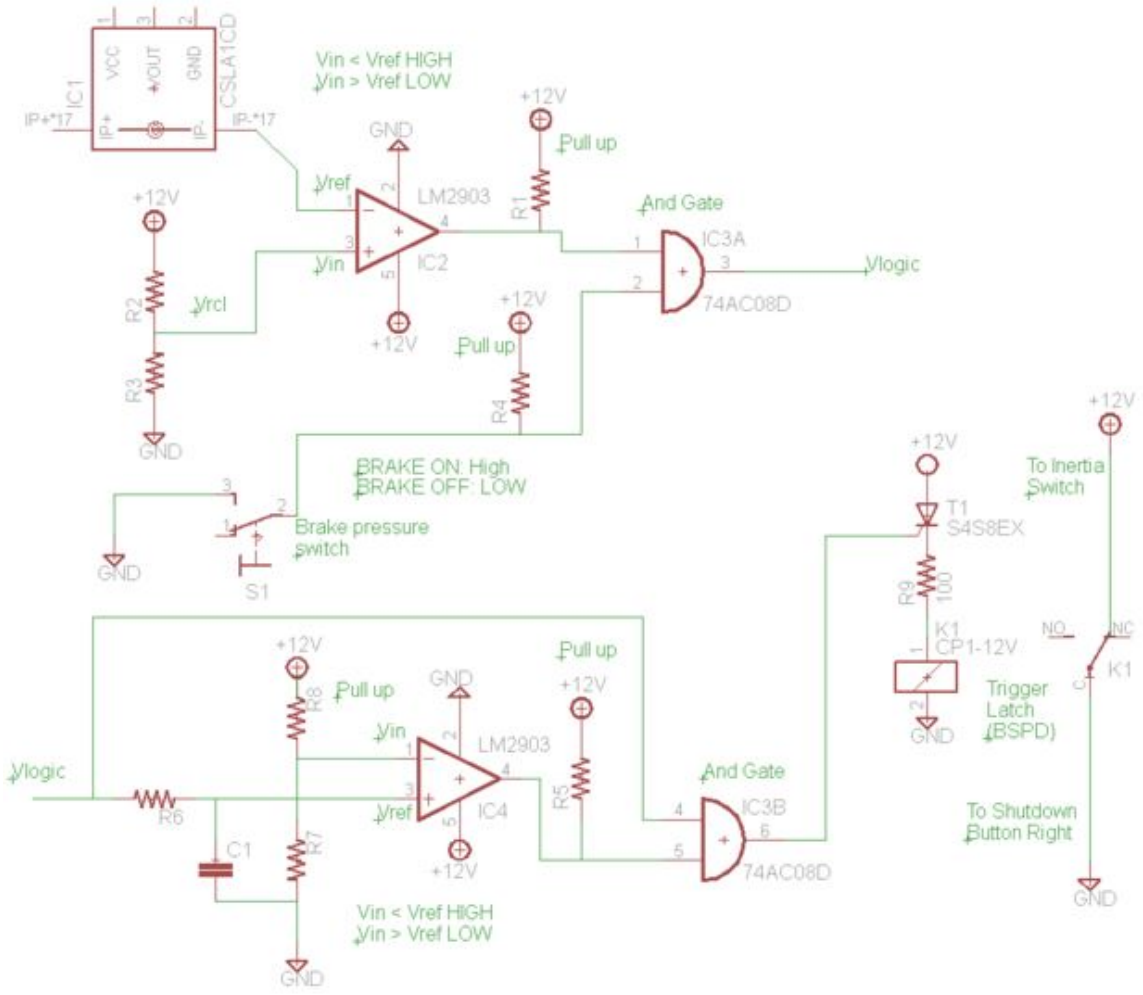

Figure 2.30: BSPD circuit: comparing the brake switch to the current sensor, timing the circuit to fault in 500 ms.[5]

An external Hall effect current sensor was around the negative DC high voltage conductor from the batteries to the motor controller, sensing tractive current. This signal and the existing brake light signal were sent to a comparator circuit, comparing it to an 8.6 V_{DC} reference voltage. If the voltage from the Hall effect sensor is greater than 8.6 V_{DC}, and the brake switch signal is sent, that creates a "high" signal that is delayed for 500 ms then opens the shutdown circuit.[5]

2.8.6 Tractive System Active Light

Since electric race cars are almost silent compared to internal combustion race cars, a highly-visible tractive system active light is required to blink at a frequency between 2 and 5 Hz. The HV+ lead is connected on the motor side of the main contactor (opposite of the battery side), and HV- is connected to the most negative lead. When the precharge circuit procedure has completed, the main contactor closes, and the tractive system voltage is at 196 V_{DC}. There is a zener diode at the HV+ input, preventing voltages less than 60 V_{DC} from activating the circuit. A LR8 high voltage linear regulator provides power to the ILD74 optocoupler, which separates HV and LV.[6] A 555 timer is powered by 12V and takes care of the 5 Hz period switching of the transistors.[5] Thus, we can switch larger loads necessary to power the lights. We tested the circuit and it provided satisfactory results. The wiring diagram is shown in Figure 2.31.

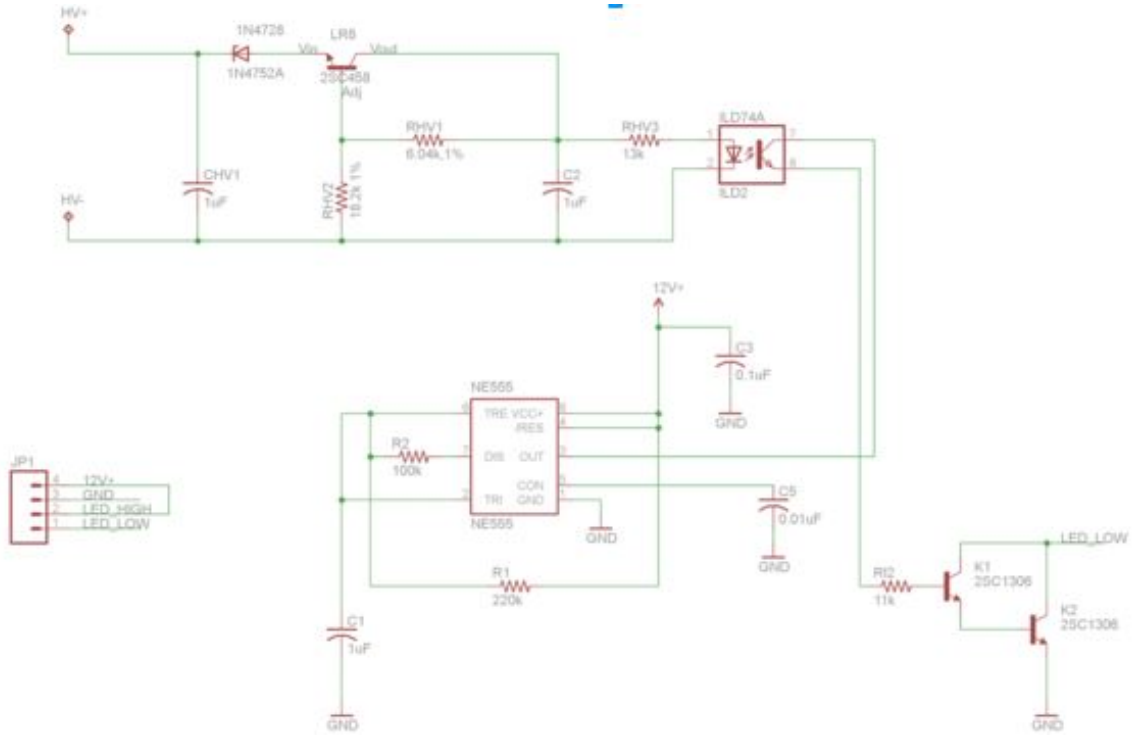

Figure 2.31: Tractive system active light circuit: when high voltage is on, the lEDs blink at 5 Hz.

2.8.7 Throttle Pedal - Torque Encoder

The torque commanded is based on an analog signal from the throttle pedal, between 0.5 V_{DC} and 4.5 V_{DC}. Any signal below 0.5 V_{DC} is an open circuit fault, and above 4.5 V_{DC} is a short circuit fault. As a safety feature, the rules require there be two throttle signals that are compared, and the signals are required to be within 10% of each other, or the shutdown circuit must open.[13] I was responsible for sourcing, testing, and implementing a reliable, consistent, accurate torque encoder component.

A traditional electric vehicle "pot box" 5 kΩ potentiometer was tested and used on a test bench for the motor. Implementing two potentiometer boxes by mechanically bolting them together was difficult because the housings got in the way, and the housings immobilized the

potentiometers. The first set of potentiometers were non-linear, and did not work. A Hall effect, two channel throttle pedal assembly was sourced, but there was not enough room in the small cabin near the pedals. The assembly is large and bulky, and a cable was run to the rear of the car. There were lots of mechanical problems with the cable, as it got pinched, bound up and bent near the pedal outside of the sheathing, and was unreliable. Finally, a Toyota pedal was implemented.[5] It has two Hall effect sensors inside the assembly, and eliminated the mechanical cable problems. The signals were compared and scaled in the EVCU.[6]

2.8.8 Charger

An AC charger was required to charge the batteries as needed, and per SAE rules, Chapter EV8.3[13] the charger must operate on a 120 V_{AC} 15 A supply from the electrical grid, have a galvanically isolated ground between the AC and DC sides, per CE standards.[55]

A new rule in 2015 stated the battery boxes were required to be removed from the vehicle and charged on a cart. This requirement only applied at the competition, and on track days or other events, a charger with more power could be used. Removing the battery boxes made packaging challenging because the IMD and BMS were required to be active during charging, shown in the charging circuit diagram 2.32. The IMD was packaged in the battery container, and the 2014 EVCU was used for the BMS charging cut off signal, opening the line AC voltage circuit.[6]

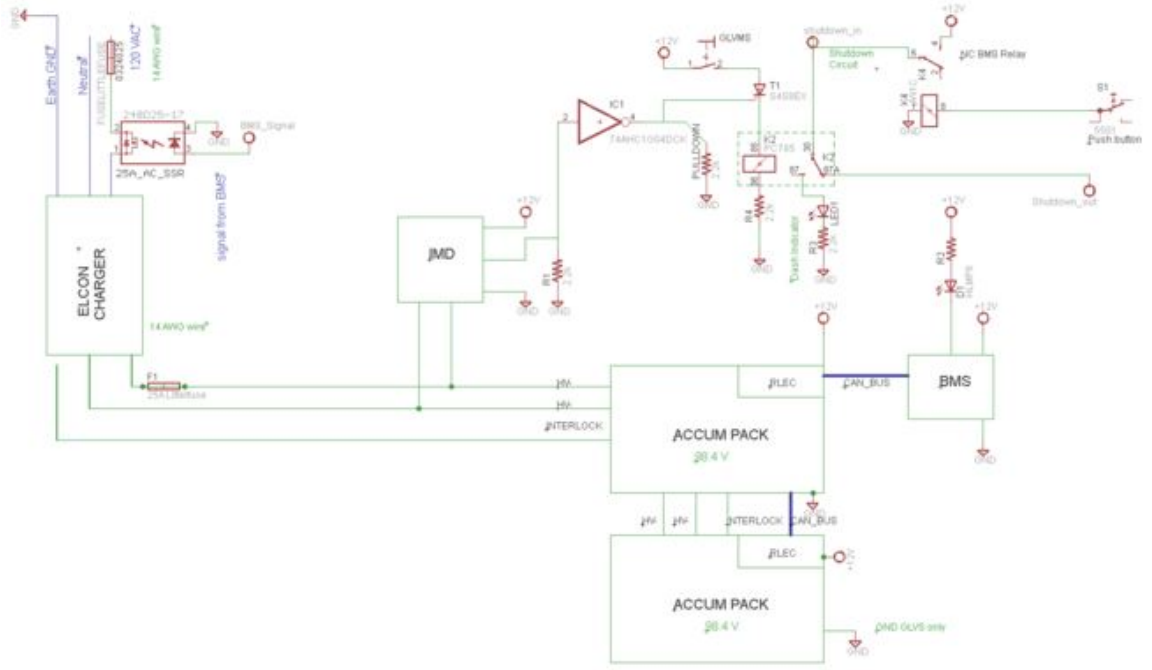

Figure 2.32: During charging, the BMS sends a low voltage signal to a solid state relay, controlling the line voltage of the 120 V_{AC} input to the charger.[5]

2.8.9 Summary

The electrical systems are crucial to safety, and emphasized during the technical inspection and throughout the competition. These circuits implement safety features unique to electric cars, such as partitioning the energy in 6 Megajoule (MJ) increments and disconnecting them in all faults, resulting in safer cars and a safer competition overall. Compared to the rules for internal combustion race cars, these systems add much complexity and effort for the designers and builders of electric race cars.

3 Testing, Simulation & Analysis

3.1 Track Test Data

VMS performed track tests of Acceleration, Skidpad, and Endurance Events in order to train drivers, gather data, examine the car's performance, compare results to calculations, simulations, and compare our results to other teams' cars from competitions. Correlation exists between the number of hours of driver training and how well a team performs at the competition.[4] All of the drivers at the competition are amateur students, as teams are not allowed to have professional drivers. Getting driver training gains experience and a feel for the race car that is crucial to dynamic performance. When the race car is first built, there are often mechanical weaknesses that can only be discovered during testing. The first generation car testing conditions were not ideal, as the track was cold and wet, decreasing track performance. The second generation car data were taken on a warm, dry track for Skid-pad, Acceleration, and longer Endurance Event testing, the ideal track testing conditions.

3.2 Track Day Data - First Generation Car (2014)

The 2014 electric race car was tested at Portland International Raceway in Portland. To get maximum performance, tire grip is significantly greater with a warm, smooth, dry track

surface. When testing the first generation race car, we had to test in the rain on a cold, wet track. The tires didn't grip as well, and the car was driven through some standing water. Over several hours of testing, the IMD faulted once, indicating there was less than 100 kΩ of insulation between high voltage and low voltage. After letting the car sit for approximately twenty minutes while attempting to diagnose the source of the problem, the fault cleared and was no longer an issue.

An Autocross test was conducted, and the length was approximately 654 m, 18.3% shorter than an actual Formula SAE 800 m course. On a single battery charge, the battery pack generated energy for 31.4 km (48 laps) of testing, a 43% greater distance than the Endurance Event requires. However, with cold, wet tires, the tire frictional force decreases from 2511 N to a range of 785 to 2354 N, a decrease of 6% to 69%.[22] Thus, the peak torque and acceleration are reduced at the same rate, and the average car speed is decreased. Therefore, the average load on the motor is less, and the energy required is much less per km versus the warm, dry conditions at the Formula SAE competition. Hence, further testing is required for estimating the car's energy use per km.

The car had an undesirable weight ratio, and handled poorly in sharp turns. The front to rear weight ratio was approximately 50/50, and should be heavier over the rear wheels. During sharp turns, the inside rear wheel would rise off of the ground several inches, and the differential transferred power to the inner wheel spinning freely, then when the wheel returned to the ground, it jerked the car sharply and was difficult to control.

The motor data showed that the peak power was approximately 51 kW, 15% less than

the 60 kW of power calculated in Equation 2.22. The peak torque was 410 Nm, 2.5% more torque than the expected value from the datasheet.[1] The ambient temperature was approximately 21°C degrees Celsius, and the motor's rotor temperature did not exceed 32°C, likely indicating a lighter load on the motor than in Formula SAE competition conditions. The broad temperature range expected was between ambient temperature and 140°C, and the temperature was 9.2% above the minimum in that range.

3.3 Track Day Data - Second Generation Car (2015)

3.3.1 Skid-pad Event Test

During Skid-pad testing, data were logged for lateral and longitudinal acceleration, Figure 3.1. The testing time was approximately 324 seconds (5.4 minutes), and was conducted to determine the testing time and actual tire forces. This emphasizes the lateral acceleration (Figure 3.2) and validation of the OptimumLap simulations.

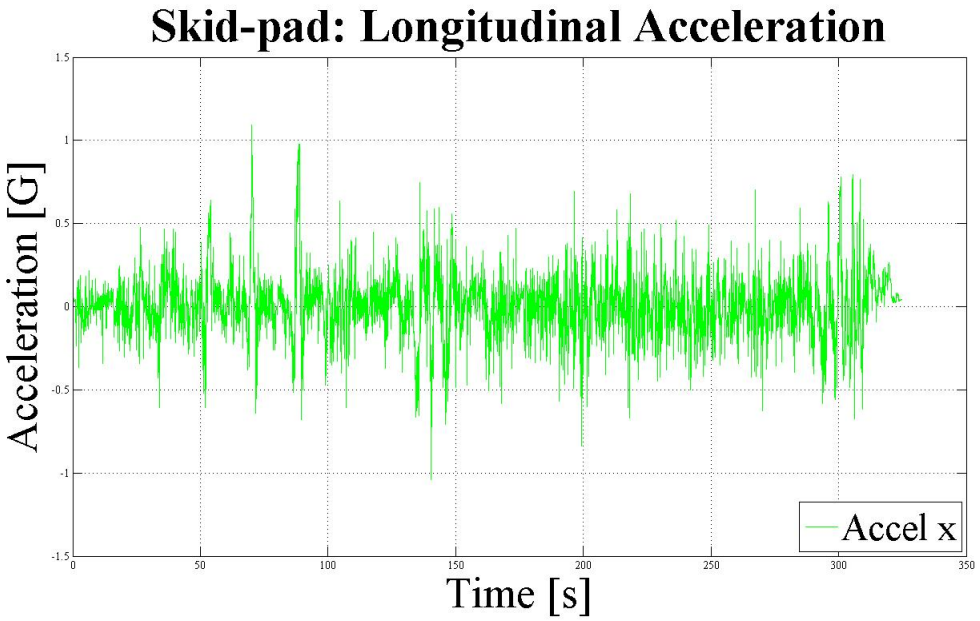

Figure 3.1: The longitudinal acceleration in G's is relatively low, when the lateral acceleration is greater than 0.8, the longitudinal acceleration is below 0.25 G's.

The maximum longitudinal acceleration is 1.1 G's, 10.7 m/s^2, for 100 ms. The mean acceleration is much less, 1.4 m/s^2, and requires 147 Nm of torque without any gear reduction included. With the 3.143/1 gear reduction, the 46.8 Nm maximum wheel torque needed for the best track time in the Skid-pad Event is much less than the 410 Nm of torque available from the Remy motor.

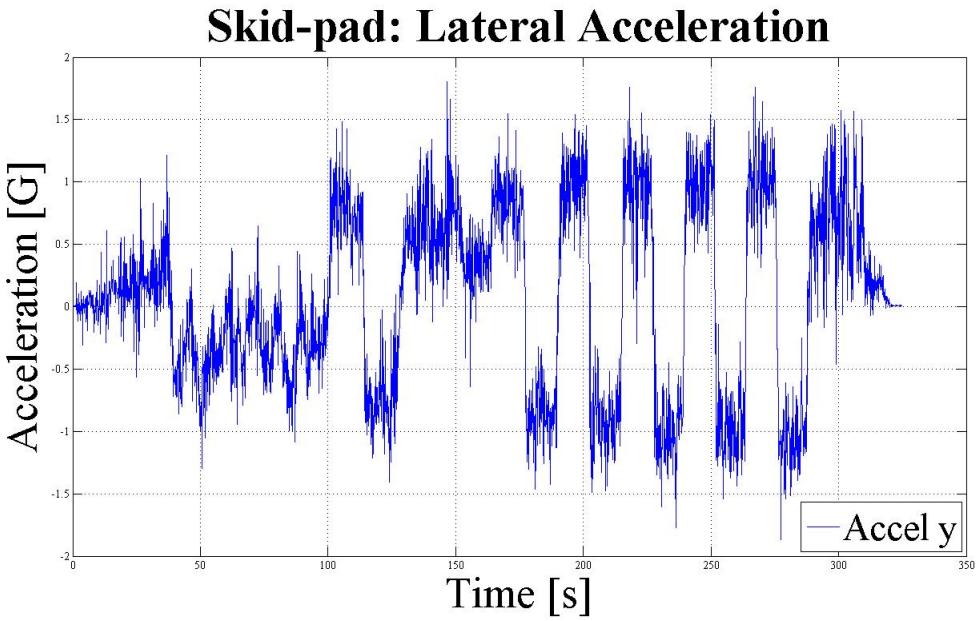

Figure 3.2: The lateral acceleration testing was one lap per side until 100 seconds, and the data is not clear. At 100 seconds, I drove two laps on the right side, two on the left, and repeated. The data from 100 to 128 seconds, and 163 to 287 seconds was much clearer.

During the testing, the tires warmed, and the force of friction gradually increased. Another variable is the driver's ability, as it is possible the driver was improving through experience driving the car. As a trend, the Skid-pad times improved from 6.85 seconds to 6.15 seconds. However, because only cold tires can be used in the Skid-pad Event at the competition, this does not include the later data from Table 3.1. A frictional force beyond μ=0.8 would not be possible, and accelerations were limited to 7.8 m/s^2 (0.8 G's) from start. Only the first row of data were used for the Skid-pad calculations, the rest are for tire coefficient modeling.

Total time (sec)	**Skid-pad time (sec)**	**Mean Accel.** (m/s^2)	**Mean Accel. (G's)**
101	6.85	7.5	0.764
128	7.25	8.4	0.856
178	6.55	8.5	0.866
191	6.0	9.7	0.989
203	6.45	9.1	0.928
216	6.15	9.4	0.958
228	5.95	9.8	0.999
240	6.1	9.9	1.01
253	6.1	9.1	0.928
264	6.1	10.1	1.03
282	6.15	10.5	1.07

Table 3.1: Skid-pad: the lateral acceleration increases with the testing time. The times improved.

Calculations and OptimumLap simulations were made to estimate the car's performance in lateral acceleration. The diameter of the track is 15.25 m, and the track width of the car, the distance between the centers of the rear wheels, is 1.2 m.

If the centripetal force is greater than the frictional force of the tires, the tires will slip. Thus, the car may slide outward of the radius of travel, and the Skid-pad Event performance decreases. Using the tire coefficient, I used the maximum frictional force to solve for the best Skid-pad time.

$$F_{friction} = (\mu)(mass)(F_{gravity}) = (0.8)(408kg)\left(9.81\frac{m}{s^2}\right) = 3202N \tag{3.1}$$

$$F_{centripetal} = F_{friction} = 3202 = (mass)(accel_c) \tag{3.2}$$

$$accel_c = \frac{F_c}{m} = \frac{3202}{408} = 7.85\frac{m}{s^2} \tag{3.3}$$

This is the maximum lateral acceleration. Next, solving for the speed from acceleration and radius.

$$speed = [(accel_c)(1.2 + diameter/2)]^{1/2} = \left[\left(7.85\frac{m}{s^2}\right)\left(8.825m\right)\right]^{1/2} = 8.32m/s \tag{3.4}$$

The distance around the circumference of the outer wheels is 55.45 m, solved for the time in seconds to complete two laps, and the ideal Skid-pad track time.

$$(2)(\pi)(radius) = 55.45m, (distance)(speed^{-1}) = \frac{55.45m}{8.32\frac{m}{s}} = 6.66sec \tag{3.5}$$

The actual data was compared to the hand calculated data and the OptimumLap simulations. The calculated time for the shortest Skid-pad lap was 6.68 seconds, but the best actual time was 6.85 seconds, a 2.5% decrease from the ideal calculations. The OptimumLap simulations resulted in a Skid-pad time of 6.43 seconds, 6.1% better than the actual. The maximum simulated lateral acceleration is 7.85 m/s^2, 5.7% better than the actual acceleration. The maximum simulated longitudinal acceleration is 9.34 m/s^2, 50% greater than the 6.23 m/s^2 figure from the MATLAB data.

A model of the tire temperature over time tested would result in a more precise figure, which would help for force equations on the tires and a more accurate prediction of performance. The coefficient increases from 0.8 to 1.05 in approximately 270 seconds (4.5 minutes). An approximate linear calculation states the maximum tire temperature would require 756 seconds (12.6 minutes) to reach the ideal operating temperature.

The longest time during the OptimumLap Endurance simulation was 30.4 minutes at the 2012 Germany Endurance. In the Endurance Event, there is a driver change half way

through the event. For the 2012 Germany course, half way is seven laps, and the second driver completes eight laps of the event. The estimated time for the first driver is 827 seconds, 9.4%, at ideal tire temperatures, and the second driver is 945 seconds, 25% at ideal tire temperatures. The total time racing at ideal temperatures is 260 seconds (14.7%). The Endurance Event average speed (49.5 kph) is approximately 71% greater than average speed of Skid-pad (29 kph), so the tires will likely increase in temperature more quickly. Accurate modeling requires both more research of the tire testing data and the collection and analysis of actual data for temperatures during Endurance testing, and it is possible performance will be better with smaller width wheels and tires.

3.3.2 Acceleration Event Test

During a track test day, data were logged from the vehicle, including power, torque, and temperatures, providing quantitative information on the car's performance in longitudinal acceleration. The temperature data were analyzed, but not expected to significantly increase from ambient temperature during a much shorter event.

For the Acceleration tests, the batteries were fully charged to 200 V_{DC}, and the controller maximum torque was set at 450 Nm, greater than the datasheet value of 408 Nm[31] to test the actual maximum value.

In addition to the data logged, some timed Acceleration tests of seventy-five meters were conducted and timed with a stop watch. The best time was 5.65 seconds, which is 71 kph, identical to the top speed during Acceleration tests. This is an average acceleration of 3.47

m/s^2. The OptimumLap Acceleration simulation was 5.38 seconds, and the actual time was 4.8% slower.

The maximum torque is 414 Nm, and peak torque was maintained for 1.3 seconds, shown in Figure 3.3. The regenerative braking feature was on, and the maximum regenerative torque was 38.9 Nm. The total torque area is much less than the Remy datasheet lists.[56] The RMS manual states performance is decreased at voltages below 320 V_{DC}, but still far below the datasheet curve.

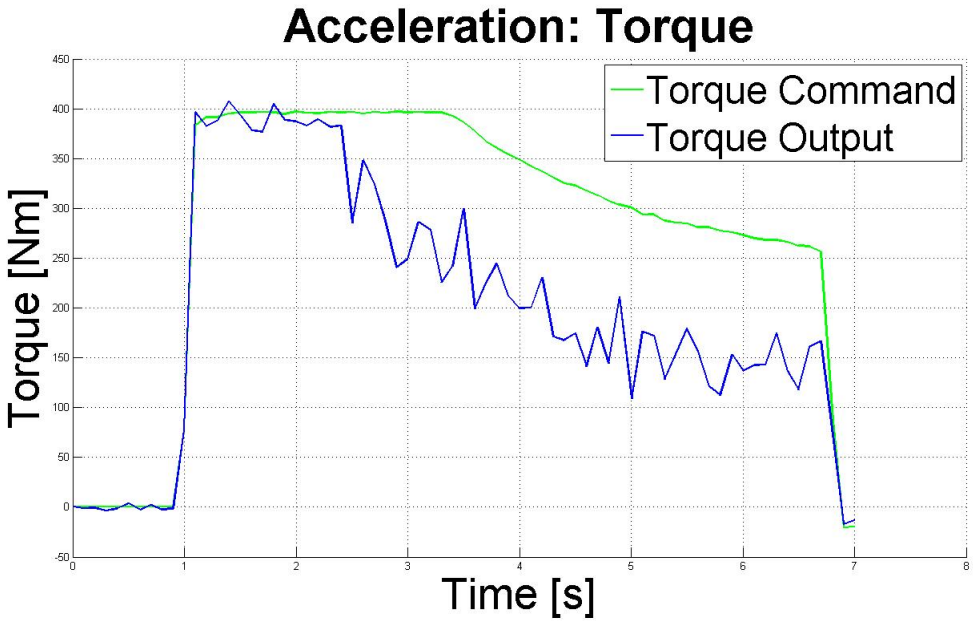

Figure 3.3: During the Acceleration test, observe the torque commanded from the controller versus the actual torque output. The actual torque varies and decreases much more quickly than expected.[6][5]

From the Remy datasheet, at 200 V_{DC}, the torque breaks sharply at a maximum of 1490 RPM, and a maximum power of 50 kW. Under load, the data listed the average voltage as 175 V_{DC}, 1.3% greater than the nominal voltage, 172.8 V_{DC}. Scaling for this decreased voltage, the datasheet states the peak torque breaks down at 1400 RPM. The torque broke at

1100 RPM, a decrease of 21%. This decrease significantly limited the torque area at peak torque draws, limiting the acceleration during testing. The batteries were out of balance, and further testing is needed to determine if the actual maximum torque breaks at 1400, or if it breaks at a lesser RPM again.

During Acceleration testing, the peak torque was reached five separate times, and analyzed. The data showed the Remy motor was capable of increasing the torque from zero to 400 Nm in approximately 100 ms. However, the motor controller can switch as fast as 7 μs, controlling peak torque much faster than the data sampling rate. The actual torque impulse time is an estimated calculation from the L/R constant.

$$5\tau = 5\frac{L}{R} = 5\frac{L}{0.667} = 100ms \tag{3.6}$$

The inductance L_q is less than 132 mH, likely in the μH range. A comparison to the known inductances of other PMSMs is shown in Table 3.2. Enstroj makes axial flux PMSMs, one has 250 Nm of torque and one with 500 Nm of torque, and the inductance for L_q ranges from 80 to 160 μH and L_d ranges from 75 to 150 μH. The Remy motor generates less torque, and the estimated inductance for the 410 Nm Remy is L_d = 123 μH, and L_q = 131 μH.

Parameter	**Emrax 228**	**Emrax 268**	**Remy HVH250**
Max current (A_{RMS})	340	360	425
Torque (Nm)	250	500	410
Flux (Wb)	0.0355	0.0664	0.168
L_d (μH)	75	150	123 (estimate)
L_q (μH)	80	160	131 (estimate)

Table 3.2: Estimations for the inductances of the Remy motor. The estimates L_d and L_q are based on similar motor inductances.[5]

If the inductance value L_q for the Remy motor is approximately 131 μH, then the impulse time for the motor is 982 μs, and the sampling rate of 100 ms samples approximately 1/100 of the data. Therefore, it is possible the actual torque spikes much more quickly than the data records it.

It is not known if motor acceleration at the ms or μs level produces useful results. Rough estimates from the data indicate 18 individual motor accelerations per minute of racing, and approximately 500 motor accelerations during an Endurance Event. The number of accelerations is significant, and analysis should be done to see if the Emrax motor with lesser inductance can improve low speed torque output. This could improve performance in both accelerating and decelerating.

If the maximum acceleration time during maximum torque is 1.5 seconds, that is 6.7% of the Acceleration time in the peak torque region, but only 2% of the total five second Acceleration time. To collect such data, the motor would need further bench testing, sending signals to an oscilloscope with a faster sampling rate of 10 kHz, and not feasible to measure with the existing setup.

During Acceleration testing, each peak had an initial spike to 400 Nm or more, then the tires slipped, resulting in the torque dropping sharply. In 300 to 500 ms, the torque went down to 200 to 275 Nm, and then spiked back to near 400 Nm.

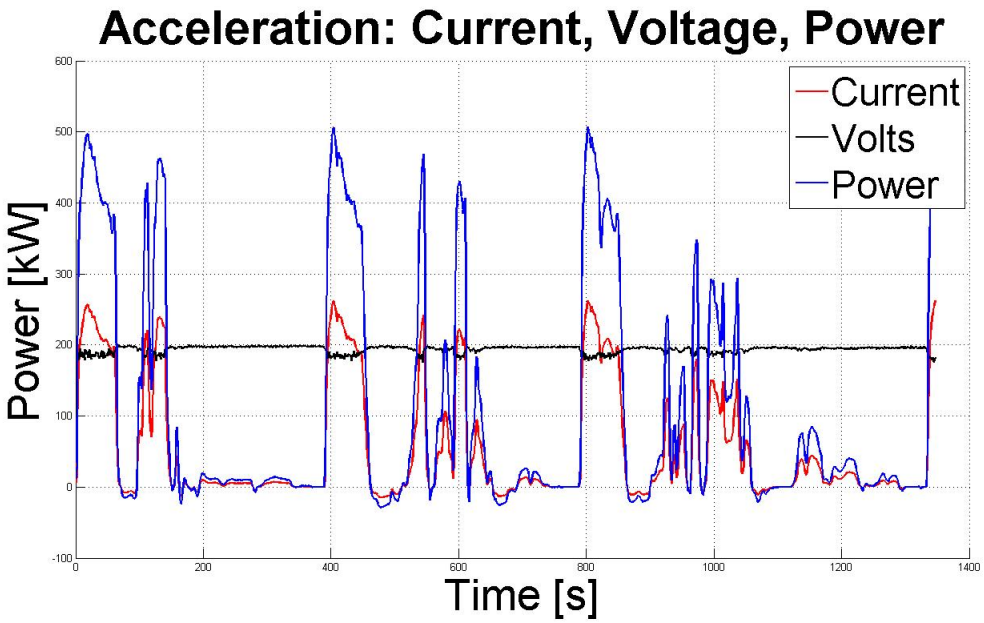

Figure 3.4: The first Acceleration test shows similar peaks for the current and power with a peak of 50.7 kW. The voltage sags from 197.6 V_{DC} to 180 V_{DC} under load.

From the same test run, the voltage, current, and power are shown in Figure 3.4. The maximum current is 262 A_{DC}, 13% less than the expected 300 A_{DC}. The maximum power is 50.7 kW, 15.5% less than the expected 60 kW. The maximum voltage is 200 V_{DC}, and the minimum is 175.8 V_{DC} under heavy current loads.

The battery cell temperatures were recorded over 240 seconds. The minimum cell temperature was the ambient temperature, 17°C, until approximately 180 seconds. The maximum cell temperature was 20°C, thus, all of the cells were acceptable temperatures, but the testing was three minutes and further cell temperature testing is needed.

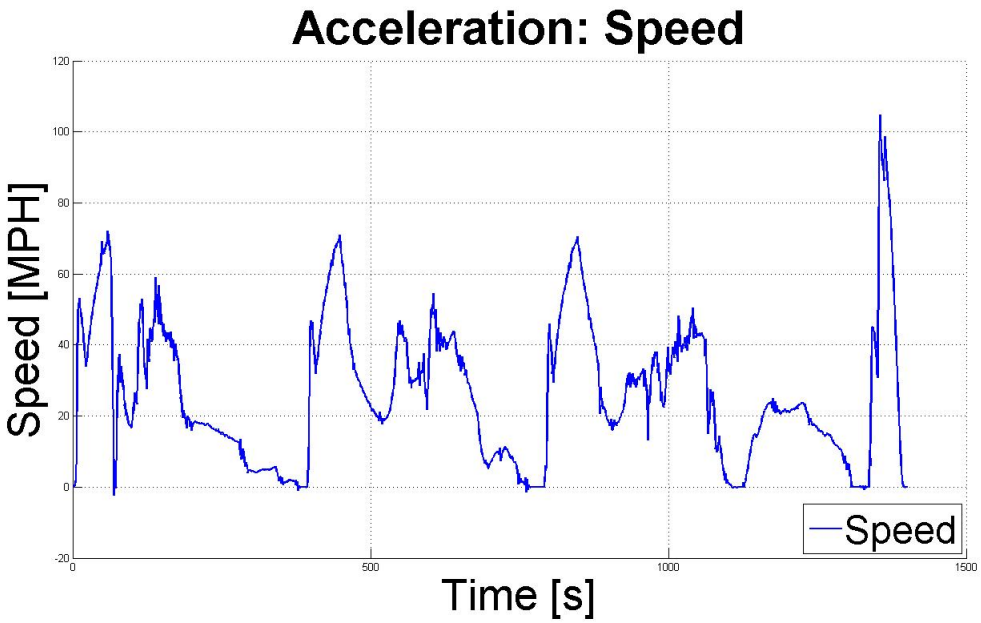

Figure 3.5: From a single Acceleration run, the speed is shown in MPH, the vehicle speed over time was recorded for straight line acceleration testing. The peak speed was 65 mph (105 kph) when the wheels were slipping. The other peaks are approximately 42-45 mph without slipping.

From Figure 3.5, the maximum motor speed was 3486 RPM during slipping, and the motor reached at least 2348 RPM without slipping on four different peaks. The speed confirms the maximum motor speed of 2500 RPM, which results in a maximum of 46 mph (75 kph). If we used the field weakening current, i_d, the top speed could be greater than 2500 RPM. The slipping demonstrates the motor has enough power to make the wheels spin. The gear reduction will need to be decreased from 3.143/1 to 2.2/1, as mentioned in Section 2.2 to attain the desired top speed of 105 kph.

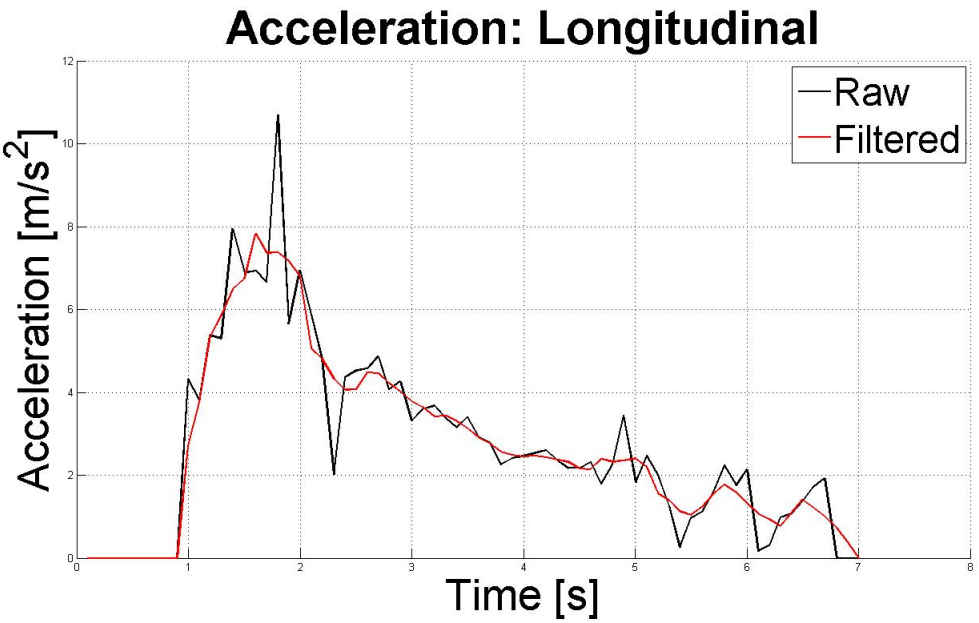

Figure 3.6: The maximum acceleration value is 10.66 m/s^2, and the maximum filtered value is 7.8 m/s^2. The acceleration decreases due to diminishing torque and power as speed increases, and the top speed is 2500 RPM.

As shown in Figure 3.6, the maximum acceleration was 10.66 m/s^2, so it was filtered for a more accurate value. The data were filtered using the convolution function in MATLAB[6], and the result is approximately 7.8 m/s^2. The maximum acceleration value in the Optimum-Lap simulations was 9.15 m/s^2. After the track testing, this was further examined. From Newton's second law, F = ma, I solved for acceleration based on the known values for force and mass:

$$accel_{max} = \frac{Force}{mass} = \frac{2511}{408} = 6.15\left[\frac{m}{s^2}\right] \tag{3.7}$$

The value contrasts the track data by 27%, so either the acceleration data is not accurate or the unknown variable, the coefficient of friction, μ, was greater than 0.8. Based on the Skid-pad results, the value μ=0.8 seems accurate for lateral acceleration and the same value

was anticipated for longitudinal acceleration. The filtered acceleration value equates to a tire coefficient of μ = 0.93, which is 16% greater than expected. The ambient temperature is 22°C, and it was assumed the tires were cold at ambient temperature, but we did not have tire temperature data.

To test the accuracy of the tablet, I took a sample of the accelerometer data, the z-axis, and compared it to the average force of gravity, 9.81 m/s^2. The first ten points of data had an average of 10.0 m/s^2, 1.9% greater than 9.81 m/s^2. Since no other means of verifying the accuracy of the vertical force were available, the assumption was made that the force of gravity in Portland, 10.0 m/s^2, will be similar in Lincoln, Nebraska in June.

Peak acceleration is a useful value, but the average acceleration over the entire Acceleration event is more important. From the MATLAB data, the average acceleration is 3.22 m/s^2, a 7.8% decrease from the stop watch Acceleration test. Further data on acceleration will be useful for modeling.

For future track days, tire temperature data will be useful to determine μ. The difference between the maximum forces that can be applied in the calculated and actual values varies by 73%, so it is important to get a closer figure to best design the car.

3.3.3 Endurance Test Performance

Data were logged during an Endurance Event from the vehicle including power, torque, and temperatures, providing quantitative information on the car's performance. We anticipated the temperatures of components would increase much more in the longer event. The data

were analyzed to test the car's performance in Endurance and compared to the OptimumLap simulations from Table 2.7, and to determine if we reached temperature specification limits for the motor, controller gate driver board, and motor.

Parameter	Ideal Value	Actual Value
Current (A_{DC})	300	252
Voltage (V_{DC}	200	182.5
Torque (Nm)	410	414
Max Regen (Nm)	50	38.9
Max Speed (kph)	75.1	54.7
Avg. Speed (kph)	49.5	36.5
Avg. Power (kW)	10.9	9.25
Energy Use (Wh/m)	0.131	0.254
Distance (km)	22	4.9

Table 3.3: For the Endurance testing, the current, voltage, and torque are compared to the Remy datasheet. The actual data was compared to the OptimumLap Endurance simulations for maximum speed, average speed, average power, and energy use. The run was made after the Acceleration testing, and the car was tested on a partial battery charge. The cells became out of balance, and drastically decreased performance.

During the test, the peak torque and current values were as expected, but the cells began going out of balance in time. The Endurance test was approximately 486 seconds, or 8.1 minutes. Shown in Table 3.3, the voltage dropped, and the car was only able to travel 4.9 km of the track. The mean power was 9.2 kW, and the mean speed was 36.5 kph. Since the average power was 9.2 kW, and the battery pack contains 4.75 kWh of energy, the car should provide 31 minutes of testing at that power. At a lower than average speed, the car consumed more energy (0.254) than faster cars (0.131) at the competition. The motor performance was acceptable, but the overall car performance suffered from unbalanced battery cells, and was unable to complete the 22 km event.

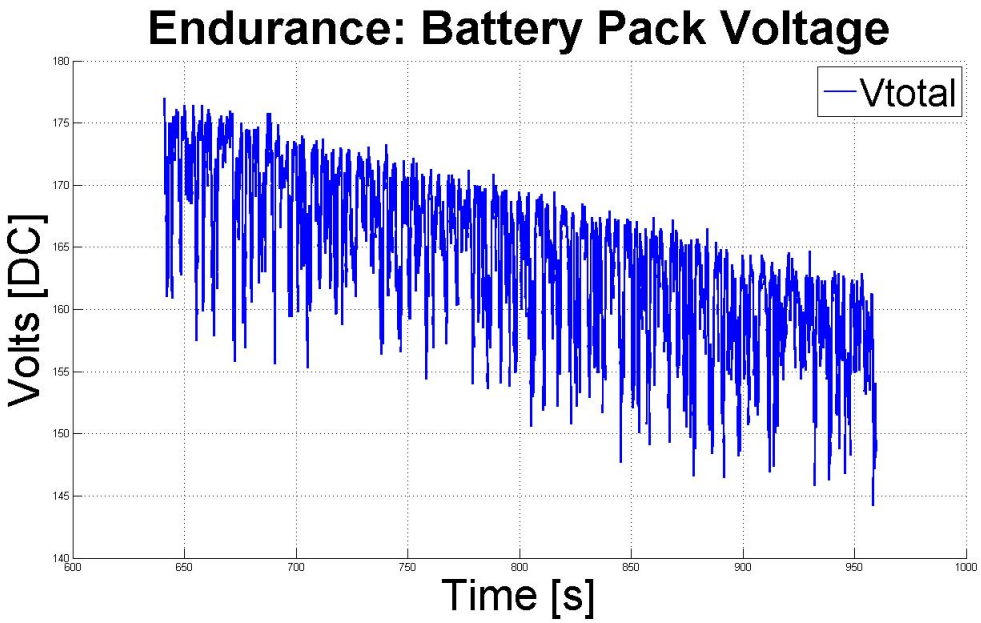

Figure 3.7: The total voltage drops over the course of the eight minute test run from 177 V_{DC} to 144 V_{DC}.

The battery pack voltage drains from 177 V_{DC} to 144 V_{DC} in 5.3 minutes. The usable voltage range is from 120 to 196 V_{DC}, and the Endurance test was started at 177 V_{DC}, shown in Figure 3.7. Note that 144 V_{DC} total is an average of 3.0 V_{DC} per cell, but if one cell drops to 2.5 V_{DC} per cell, the car must shut down, and it did. The maximum current was 248 A_{DC}, the minimum was -26.1 A_{DC} during regenerative braking, and the mean was 64.8 A_{DC}. Testing the car on a full charge with balanced batteries would be useful to create a baseline discharge curve to provide more accurate modeling and compare against the Enerdel datasheet.[47]

The IGBT gate and the cell maximum temperatures peaked in the low thirties in the 8.1 minute test, shown in Figure 3.8. The cell temperature increased four degrees, and scaling that for an entire Endurance test results in 38°C, 13°C greater than ambient temperature.

The cell temperature is crucial to both performance and avoiding faults, and well below the maximum 55°C temperature. The IGBT board is not a great concern for faults, but useful for controller conditions and efficiency, and 31°C is acceptable. The motor temperature increases to 65°C, and is increasing in temperature at a rate of 5°C per minute. The increase is acceptable to 140°C when the efficiency drastically decreases[56], and the limit is 160°C.[1] At the rate of increase, the temperatures could reach 153°C, and will decrease motor efficiency. After 160°C, damage may result to the insulation windings or other motor parts.

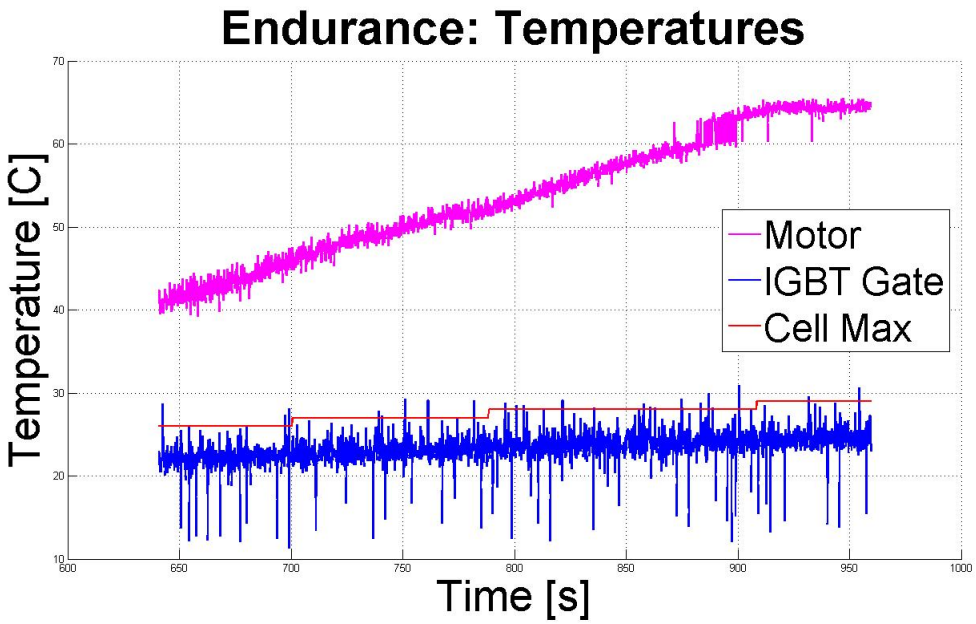

Figure 3.8: The motor maximum temperature is 65°C, gate temperature maximum is 31°C, and cell temperature maximum is 29°C.

During the Formula SAE Endurance Event, there is a break of at least three minutes in the middle of the event. While the break is challenging for combustion race cars completing a "hot start", it is an advantage for electric race cars, as the motor does not need starting.

Also, the break allows the power electronics, motor, and batteries to cool. All temperatures should be further tested for modeling actual values during a demanding Endurance test, including the rate of cooling to determine expected temperatures.

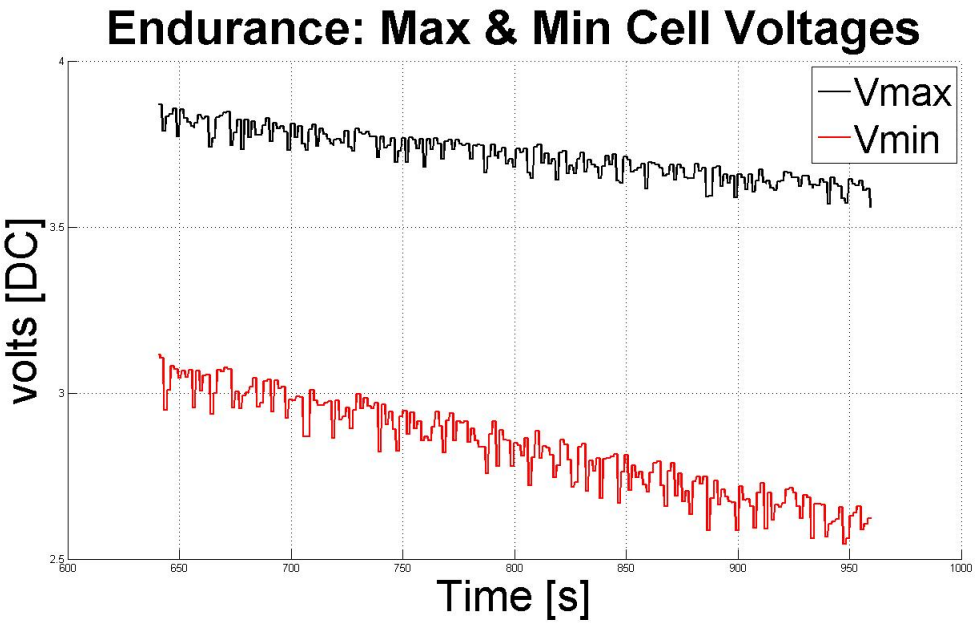

Figure 3.9: The individual maximum and minimum cell voltages. The maximum and minimum cell voltages started at 3.9 V_{DC} and 3.25 V_{DC} and ending at 3.6 V_{DC} and 2.6 V_{DC}, respectively.

The batteries were out of balance and a major problem, hindering performance. The cutoff voltage is 2.5 V_{DC}.[47] In Figure 3.9, the cell with the greatest voltage experienced a voltage drop of 0.3 V_{DC}. The minimum cell voltage is 0.65 less than the original value, 3.6 V_{DC}, a 117% greater drop. The cells are out of balance, and it decreased the range and power output. There must be a procedure to balance cells more quickly, as the EVCU takes at least 24 hours to fully balance them. The battery balancing is a major problem that will need to be addressed for both cell performance and protection from damages.

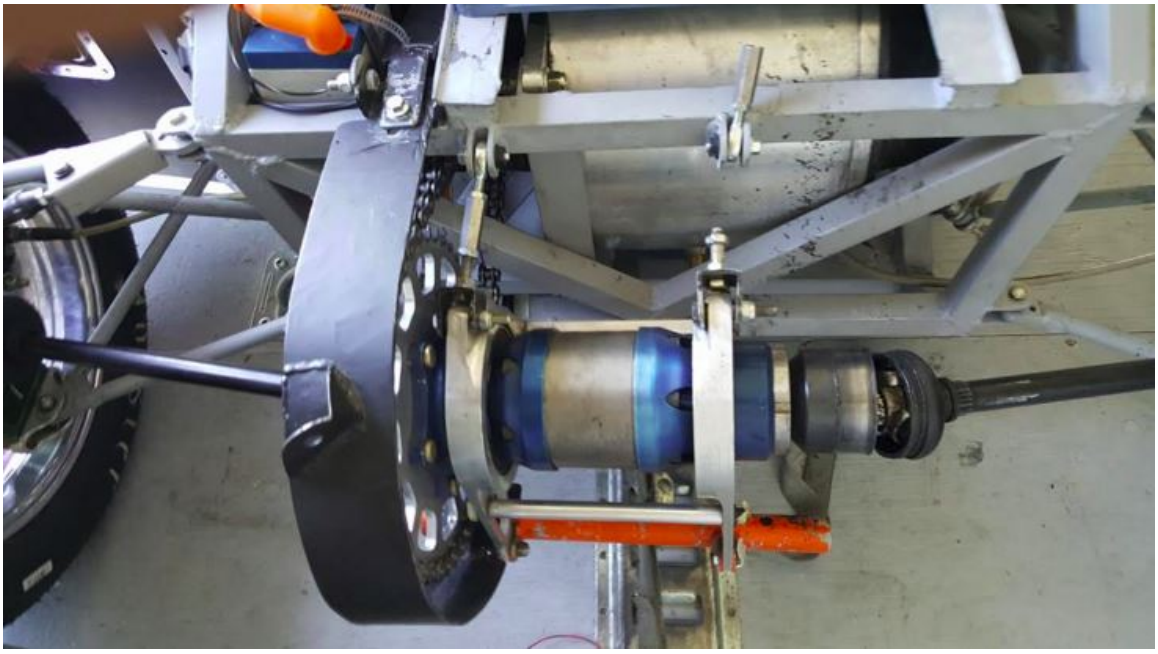

Figure 3.10: The drivetrain failed, the differential was not damaged, but the halfshaft teeth were damaged and not usable.

After this data was collected, there was a mechanical failure with the drivetrain, shown in Figure 3.10. Because of the 13° angle placed on the halfshafts, there were undesired forces placed on the differential. The turnbuckles became unscrewed, and the differential was dismounted from the chassis. The differential mounting broke, ending the testing during the summer of 2015. An improved design was created to avoid repeating this mechanical failure.

3.4 OptimumLap Model

The race car was tested for its maximum performance in all of the dynamic events. Next, possible improvements were considered for the electric race car. Some improvements would be decreasing the weight of the car by replacing the motor. The car was simulated in

OptimumLap, keeping all variables the same, except the motors. Each motor would be simulated, and the optimum gear ratio was found. Once the ideal gear ratio was found, the motor, gear ratio, and total mass variables were entered into OptimumLap, simulated, and compared against other motors.

Race Car Motor	**Remy**	**Emrax 1**	**Emrax 2**	**Honda**
Motor model	HVH250-115S	207	228	CBR600
Motor type	PMSM	PMSM	PMSM	Gasoline
Vehicle Weight (kg)	408	363	370	318
Germany Endur. '12(s)	92.4	91.3	90.8	90.7
Autocross (s) NE '13	57.0	56.8	56.7	56.1
Skid-pad (s)	5.18	5.84	5.55	4.91
Acceleration (s)	5.8	5.6	5.6	5.0
Rotating Mass (kgm^2)	0.069	0.0421	0.0421	unknown
Cooling medium	air	water	water	water
Max efficiency (%)	94	98	98	30
Peak speed (RPM)	10500	6500	6500	13000
Peak torque (Nm)	400	70	240	63
Peak power (kW)	80	59	100	72

Table 3.4: Simulated dynamic event results. Note the combustion car is the lightest, and performs best in many of the events even with much less power.

In Table 3.4, the VMS combustion race car was compared against the existing VMS electric car with a Remy motor, and two potential cars with light, high performance motors. The combustion car is 12% lighter than the lightest electric car option, has the least power, and performed better in every event. The electric car meets the maximum forces applied to the tires, and it needs to scale down the weight from all areas of the car. The OptimumLap simulation on the Emrax 228 motor comparing different total weights found the car did best in Skid-pad with a mass of 335 kg and best in Acceleration with a mass of 300 kg. The best

results will be found decreasing the car weight closer to 300 to 335 kg, and further modeling is required when changes are more defined.

3.4.1 Formula SAE Electric Competition Records

All of the data from past Formula SAE competitions are listed in the Appendix A. The VMS car times were compared against those times.

Event/Parameter	Achievement	Year	College/Team
Lightest (kg)	151	2015	Illinois Inst. of Tech
Design Score	150	2013, 2014	UniCamp, McGill
Presentation	75	2013,'14,'15	UWash, UWash, UPenn
Cost Score	93.55	2013	UniCamp
Cost (US $)	$\$15,540$	2015	Univ of Akron
Acceleration (sec)	4.164	2015	Univ. of Pennsylvania
Skid-pad (sec)	5.431	2014	UniCamp
Autocross (sec)	53.514	2014	McGill
Endurance (sec)	1526.348	2014	UniCamp
Efficiency Score	100	2013, 2014	UniCamp, UniCamp
Energy Used (kWh)	2.891	2014	UniCamp
Total Score	985.4	2013	UniCamp

Table 3.5: Formula SAE competition records: summary of results, best scores, year and team.

The most electric race car teams to complete all dynamic events is three in 2014. In both 2013 and 2015, only one team completed all of the dynamic events. In Table 3.5 Design (150) and presentation (75) are the maximum possible scores, awarded to UniCamp from Brazil and McGill from Montreal. Skid-pad and Acceleration are valuable testing metrics, as they isolate lateral and longitudinal acceleration and are easy to replicate for testing. The best electric Skid-pad time was 5.431 seconds, and comparing to the 2015 combustion results, that would rank 28th out of 40. Electric cars still do not perform as well in Skid-pad,

likely due to the extra weight from batteries and increased center of gravity. The University of Pennsylvania electric race car completed Acceleration in 4.164 seconds, which would have been 4th place out of 42 in the combustion Acceleration Event. The fastest combustion cars are approximately 11% faster in Autocross, and 13% faster in Endurance. The best total score was 985.4 in 2013, and UniCamp was the only team to compete in any dynamic events, achieving almost all of the possible points. For combustion, the best score in 2015 was 890.4 by San Jose State, finishing first out of 65. For Formula SAE Electric, in 2016 and beyond, there are 40 registered teams and the competition has been growing. It is unlikely that only one team passes technical inspection and competes in all dynamic events, making the score 985.4 very challenging to surpass.

Event/Parameter	**Achievement**	**EV Record**	**% From Record**
Weight (kg)	408	151	63%
Design Score	70	150	114%
Presentation	67.5	75	11.1%
Cost Score	33.13	93.55	182%
Cost (US $)	*$33,248	$15,540	53.3%
Acceleration (sec)	5.65	4.164	26%
Skid-pad (sec)	6.85	5.431	21%
Autocross (sec)	unknown	53.514	unknown
Endurance (sec)	2170	1526.348	30%
Efficiency Score	unknown	100	unknown
Energy Use/km (kWh/km)	0.254	0.1314	48%
Total Score	110.7	985.4	790%

Table 3.6: VMS EV versus Formula SAE Electric performance. *The cost event results state the VMS car cost is $33,248, but our bill of materials A.1 states the car was $27,042.73.

The VMS electric car is heavier than most electric race cars. In 2014, the design score was 70/150, signifying much room for improvement, shown in Table 3.6. The presentation

was 67.5/75, a great score. The cost was far too much, twice as much as the lowest. Scaling down the car with a smaller motor, battery pack, and chassis results in much less weight, and better track times. The team lost 60 points due to late documentation. Thus, the overall score was 110.7 out of 225 possible static events, and 0 out of 675 for dynamic events.

The car did not pass technical inspection, and did not compete in dynamic events. The TSAL did not turn on without manually pressing the button, thus, did not meet the rules.[13] The BSPD used the calculated current from the 0-5 V_{DC} throttle position signal that results in 5 kW of motoring power, and the rules state the actual power measurement is required.[13] The IMD did not drive enough current to open the shutdown circuit, and the latching relay circuit was incomplete.

Only three cars out of twenty passed in 2014 and 2015. Passing technical inspection and competing in dynamic events will be major accomplishments for VMS. Rather than just drive on the track, we strive to compete and perform well against great competitors.

3.5 Summary

Track testing was conducted to gather performance data for the Formula SAE dynamic events, compare results to calculations and simulations, and compare our results to other teams' electric race cars from past competitions. The testing was done to gather performance data, including peak torque, peak power, and temperatures over time. The first generation car was tested on an Autocross course in the rain, and went 31.4 km on a single battery charge, but the range in ideal conditions is less. The peak power was 51 kW, 15% less than

the calculated peak, because the current was 14.5% less than the Remy datasheet. However, the peak torque met the 400 Nm value on the Remy datasheet. The car handled poorly in sharp turns, and the inner rear wheel came off the ground during cornering. The second generation car was tested in Skid-pad, Acceleration, and Endurance courses.

In Skid-pad, the car required only 11% of the motor's peak torque, and the time with cold tires was 6.85, 21% slower than the fastest record from the competition. Lap times improved over the duration of the run, likely due to tire frictional forces increasing with temperature, but there were no tire temperature sensors to confirm this. The actual time was 2.5% worse than the calculated time, and 6.1% worse than the OptimumLap simulation.

The best Acceleration time was 5.65 seconds, 26% slower than the fastest record from the competition. The actual time was 4.8% slower than the OptimumLap simulation of 5.38 seconds. This difference is relatively low, but could be from the actual frictional force of the tires having less grip, less weight transfer, battery cell imbalances decreasing average power, or the driver not driving the car at its maximum performance. The calculated average acceleration from the fastest run was 3.47 m/s^2, and the track data calculated an average acceleration of 3.22 m/s^2, 7.8% less. The maximum speed was 75 kph, which was the expected speed. The peak torque was 414 Nm, but the torque broke 21% sooner than expected. This is likely due to the battery cells being out of balance, which showed later in the Endurance test.

The Endurance Event is 22 km, but due to battery cell voltage imbalances, the test ended after 4.9 km from an undervoltage fault. We knew that the cells were capable of

propelling the car for 31.4 km with cold tires, but were unable to get a full Endurance Event test with hot tires, as a drivetrain failure ended the testing for 2015. Therefore, the projected Endurance time for 22 km was based on the 4.9 km test data, and the result was a time of 2170 seconds. This is 30% slower than the fastest record. However, the average Endurance Event time from the OptimumLap simulations was 1600 seconds, only 4.8% slower than the Endurance record. The actual best case Endurance time is likely between the ideal OptimumLap simulation and the shortened test run with diminished battery power from imbalanced cell voltages. This actual case requires further testing to determine the Endurance time.

At the 2014 Formula SAE competition, the car did not pass the Formula SAE Electric judges' technical inspection. The main problems were the TSAL, BSPD, IMD, and latching circuits. The TSAL was not blinking when high voltage was on without pressing a button (not meeting the rules), the BSPD was a bad design that did not work, the IMD circuit did not drive enough current to open the shutdown circuit, and the latching relay circuits were not wired correctly, thus, not working to latch fault signals from the IMD and BMS. After working on the circuits for two days and testing each circuit independently, we were uable to fix all circuits and meet the rules. For the 2015 competition, VMS withdrew from the competition because the high voltage circuits were not completed, thus, no track testing was done. Regardless of Formula SAE competition performances, we were able to design, implement, and evaluate two generations of electric race cars and compare the results to our calculations, simulations, and performances of other electric cars from past competitions.

4 Discussion

4.1 Successes

A foundation of research, design, manufacturing, and performance data was obtained through the first two generations of the electric race car at Portland State University. This included the strengths and weaknesses of different design parameters and performance metrics such as: power, torque, temperature, acceleration, motor and vehicle speeds. The performance data was compared to the competition performance data of the other Formula SAE Electric race cars.

The electrical engineering efforts for the race car have been productive. The hardware and software have been built and tested for the TSAL, IMD, latching circuits, precharge and discharge, the charging system, high voltage tractive system. Research and selection of the motor, controller, and battery cells have been used to create a high performance race car. The throttle plausibility was accomplished in software. Much analysis has been done with data in MATLAB on existing data, which is valuable to validating designs and making improved ones. A new and improved EVCU is being built that has consolidated many circuits on one board.

Every aspect of the electric race car can be improved, and the entire race car must be scaled down in size. An EVCU and accurate data logging were established, but more testing

and data would be useful. Only two tests of the longer Endurance events were conducted, and the batteries were out of balance, not displaying their maximum performance. This will further the modeling of the battery state of charge calculations that are crucial to properly size the battery pack.

It will be important to get more precise battery models. For optimal performance, it is critical to balance peak acceleration by decreasing the battery pack weight, but having enough battery energy to perform well and complete the Endurance Event. The technology and applications continue to evolve, and it will be interesting to see how the next generation car performs against the calculations and models.

When redesigning the car, it will be useful to repeat method outlined in Section 2.1: navigate the design process with the known constraints, examine them individually, and then adjust the overall model for the improved variables.

4.2 Failures

VMS did not pass the Formula SAE Electric judges' technical inspection in 2014. There were several circuits that were incomplete or did not work, causing it to fail (listed in Section 3.5). The race car weighed 456 kg with a driver, and cost approximately $27,043. All of these issues needed to be drastically improved.

VMS withdrew from the 2015 competition due to not completing the race car. The weight was decreased, but the battery containers did not get finished, and not all of the circuits were complete. The differential carrier was a weakness, too much angle was placed

on the halfshafts, creating a large angle that added losses. The carrier eventually broke during testing, ending the 2015 season.

5 Conclusion

5.1 Looking Forward

5.1.1 Future Designs

There are several aspects of the electric race car that can be improved that are simple in concept, but much more difficult to execute. Implementing the lighter, axial flux Emrax motor, increasing the battery voltage to 300 V_{DC}, decreasing the total mass, testing the tire temperatures, optimizing the gear reduction, and creating simpler, consolidated circuits will increase the performance and design of the race car.

Using a smaller motor with less weight allows for quicker acceleration and deceleration, both in terms of the inrush current time of increasing the electromagnetic field, and in mechanical inertia resisting rotor movement. For example, the inertia of the Remy motor's rotor is 0.069 kgm^2, while the Emrax rotor is 0.0421 kgm^2, a reduction of 39%. Remy provides thorough information on the counter EMF of a decrease of 80 volts per 1000 RPM. In the radial flux Remy motor, when motor speed increases, the EMF can not be maintained. Therefore, torque and power decrease with speed. There is some skepticism regarding an axial flux motor essentially eliminating counter EMF, a major drawback characteristic in radial flux motors. The Emrax datasheet states the counter EMF reduction is true[2], and

VMS looks forward to testing this dynamic, high performance motor in the future.

At 300 V_{DC}, the motor will have greater peak power, thus, the car will have an improved average acceleration. For the Remy motor and RMS motor controller combination, the derived maximum theoretical power at the motor's rotor(2.21) was 60 kW. The actual motor power was 50.7 kW before drivetrain losses, 15.5% less than expected. At 300 V_{DC}, the theoretical maximum power is 90 kW, but limited to 80 kW by rule4s, and the actual power should be at least 76.5 kW. Increasing to 300 V_{DC} increases the peak power by 50%[25], and could achieve an average acceleration of 5.2 m/s^2.

During track testing at PIR, the peak current draw was much less than the available peak current, thus, the power density was not as important as the energy density. The maximum current draw from the Remy motor was 262 A_{DC}, and 480 ADC is the peak battery current. For the Emrax motor, the maximum current for 80 kW at 300 V_{DC} is approximately 267 A_{DC}. Many power cells can generate the maximum power required. The Enerdel 16 Ah cell used outputs 240 A_{DC} peak, 11.3% less than the ideal maximum. However, that is the peak rating for ten seconds, and the cell might reach the peak goals. Going forward, it is important to create a 300 V_{DC} battery pack with enough kWh to race 22 km, reach approximately 267 A_{DC}, and minimize the total battery pack weight.

When the voltage is increased to 300 V_{DC}, this decreases the average current and the discharge rate. The internal impedance is constant regardless of the voltage or current, so it is ideal to reach the greatest voltage allowed. An estimate of the discharge rates for the current 200 V_{DC}, 48 cells in series and 2 parallel configuration, battery pack is 1.97 C. The

calculations and OptimumLap simulations show this allows for approximately 30.5 minutes of Endurance testing. At 300 V_{DC}, 75 cells in series and 1 parallel, the discharge rate is 2.63 C, allowing approximately 22.8 minutes of Endurance testing at the average power rate of the current car. However, when the mass decreases significantly, the average force decreases significantly, and less energy is required to drive 22 km. The car mass, cell's peak current, and total energy use for 22 km will need to be reevaluated and further tested for more accurate modeling and improved designs.

The total mass of the car needs to be reduced by 100 kg, which is a difficult task requiring a complete redesign and build of many subsystems, shown in Table 5.1. The future electric motor will reduce the car mass 38 kg and not sacrifice the power output. Eliminating one of the two battery boxes will save much weight for the container, half of the high voltage cables, low voltage wiring harnesses, three one pound contactors, fuses, insulating material, fasteners, and chassis mounting. Aluminum boxes are more difficult to weld than steel, but decrease the weight. Changing from 200 to 300 V_{DC} with balanced batteries reduces the cell mass from 42 kg to 33 kg. The chassis and all other components on the car should be reconsidered for weight, including the wheels and tires. These reductions in weight also decrease the total cost of the car, improving the competition score. After reducing the weight 100 kg (Equation 2.10), if the weight transfer during acceleration is kept proportional, 78% or more, the average acceleration rate over the entire Acceleration test (3.47 m/s^2) will also increase.

Parameter	change (kg)	total (kg)
2015 EV	0	408
Replace motor	-38	370
Eliminate one battery box	-15	355
Make aluminum box	-6	349
Increase from 200 to 300 V_{DC}	-9 max	340
Decrease chassis weight	-32	308
Total		308

Table 5.1: The main weight factors and the estimated differences between the 2015 EV and potential electric race car. The motor, batteries, and chassis are the main factors considered.

The race car does not have tire temperature sensing, which is useful for determining optimal tire temperatures for the Endurance Event. The tires do not get to the optimal temperature (93°C) during Skid-pad, Acceleration, and the Autocross Events, and wider wheels and tires could be decreasing performance. OptimumLap does not have a setting for tire width adjustments, but OptimumTire[57] software does. VMS did not have this software, but it would be useful to make simulations. Then, the car is tested at the track and tire simulations are compared to tire temperature readings and Endurance test times. When the changes in mass are completed, the tire temperature data is also very important, and the 6 or 6.5 inch tires and wheels could possibly perform the best.

With the Emrax motor, the torque is 240 Nm instead of 410 Nm, and the load transfer on the rear wheels is less at the decreased weight. If the car weight is much less, the frictional forces and load transfer change. This requires new calculations, and likely a new rear sprocket. If the mass is 308 kg, the new frictional force is:

$$f_{friction} = \mu N = (0.8)(W_T)(g) = (0.8)(241.5(kg))\left(9.81\frac{m}{s^2}\right) = 1895N \tag{5.1}$$

The force from the torque is 957 N, a gear reduction of 2.286/1 after 86.5% losses is approximately the ideal ratio.

The circuits created are crucial to the car passing technical inspection, and they need to work under harsh conditions. Even if the car passes the rigorous technical inspection, the hardware needs to withstand high temperatures, harsh vibrations, and high EMI during track events. During past competitions, some circuits did not meet the rules, were not complete or did not work properly. At the 2014 Formula SAE competition, the car did not pass technical inspection, and the main problems were the TSAL not blinking without pressing a button (not meeting the rules), the BSPD was a bad design that did not work, the IMD circuit did not drive enough current to open the shutdown circuit, and the latching relay circuits were not wired correctly, thus, not working to latch faults from the IMD and BMS. For the 2015 competition, VMS withdrew from the competition because the high voltage circuits were not completed, thus, no track testing was done. VMS is currently creating a 2016 Formula SAE Electric race car, and efforts have been made to consolidate all circuits with any high voltage (shutdown circuit: IMD, precharge, discharge) into the main battery box, and all circuits with exclusively low voltage (BMS, BSPD, status indicators, latching circuits) into the EVCU container.

The Formula SAE Electric competition is a challenging and requires much planning and coordination between engineering and other students to design, build, and test the electric race car. It is important to make realistic goals and timelines based on the team's budget, number of teammates and abilities, and fabrication resources. VMS is track testing the 2016

car in May, and looking forward to improving our track performance.

Bibliography

[1] HVH250 Motor Manual. [Online], (2016). http://www.neweagle.net/support/wiki/images/archive/a/a6/20140501174637!HVH250_MotorManual20110408.pdf.

[2] Manual For Emrax Motor, (2016). http://www.enstroj.si/download.php?f=images/stories/emrax_228_tech_data_table_dec_2014.pdf.

[3] ENERDEL DEBUTS PPA 300-689 VIGOR+ ENERGY STORAGE SYSTEM (ESS) FOR USE IN ALLISON NiMH-BASED HYBRID BUSES. [Online], (2015). http://www.enerdel.com/wp-content/uploads/2013/04/ENERDEL-DEBUTS-PPA-300-689-VIGOR-ENERGY-STORAGE-SYSTEM-ESS.pdf.

[4] Evan Waymire. Email communications with Evan Waymire, PE, Racing Industry Adviser, (2016).

[5] Viking Motorsports: Work Completed by Quinn Sullivan, PSU ECE Student, (2014)(2015)(2016).

[6] Viking Motorsports: Work Completed by Michal Podhradsky, PSU ECE Student, (2014)(2015)(2016).

[7] Viking Motorsports: Work Completed by Tyler Gilbert, PSU ECE Student, (2015)(2016).

[8] Viking Motorsports: Work Completed by Trevor Conant, PSU ECE Student, (2014)(2015).

[9] Viking Motorsports: Work Completed by Xander Jole, PSU ME Student, (2015).

[10] Viking Motorsports: Work Completed by Troy Brown, PSU ECE Student, (2013)(2014).

[11] Viking Motorsports: Work Completed by Nick Cho, PSU ME Student, (2015)(2016).

[12] About Formula SAE Series. [Online], (2016). http://students.sae.org/cds/formulaseries/about.htm.

[13] 2015-16 fsae rules. [Online], (2016). http://students.sae.org/cds/formulaseries/rules/2015-16_fsae_rules.pdf.

[14] FSAE Lincoln Courses. [Online], (2016). https://drive.google.com/folderview?id=0Bxeyn45rNs51M3FXb21DcnBVNzQ&usp=sharing.

[15] OptimumG: OptimumLap. [Online], (2016). http://www.optimumg.com/software/optimumlap/.

[16] Viking Motorsports. [Online], (2016). http://vms.groups.pdx.edu/.

[17] James B. Spicer. Effects of Frictional Loss on Bicycle Chain Drive Efficiency. *ASME*, 123, (2001).

[18] Efficiency of the Planetary Gear Hybrid Powertrain. [Online], (2016). file:///C:/Users/qsullivan11/Downloads/Article.pdf.

[19] Optimisation of the Chain Drive System on Sports Motorcycles. [Online], (2016). http://www.ducati-upnorth.com/tech/chain.pdf.

[20] Bob Brant Seth Leitman. *Build Your Own Electric Vehicle*. McGraw-Hill, 2009.

[21] Vehicle Longitudinal Load Transfer parts. [Online], (2013). http://www.slideshare.net/billharbin/vehicle-load-transfer-parts-iiimar13.

[22] Friction and Coefficients of Friction. [Online], (2016). http://www.engineeringtoolbox.com/friction-coefficients-d_778.html.

[23] Carbon Fiber Wheels. [Online], (2016). https://kb.osu.edu/dspace/bitstream/handle/1811/58422/carbon_wheel_thesis_FINAL.pdf?sequence=1.

[24] Remy - NewEagleWiki. [Online], (2015). http://www.neweagle.net/support/wiki/index.php?title=Remy.

[25] HVH250 r3 Sept 2010. [Online], (2016). https://www.remyinc.com/docs/HVH250_r3_Sept_2010.pdf.

[26] EV Source - NetGain WarP 13 Electric Motor. [Online], (2015). http://www.evsource.com/tls_warp13.php.

[27] White Zombie. [Online], (2016). http://datsun1200.com/modules/mediawiki/index.php?title=White_Zombie#White_Zombie_2000_Specification.

[28] Iqbal Husain. *Electric and Hybrid Vehicles: Design Fundamentals*. CRC Press, 2003.

[29] General Purpose Permanent Magnet Motor Drive without a Speed Sensor. [Online], (2016). http://www.automation.com/pdf_articles/yaskawa/WP.AFD.05.pdf.

[30] Reduction of Cogging Torque in Permanent Magnet Machine. [Online], (2016). http://www.slideshare.net/krithikk/reduction-of-cogging-torque-in-permanent-magnet-machine.

[31] Pm100 and pm150 family propulsion inverters. [Online], (2016). http://www.rinehartmotion.com/uploads/5/1/3/0/51309945/pm100-150datasheet_2.pdf.

[32] Remy HVH250R3. [Online], (2016). http://www.remyinc.com/docs/HVH250R3.pdf.

[33] Parker GVM210 datasheet. [Online], (2016). https://www.parker.com/parkerimages/Parker.com/Divisions-2011/Electromechanical Division - North America/Markets/Photos/GVM210 Traction Motors.pdf.

[34] eAssist AC Induction Motor [Archive] - ElMoto.net - The Electric Motorcycle Forum. [Online], (2016). http://elmoto.net/archive/index.php/t-2676.html.

[35] Motors for Electric Cars - Electronic Products. [Online], (2016). http://www.electronicproducts.com/Electromechanical_Components/Motors_and_Controllers/Motors_for_electric_cars.aspx.

[36] Stephen J. Chapman. *Electric Machinery and Power System Fundamentals*. McGraw-Hill, 2002.

[37] First Run: 2012 Buick LaCrosse With eAssist. [Online], (2016). http://www.thevirtualdriver.com/drivers-seat/2011/7/29/first-run-2012-buick-lacrosse-with-eassist.html.

[38] Harmonics in Power Systems. [Online], (2016). https://www.industry.usa.siemens.com/drives/us/en/electric-drives/ac-drives/Documents/DRV-WP-drive_harmonics_in_power_systems.pdf.

[39] Definition of an Axial Flux Permanent Magnet Alternator. [Online], (2016). http://www.aerco.co/uploads/Definition_of_an_Axial_Flux_Permanent_Magnet_Alternator.pdf.

[40] A Comparison Between the Axial Flux and the Radial Flux Structures for PM Synchronous Motors. [Online], (2016). http://ieeexplore.ieee.org.proxy.lib.pdx.edu/stamp/stamp.jsp?tp=&arnumber=955750.

[41] Curtis PMC Manual. [Online], (2016). http://www.evsource.com/datasheets/curtis/Curtis_manual.pdf.

[42] IGBT or MOSFET: Choose Wisely. [Online], (2016). http://www.irf.com/technical-info/whitepaper/choosewisely.pdf.

[43] Types of Lithium-ion Batteries – Battery University. [Online], (2016). http://batteryuniversity.com/learn/article/types_of_lithium_ion.

[44] Professor Jeff Dahn - Waterloo Institute for Nanotechnology Seminar Series. [Online], (2016). https://www.youtube.com/watch?v=9qi03QawZEk.

[45] Quinn Sullivan's photographs, (2016).

[46] 38120S 10Ah Headway Energy Cell. [Online], (2016). http://www.headway-headquarters.com/38120s-10ah-headway-energy-cell/.

[47] Enerdel Cells Datasheet. [Online], (2015). http://www.enerdel.com/wp-content/uploads/2013/11/Cell-Binder.pdf.

[48] TH!NK A306 Remote Lithium Energy Controller (RLEC) CAN Programmers Guide. [Online], (2013). https://drive.google.com/open?id=0By_GkproEtO8VVhWSDRuNkJRNXM.

[49] G-10/FR-4 Sheets. [Online], (2015). http://www.professionalplastics.com/cgi-bin/pp.pl?pgm=co_disp&func=displ&prrfnbr=124679&child=144952&sesent=0,0&strfnbr=3.

[50] CANopeners and Battery Life. Heat does appear to matter. [Online], (2016). http://evtv.me/2014/02/canopeners-battery-life-heat-appear-matter/.

[51] Introduction to the Controller Area Network (CAN). [Online], (2016). http://www.ti.com/lit/an/sloa101a/sloa101a.pdf.

[52] RMS CAN Protocol. [Online], (2015). https://app.box.com/s/4fb49r9p6lzfz4uwcb5izkxpcwh768vc.

[53] Sensors Overview. [Online], (2016). http://developer.android.com/guide/topics/sensors/sensors_overview.html.

[54] Ok..Maybe it was Just a Little Gas Pain. [Online], (2016). http://evtv.me/2014/06/ok-maybe-just-little-gas-pain/.

[55] What is CE Marking. [Online], (2016). http://www.ce-marking.org/what-is-ce-marking.html.

[56] Remy HVH Application Manual. [Online], (2016). http://www.neweagle.net/support/wiki/images/c/c2/Remy_Hybrid_Application_Manual_Rev_2-TRB-9-25-2013.pdf.

[57] OptimumG: OptimumTire. [Online], (2016). http://www.optimumg.com/software/optimumtire/.

Appendix A: Supplemental Files

A.1 Cost Report (2014), file type: .xml, size: 4 MB, required software: Microsoft Excel or Google Drive

A.2 Electrical Systems Form (2014), file type: .pdf, size: 4.80 MB, required software: Adobe Reader or Google Drive

A.3 Electrical Systems Form (2015), file type: .pdf, size: 6.35 MB, required software: Adobe Reader or Google Drive

A.4 Formula SAE Electric results (2013), file type: .xml, size: 369 KB, required software: Microsoft Excel or Google Drive

A.5 Formula SAE Electric results (2014), file type: .xml, size: 310 KB, required software: Microsoft Excel or Google Drive

A.6 Formula SAE Electric results (2015), file type: .xml, size: 324 KB, required software: Microsoft Excel or Google Drive

A.7 GEVCU Manual, file type: .pdf, size: 34 MB, required software: Adobe Reader or Google Drive

A.8 RMS GUI Settings, file type: .pdf, size: 244 KB, required software: Adobe Reader or Google Drive

A.9 Thesis Powerpoint (2016), file type: .pdf, size: 4 MB, required software: Google Drive or Adobe Reader

A.10 TH!NK RLEC CAN Programmers Guide, file type: .pdf, size: 1 MB, required software: Google Drive or Adobe Reader